ornl

ORNL/NPR-92/9

OAK RIDGE NATIONAL LABORATORY

MARTIN MARIETTA

HRB-17 and HRB-18 HEU TRISO UCO Unbonded Irradiated Particle Core Conduction Cooldown Tests

R. N. Morris
C. A. Baldwin
J. L. Collins
T. L. Collins
C. M. Malone
W. A. Gabbard
J. Travis
C. S. Webster
J. C. Whitson
J. L. Wright
M. J. Kania

This document does not contain UCNI, ECI, or other unclassified sensitive information and has been approved for release to the public by:

David R. Hamrin 6/16/2011

David R. Hamrin, ORNL Classification Officer Date

[redacted]

MANAGED BY
MARTIN MARIETTA ENERGY SYSTEMS, INC.
FOR THE UNITED STATES
DEPARTMENT OF ENERGY

This report has been reproduced directly from the best available copy.

Available to DOE and DOE contractors from the Office of Scientific and Technical Information, P.O. Box 62, Oak Ridge, TN 37831; prices available from (615) 576-8401, FTS 626-8401.

This report was prepared as an account of work sponsored by an agency of the United States Government. Neither the United States Government nor any agency thereof, nor any of their employees, makes any warranty, express or implied, or assumes any legal liability or responsibility for the accuracy, completeness, or usefulness of any information, apparatus, product, or process disclosed, or represents that its use would not infringe privately owned rights. Reference herein to any specific commercial product, process, or service by trade name, trademark, manufacturer, or otherwise, does not necessarily constitute or imply its endorsement, recommendation, or favoring by the United States Government or any agency thereof. The views and opinions of authors expressed herein do not necessarily state or reflect those of the United States Government or any agency thereof.

ORNL/NPR-92/9

Metals and Ceramics Division

HRB-17 AND HRB-18 HEU TRISO UCO UNBONDED IRRADIATED PARTICLE CORE CONDUCTION COOLDOWN TESTS

R. N. Morris, C. A. Baldwin, J. L. Collins, T. L. Collins,
C. M. Malone, W. A. Gabbard, J. Travis, C. S. Webster,
J. C. Whitson, J. L. Wright, and M. J. Kania

Date Published—June 1992

[redacted]

[redacted]

Prepared for the
New Production Reactors Department
EG&G Idaho
under funding from DOE
62 70 35 20 1

prepared by the
OAK RIDGE NATIONAL LABORATORY
Oak Ridge, Tennessee 37831-6285
managed by
MARTIN MARIETTA ENERGY SYSTEMS, INC.
for the
U.S. DEPARTMENT OF ENERGY
under contract DE-AC05-84OR21400

[redacted]

[redacted]

CONTENTS

LIST OF FIGURES v

LIST OF TABLES ix

ACRONYMS xi

SUMMARY xiii

ABSTRACT 1

1.0 INTRODUCTION 2

2.0 TEST OBJECTIVES 4

3.0 PRETEST RESULTS 7
- 3.1 TEST ARTICLE, HANDLING, AND GAMMA SCANNING 9
- 3.2 BURNUP ANALYSIS 26
- 3.3 METALLOGRAPHY 26
- 3.4 SEM AND MICROPROBE ANALYSIS 30
- 3.5 RADIOGRAPHY 30
- 3.6 HRB-17 PREHEATING RADIOCHEMISTRY ANALYSIS 30
- 3.7 HRB-18 PREHEATING RADIOCHEMISTRY ANALYSIS 30

4.0 EXPERIMENTAL CONDITIONS 31
- 4.1 1600°C TEST TEMPERATURE HISTORY 31
- 4.2 1400°C TEST TEMPERATURE HISTORY 33
- 4.3 1600°C TEST FURNACE SWEEP GAS AND FLOWS 35
- 4.4 1400°C TEST FURNACE SWEEP GAS AND FLOWS 35
- 4.5 CCCTF COMPONENTS 42
- 4.6 PERSONNEL 42

5.0 EXPERIMENTAL HEATING RESULTS 43
- 5.1 GAMMA-EMITTING FISSION PRODUCT RELEASE AT 1600°C 43
  - 5.1.1 Metallic Fission Products 43
  - 5.1.2 Gaseous Fission Products 54
- 5.2 GAMMA-EMITTING FISSION PRODUCT RELEASE AT 1400°C 54
  - 5.2.1 Metallic Fission Products 54
  - 5.2.2 Gaseous Fission Products 65
- 5.3 STRONTIUM RELEASE AT 1600°C 67
- 5.4 STRONTIUM RELEASE AT 1400°C 71
- 5.5 COMPARISON OF 1400 AND 1600°C TEST RELEASE BEHAVIOR 72
- 5.6 1600°C TEST FISSION PRODUCT MASS BALANCE 77
- 5.7 1400°C TEST FISSION PRODUCT MASS BALANCE 80
- 5.8 1400/1600°C PARTICLE CONTAMINATION COMPARISON 81

6.0 METALLOGRAPHY, SEM, AND RADIOGRAPHY 83
6.1 1600°C TEST METALLOGRAPHIC RESULTS 83
6.2 1400°C TEST METALLOGRAPHIC RESULTS 87
6.3 SEM AND MICROPROBE ANALYSIS 87
6.4 RADIOGRAPHY 87
7.0 CONCLUSIONS 87
8.0 ACKNOWLEDGMENTS 88
9.0 REFERENCES 88
APPENDIX A. BURNUP CALCULATIONS HEU UCO TRISO PARTICLES - CAPSULES HRB-17/-18 91

LIST OF FIGURES

Figure		Page
1	Schematic diagram of the CCCTF	3
2	Planned temperature control profile for the core conduction cooldown test of HRB-17 fuel particles	6
3	Planned temperature control profile for the core conduction cooldown test of HRB-18 fuel particles	8
4	Furnace internal geometry	27
5	HRB-17/-18 particle pretest metallography. This work was done at GA. Recent calculations indicate burnup was 67% rather than the initial estimate of 78%	28
6	HRB-17/-18 kernel pretest metallography. This work was done at GA. Recent calculations indicate burnup was 67% rather than the initial estimate of 78%	29
7	Furnace temperature history as measured by the pyrometer, BGT, and Type C thermocouple for the HRB-17 test	32
8	Furnace temperature history as measured by the pyrometer, BGT, and Type C thermocouple for the HRB-18 test	34
9	Furnace sweep gas flow history for each region showing the flow spikes and drift for the 1600°C test	36
10	Furnace sweep gas flow history for each region showing the trap blockage, flow spikes, and drift for the 1400°C test	37
11	Sweep gas flow history during trap blockage, trap warmup, and flow restoration for the 1400°C test	39
12	Trap temperature histories during trap blockage, trap warmup, and flow restoration for the 1400°C test	40
13	History of RGA monitoring of mass 18/28 impurities in the furnace internal region for the 1400°C test. These data are only qualitative in nature	41
14	Integrated deposition cup cesium collection as a function of time for the 1600°C test. Corrected to 5 Feb 1986	44

Figure		Page

15 Deposition cup cesium collection rate as a function of time for the 1600°C test. Corrected to 5 Feb 1986 46

16 Measured change in particle Cs-134 inventory on a particle-by-particle basis for the 1600°C test. Note indicated losses 48

17 Measured change in particle Cs-137 inventory on a particle-by-particle basis for the 1600°C test. Note indicated losses and downward trend 49

18 Measured change in particle Ce-144 inventory on a particle-by-particle basis for the 1600°C test 50

19 Measured change in particle Eu-154 inventory on a particle-by-particle basis for the 1600°C test. Note indicated losses 51

20 Cumulative cold trap activities during 1600°C particle heatup test. No krypton release was observed 55

21 Integrated deposition cup cesium collection as a function of time for the 1400°C test. Corrected to 5 Feb 1986 57

22 Deposition cup cesium collection rate as a function of time for the 1400°C test. Corrected to 5 Feb 1986 59

23 Measured change in particle Cs-134 inventory on a particle-by-particle basis for the 1400°C test. Note downward trend 60

24 Measured change in particle Cs-137 inventory on a particle-by-particle basis for the 1400°C test. Note downward trend 61

25 Measured change in particle Ce-144 inventory on a particle-by-particle basis for the 1400°C test. Note random scatter 62

26 Measured change in particle Eu-154 inventory on a particle-by-particle basis for the 1400°C test 63

27 Cumulative cold trap activities during 1400°C particle heatup test. No Krypton-85 release was observed 66

28 Integrated deposition cup strontium collection as a function of time for the 1600°C test. Corrected to 5 Feb 1986 68

29 Deposition cup strontium collection rate as a function of time for the 1600°C test. Corrected to 5 Feb 1986 70

Figure		Page
30	Integrated deposition cup strontium collection as a function of time for the 1400°C test. Corrected to 5 Feb 1986	73
31	Deposition cup stronium collection rate as a function of time for the 1400°C test. Corrected to 5 Feb 1986	75
32	Comparison between the 1600 and 1400°C integrated deposition cup cesium collection as a function of time. Corrected to 5 Feb 1986	76
33	Comparison between the 1400 and 1600°C deposition cup cesium collection rate as a function of time. Corrected to 5 Feb 1986	78
34	Metallographic cross section of particle H17D-H42. No evidence of chemical attack. SiC appears dense and non-porous	84
35	Metallographic cross section of particle H17D-H51, which released europium but not cesium	85
36	Metallographic cross section of particle H17D-H62, which released cesium but little europium	86

LIST OF TABLES

Table		Page
1	1600° C particle pre- and postheating inventories. Activities are in Bq corrected to 5 Feb 1986	10
2	1400° C particle pre- and postheating inventories. Activities are in Bq corrected to 5 Feb 1986	18
3	1600° C deposition cup cesium data. Corrected to 5 Feb 1986	45
4	1600° C deposition cup cesium data. Corrected to 5 Feb 1986	58
5	1600° C deposition cup strontium data. Corrected to 5 Feb 1986	69
6	1400° C deposition cup strontium data. Corrected to 5 Feb 1986	74
A-1	Actinide fission fraction data and fission product yield data for HRB-17/-18 HEU UCO TRISO particle burnup calculations	93
A-2	Irradiation history for test capsules HRB-17/-18 in HFIR	94
A-3	Calculations for the fission rate and number of fissions for HEU UCO TRISO particles irradiated in test capsules HRB-17 and HRB-18A	95
A-4	Burnup determinations for HEU UCO TRISO-coated particles irradiated in test capsules HRB-17 and HRB-18	97
A-5	Comparison of the fission product inventories measured (gamma spectrometry) and calculated (burnup determinations) for HEU UCO TRISO particles irradiated in test capsules HRB-17 and HRB-18	97

ACRONYMS

BGT	Boron Graphite Thermocouple
CCCTF	Core Conduction Cooldown Test Facility
DTF	Designed-to-Fail
FIMA	Fissions per Initial Metal Atom
HEU	Highly Enriched Uranium
IPyC	Inner Pyrolytic Carbon Coating
OPyC	Outer Pyrolytic Carbon Coating
MDAL	Minimal Detectable Activity Level
MHTGR	Modular High-Temperature Gas-Cooled Reactor
NP	New Production (Reactor)
RGA	Residual Gas Analyzer
SiC	Silicon Carbide
TRISO	TRI-material (buffer, silicon carbide, pyrolytic carbon), isotropic material coating layers coated particle design
UCO	Uranium Oxycarbide (UO_2+UC_2) two-phase mixture

SUMMARY

This report describes the core conduction cooldown (CCC) heating experiment performed on the HRB-17 and HRB-18 unbonded, irradiated, highly enriched uranium (HEU), uranium oxycarbide (UCO) TRISO particles and the results of those experiments. The goal of these two heating experiments was to use the Core Conduction Cooldown Test Facility (CCCTF) to heat the irradiated, unbonded, HEU UCO particles from the HRB-17 capsule at a temperature of 1600°C for a period of 100 h and to heat identical particles from the HRB-18 capsule at a temperature of 1400°C for a period of 300 h and monitor the cesium (^{134}Cs and ^{137}Cs) and krypton (^{85}Kr) releases.

The 1600°C (HRB-17) heating program proceeded as planned with only minor difficulties, but the 1400°C (HRB-18) test suffered an unplanned shutdown late in the test. The major portion of the 1400°C heating program had proceeded as planned, but the experiment ended prematurely due to the malfunction of a power supply cooling flow control valve. Fortunately, 86% of the heating (over 259 h) at the planned temperature had been completed before the malfunction occurred. In addition, the experiment had proceeded well past the transient stage of metallic fission product release.

No gaseous release from either set of fuel particles was observed. However, a cesium release was observed in both experiments. For both heating tests, the cesium collection by the deposition cup began during the temperature ramp from 800°C up to the test temperature (1400 or 1600°C), peaked soon after the test temperature was reached, and then decreased to a small, steady-state level after approximately 1 d at the test temperature. After a short time at this low level, the 1600°C test release rate increased to a much higher level where it stayed until the termination of the test. The 1400°C test release rate continued to decrease after the initial release until the termination of the experiment. In addition to cesium, a strontium (^{90}Sr) release was also observed. The strontium release for the 1600°C test started after the test temperature was achieved and continued until rampdown. Strontium release for the 1400°C test followed the cesium release pattern, and only trace amounts of the material were observed.

The metallic fission product release is believed to be composed of two components. The early releases during the ramp up to test temperature are due to surface contamination on the particles. The second, later release is due to particle fission product release, which may indicate particle coating failure.

Two problems were encountered during the 1600° C test. The first was a motor binding problem on the deposition cup drive motor. This problem was repaired in situ and resulted in a 2-h delay of the deposition cup change at hour 60. No further problems with the deposition cup system were encountered during the run. The other problem was a change in the detector system background at the cold trap during the test caused by the migration of contaminated dust. The net effect of the detector problem was to raise the minimum detectable activity level for ^{85}Kr. The level was still far below the ^{85}Kr inventory of a single particle. Hence, the sensitivity for detecting ^{85}Kr diffusion through the particle coating was reduced somewhat, but the capacity to detect coating failure was maintained.

Two problems were also encountered during the 1400° C test. During the 800° C heating plateau phase, at approximately hour 35, the trap system plugged up. Flow adjustments were not successful in increasing the flow or freeing the blockage. The first cold trap was then slowly warmed in an effort to melt/remove the blockage and restore flow. No krypton activity had been detected up to this time in either trap. While the first trap was being warmed up, the second trap was held at its nominal temperature as a backup should a sudden release of krypton take place. The warmup was successful in removing the blockage and restoring flow. The first trap then resumed normal operation. No interruption in krypton monitoring had taken place.

The shutdown of the 1400° C test was caused by the second problem. At hour 319.5, the power supply cooling flow interlock switch either malfunctioned or became temporarily blocked by debris, resulting in a shutdown of the power supply. The furnace immediately began to cool and did not recover. This effectively terminated the experiment. Fortunately, 259.5 h of the planned 300 h at temperature had been completed.

Postheating visual examination and gamma spectrometric analysis of the individual particles heated at 1600° C revealed that four of the particles had suffered large releases of cesium and/or europium. Loss of the metallic fission product contamination on the surface of the particles was expected early in the test, and results indicate that, on average, each particle lost 1.8% of its cesium inventory as the contamination left the particle. However, in addition, four particles lost a large amount of their cesium and/or europium inventory, 2 and 57%, 6 and 7%, 60 and 5%, and 35 and 99%, respectively. This loss, due to particle release, increased the aggregate cesium loss by 1.2% to bring the postheating cesium difference to 3%. As a reference, the inventory of the nonvolatile cerium isotope was measured as well as that of cesium and europium to provide an internal baseline for a consistency check. No cerium release was observed.

Postheating visual examination and gamma spectrometric analysis of the individual particles heated at 1400°C revealed that none of the particles had suffered a coating failure. Loss of the metallic fission product contamination again resulted in a 1.8% decrease in the postheating particle cesium inventory. Again, the inventory of the nonvolatile cerium isotope was measured, as well as that of cesium, to provide an internal baseline for a consistency check.

Both the HRB-17 and HRB-18 unbonded particles were irradiated in a capsule that contained designed-to-fail (DTF) particles which released cesium. The cesium collected during and just after the ramp up to test temperature was determined to be contamination from the DTF particles, while the cesium collected later in the test resulted from releases through the SiC coatings. The double-peaked nature of the cesium collection rate history at 1600°C supports this belief, with the first peak due to release of surface contamination and the second, later peak due to release of cesium through the SiC coating.

Postheating examination of the CCCTF furnace used for the 1400 and 1600°C tests revealed that only the muffle tube liner and the furnace components exposed to the fuel heating region became contaminated with radioactive material. The graphite muffle tube had only a slight amount of activity, and the furnace components external to the heating zone were free from contamination. In addition, the furnace components were noted to be in good condition with no serious degradation from the time-at-temperature period.

HRB-17 AND HRB-18 HEU TRISO UCO UNBONDED IRRADIATED PARTICLE CORE CONDUCTION COOLDOWN TESTS*

R. N. Morris, C. A. Baldwin, J. L. Collins†, T. L. Collins,
C. M. Malone, W. A. Gabbard, J. Travis†, C. S. Webster,
J. C. Whitson‡, and J. L. Wright, and M. J. Kania†

ABSTRACT

This report describes the performance of the HRB-17/18 irradiated, highly enriched uranium (HEU), uranium oxycarbide (UCO) TRISO particles under core conduction cooldown (CCC) conditions. The goal of these two heating experiments was to use the Core Conduction Cooldown Test Facility (CCCTF) to heat the irradiated, unbonded, HEU UCO particles from the HRB-17 capsule at a temperature of 1600°C for a period of 100 h and to heat identical particles from the HRB-18 capsule at a temperature of 1400°C for a period of 300 h and monitor the cesium and krypton releases. This goal was achieved with minimal problems for the HRB-17 test. A power supply safety system malfunction prevented the entire HRB-18 heating program from being accomplished, but 86% (over 259 h) of the time at temperature was completed with generally good overall system performance. Postheating examination of the furnace and its components revealed no serious degradation of the components from the heating cycle for either test.

Gamma spectroscopic measurements of each HRB-17 particle after heating revealed that four particles had suffered large, fractional inventory releases. These four particles lost a large amount of their cesium and/or europium inventory, 2 and 57%, 6 and 7%, 60 and 5%, and 35 and 99%, respectively. In addition, the particles' cesium surface contamination was released as well. Overall, the aggregate particle cesium release was 3%, of which 1.8% was due to surface contamination and 1.2% was due to particle fission product release. The total europium release was 2.1%. A strontium release was also observed, totalling 1.5% of the aggregate inventory. No krypton release was observed in the HRB-17 test.

*Research sponsored through EG&G Idaho by the Office of New Production Reactors, U.S. Department of Energy, under contract DE-AC05-84OR21400 with Martin Marietta Energy Systems, Inc.

†Chemical Technology Division.

‡Computing and Telecommunications Division.

Metallography of the HRB-17 particles to characterize the condition of the SiC in the particles releasing significant amounts of cesium or europium has not passed the preliminary polishing stage due to administrative problems. Early work indicates that the SiC in the releasing particles may differ from that in the non-releasing particles. No firm conclusions have been drawn. Fission product corrosion does not appear to be present.

In contrast to the HRB-17 test, the lower temperature HRB-18 test (1400° C) suffered no particle fission product releases. These particles also released their surface contamination, for a total cesium inventory loss of 1.8%. Only trace amounts of strontium were collected in the test, and the likely source of this strontium is surface contamination. No gaseous fission product releases were observed during the HRB-18 test.

1.0 INTRODUCTION

Postirradiation heating of the unbonded, highly enriched uranium (HEU), uranium oxycarbide (UCO) TRISO-coated particles irradiated in capsules HRB-17 and HRB-18 was carried out in accordance with the requirements of the test specification as outlined by the test plan, which provides the background justification and description of the test.[1,2] The experiments provided an opportunity to provide the initial proof-of-principle operation of the CCCTF and to provide an indication of the off-normal performance of an HEU UCO irradiated fuel, which is similar to the New Production-Modular High-Temperature Gas-Cooled Reactor (NP-MHTGR) particle design, except for the lack of seal coats and an outer protective coating. In addition to providing a shakedown of the CCCTF, this set of experiments provided a demonstration of U.S. irradiated HEU UCO TRISO fuel thermal performance under accident conditions and contributed to the data base for this fuel type at temperatures of interest for the NP-MHTGR design.

A schematic diagram of the CCCTF[3,4] is shown in Fig. 1. Briefly, the fuel specimen is heated according to a predetermined program in an instrumented furnace contained in a hot cell. A sweep gas flows up through the furnace, past the fuel specimen, over a cold finger assembly, and out to the cold trap system. Condensible fission products released by the fuel specimen are collected by the cold finger assembly, while the gaseous fission products are carried by the sweep gas to the cold traps. The cold finger assembly can be removed from the furnace via an airlock,

ORNL-DWG 92-5157

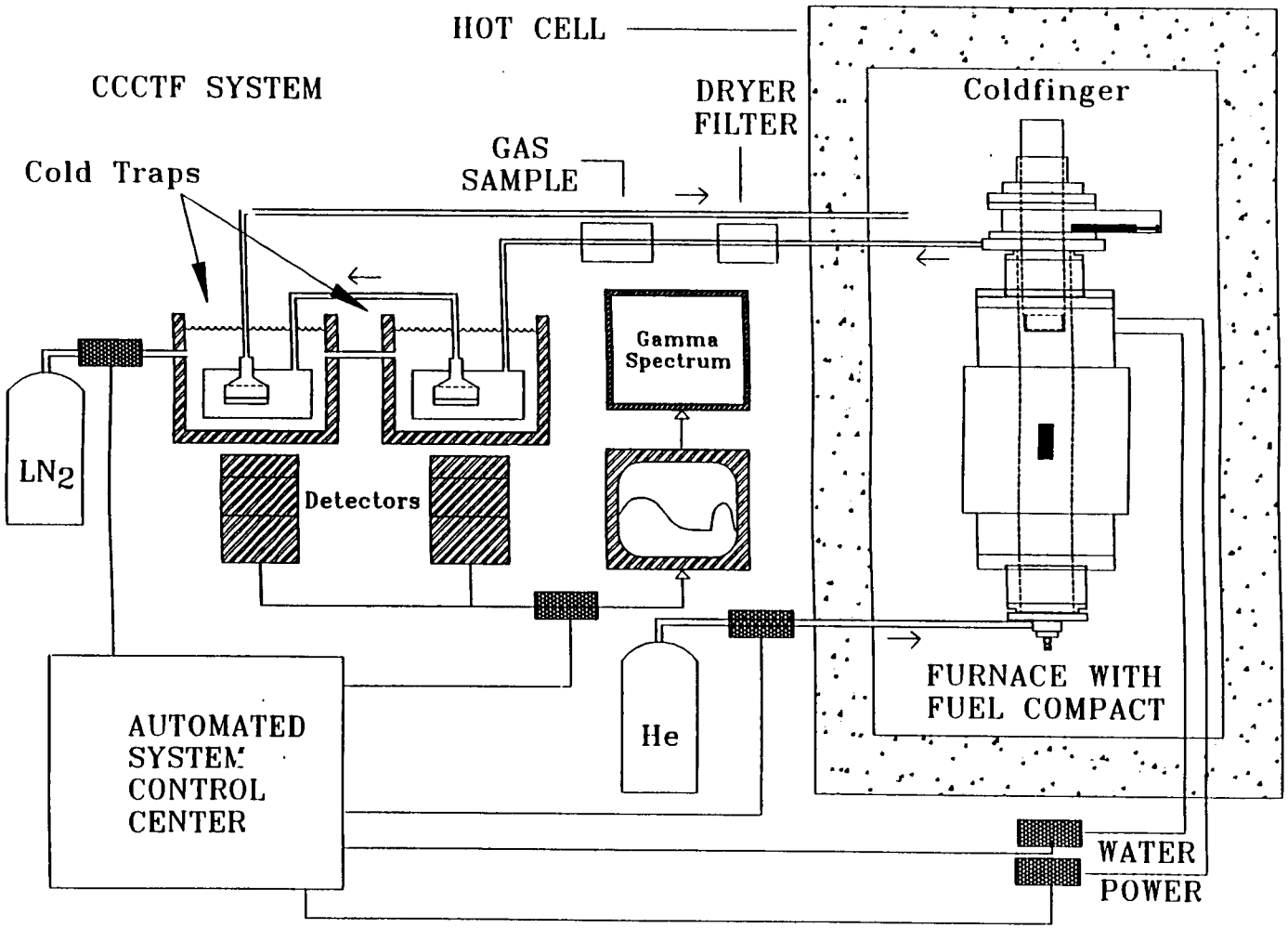

Fig. 1. Schematic diagram of the CCCTF.

the deposition surface (cup) changed, and the assembly reinserted into the furnace without disturbing the heating program. The fission gases are sorbed/frozen onto a low-temperature charcoal bed just above an NaI(Th) detector that provides continuous monitoring of the trap inventory. Two cold traps are connected in series for redundancy. Together, the deposition cup record and the cold trap activity provide a time-release history of fission products from the fuel specimen.

The first experiment in the CCCTF was at 1400° C using HRB-18 unbonded fuel particles, and the second experiment was at 1600° C using HRB-17 unbonded fuel particles.[5,6] These two experiments also marked the initial operation of the CCCTF with irradiated fuel. The primary focus of the 1600° C unbonded fuel heating experiment was to examine the cesium and krypton releases from a modest number (80) of unbonded particles when heated for 100 h in an inert gas atmosphere. The focus of the 1400° C unbonded fuel heating experiment was to examine the cesium and krypton releases from 80 unbonded particles when heated for 300 h in an inert gas atmosphere. These temperatures represent peak and average fuel temperatures for an MHTGR during a depressurized, core-conductor cooldown event. An important part of both experiments was to individually track each particle throughout the experiment so that its radionuclide inventory could be compared before and after the heating. This tracking allowed the identification of the particles that released fission products and quantified the amount released.

During heating, the released cesium was collected on a removable deposition cup that was changed twice daily. The furnace sweep gas was routed through the cold traps, and the individual trap activity was monitored for krypton. No krypton was detected in the traps for either test, but cesium was collected on the deposition cups for both tests. Europium was found on the furnace components used in the 1600° C test but not on the deposition cups. Trace amounts of strontium were also found on the deposition cups used in the 1400° C test. Much larger amounts of strontium were collected by the cups during the 1600° C test. After the heating was complete, the furnace was disassembled and the components examined for degradation and radioactive material inventory.

2.0 TEST OBJECTIVES

The objectives of the heatup experiments were to:

1. contribute to the data base in support of validation of fuel performance models (DDN 11.20);
2. provide the first demonstration of the expected chemical compatibility of high-burnup, dense UCO with the TRISO coating after exposure to temperature-time conditions simulating NP-MHTGR accident conditions;

3. test the four-layer HEU UCO TRISO irradiated fuel performance under accident conditions to provide data for later comparison with the improved, eight-layer TRISO design adapted for the NP-MHTGR; and
4. provide valuable experience in operation of the CCCTF prior to tests with reference NP-MHTGR fuel from capsule NPR-1 and NPR-2.

For the 1600°C test, these objectives were achieved by the following test logic:

1. Catalog and individually identify the test particles throughout the experiment; catalog a subset of their gamma-emitting radionuclide inventories by gamma spectrometry; and destructively analyze a small number of the particles for burnup, kernel microstructure, and ^{90}Sr inventory.
2. Expose the test particles to postulated, dry, depressurized conduction cooldown accident conditions and measure any resulting cesium and krypton releases. The test temperature was 1600°C (±10°C) and the scheduled heating time 100 h. The heatup was to take place in a series of ramps so that a bakeout of the furnace materials could occur and for the fuel to stabilize near its irradiation temperature before ramping up to the test temperature. Cesium and krypton measurements were taken at least twice daily to provide a time-release history. In addition, the furnace atmosphere was monitored by a residual gas analyzer (RGA) to ensure a stable environment.
3. Complete a postheating examination of the particles, both visual and by gamma spectrometry; destructively analyze a small number of the particles for kernel microstructure and ^{90}Sr inventory; examine and gamma count the furnace components; and perform a mass balance for the released fission products.

The planned temperature history for the 1600°C test was:

Ramp from 25 to 300°C in 1.5 h,
Hold at 300°C for 16 h,
Ramp from 300 to 800°C in 2.5 h,
Hold at 800°C for 22 h,
Ramp from 800 to 1600°C in 24 h,
Hold at 1600°C for 100 h, and
Ramp from 1600 to 25°C in 8 h.

The details of the planned temperature profile are shown graphically in Fig. 2, along with the calendar dates for the primary events.

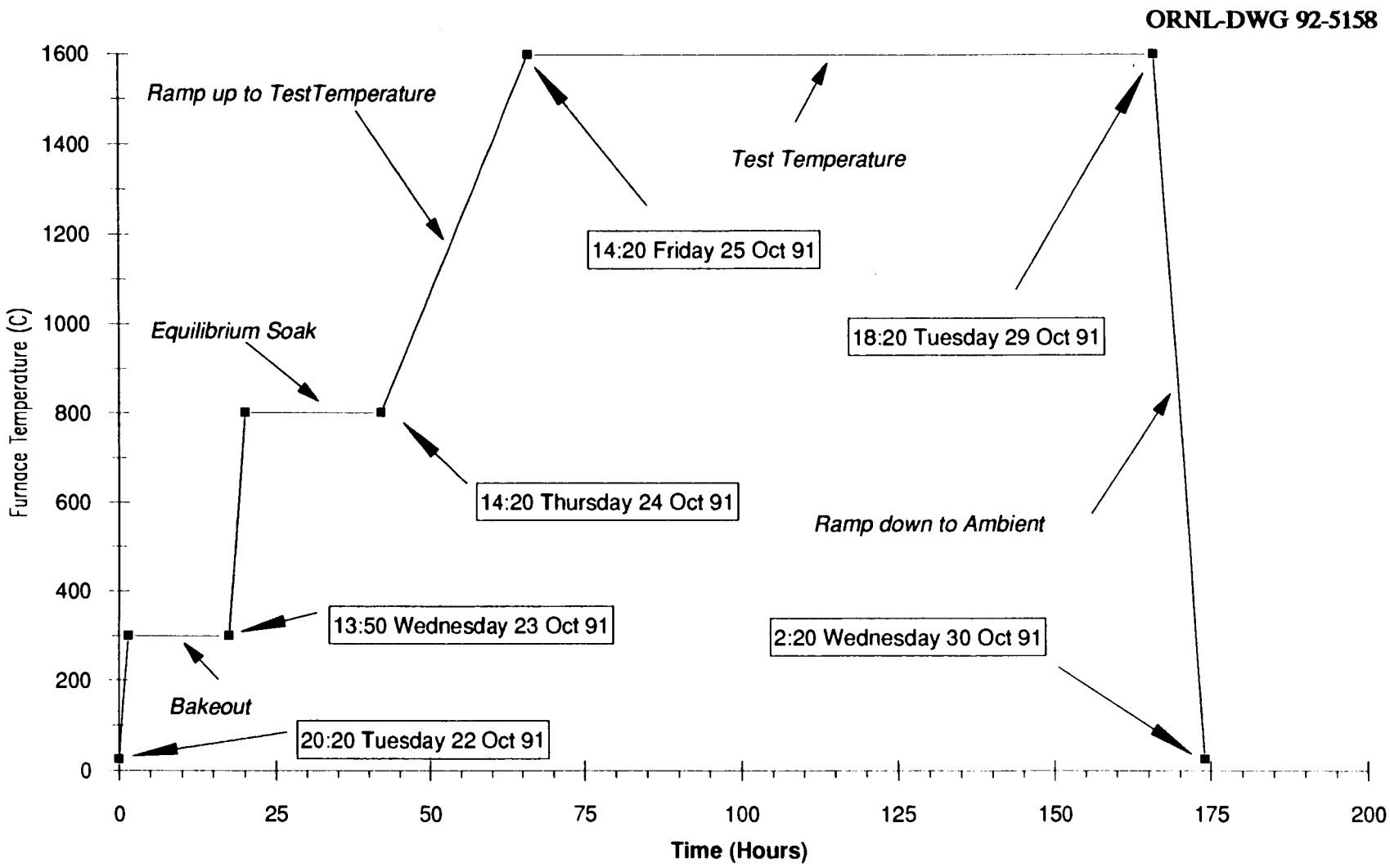

Fig. 2. Planned temperature control profile for the core conduction cooldown test of HRB-17 fuel particles.

The test logic of the 1400°C core conduction simulation experiment was the same as for the 1600°C test, except for item 2, which reflects the lower operating temperature and longer time period:

2. Expose the test particles to postulated, dry, depressurized conduction cooldown accident conditions and measure any resulting cesium and krypton releases. The test temperature was 1400°C (±10°C) and the scheduled heating time 300 h. The heatup was to take place in a series of ramps so that a bakeout of the furnace materials could occur and the fuel could stabilize near its irradiation temperature before ramping up to the test temperature. Cesium and krypton measurements were taken at least twice daily to provide a time-release history. In addition, the furnace atmosphere was monitored by an RGA to ensure a stable environment.

The planned temperature history for the 1400°C test was:

Ramp from 25 to 300°C in 1.5 h,
Hold at 300°C for 16 h,
Ramp from 300 to 800° in 2.5 h,
Hold at 800°C for 22 h,
Ramp from 800 to 1400° in 18 h,
Hold at 1400°C for 300 h, and
Ramp from 1400 to 25°C in 7 h.

The details of the planned temperature profile are shown graphically in Fig. 3, along with the calendar dates for the primary events.

Because of a malfunction of a coolant flow switch, the experiment was stopped earlier than planned. A total of 259.5 h at 1400°C were completed prior to a rapid shutdown, which cooled the furnace from 1400 to 400°C in approximately 30 min.

3.0 PRETEST RESULTS

This section describes the test article, handling of the test article, and analyses performed to the test article.

ORNL-DWG-92-5159

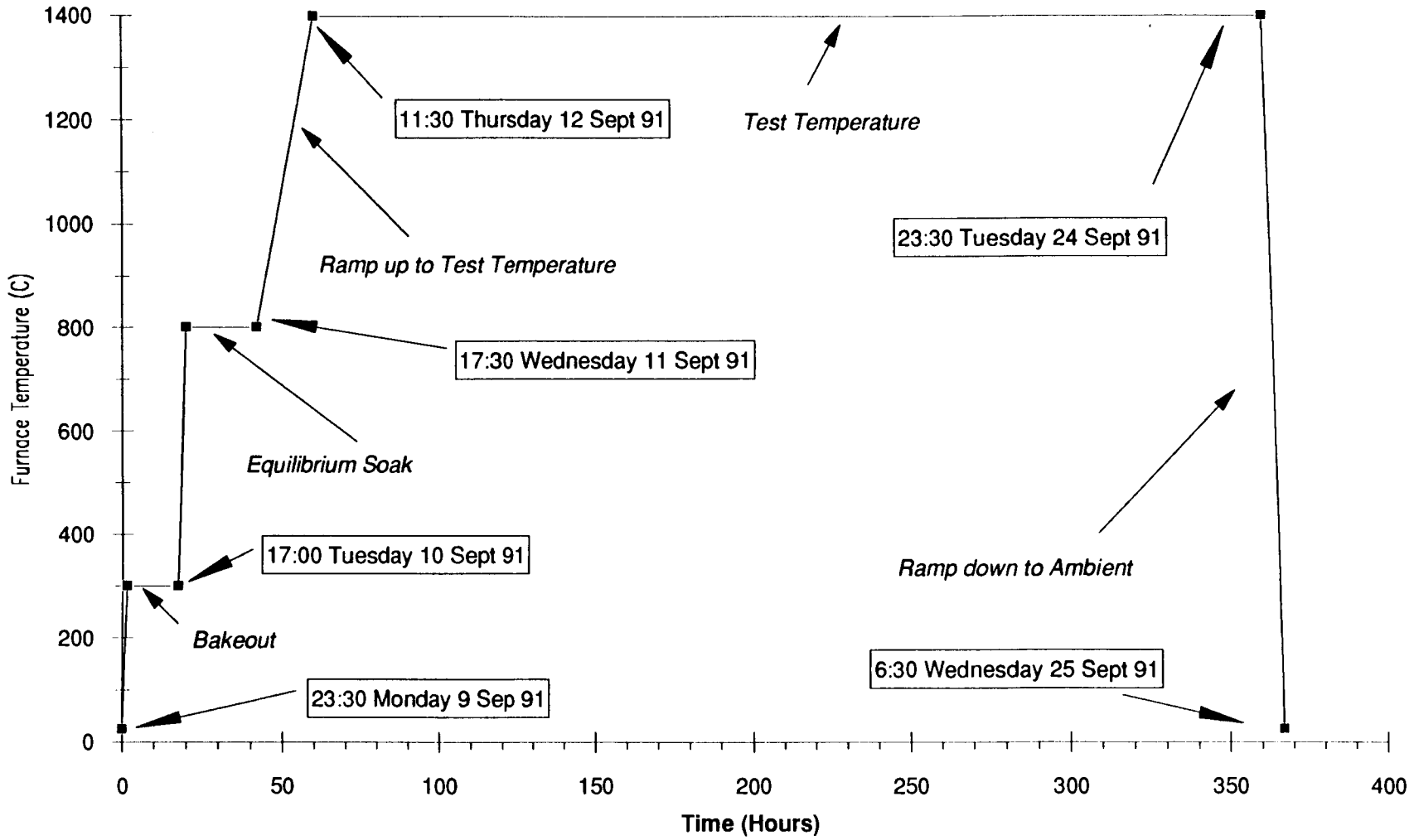

Fig. 3. Planned temperature control profile for the core conduction cooldown test of HRB-18 fuel particles.

3.1 TEST ARTICLE, HANDLING, AND GAMMA SCANNING

The HEU UCO fuel particles to be used in the heatup experiments were irradiated in unbonded particle trays contained in the piggyback experiments in capsules HRB-17 and HRB-18. These trays contained HEU UCO TRISO particle types as well as DTF particles. The design of the irradiation experiment inadvertently allowed the releases from the DTF particles to contaminate the particles used in this test with cesium.

The HEU UCO fuel particles were removed from the original particle trays; individually gamma scanned; visually inspected for gross defects; and placed in new, clean graphite particle trays designed for the CCCTF. The locations of the particles in the holder were recorded so that the particles could be tracked throughout the experiment. The particles were subjected to gamma spectrometry to determine their inventories of ^{134}Cs, ^{137}Cs, ^{144}Ce, ^{154}Eu, ^{155}Eu, and ^{106}Ru. Other isotopes, such as ^{125}Sb, yielded poor counting statistics and were not used for analysis. Because of its very small inventory, due to the age of the fuel specimen, ^{110m}Ag was not characterized. The particle inventories are detailed in Table 1 for HRB-17 and Table 2 for HRB-18. The gamma spectrometric equipment has an overall repeatability of 1 to 12% depending on the radionuclide and its amount. Particle inventory losses in excess of this amount can be determined on an individual basis. Losses of a particular radionuclide smaller than this amount cannot be reliably determined on an individual particle basis, but the aggregate total of a group can provide some approximate information about average losses. Deposition cup data must be relied upon for the measurement of very small losses.

The parameters of the unbonded particles contained in trays 17B, 17D, and 17F of HRB-17 and trays 18B, 18D, and 18F of HRB-18 are:[7]

Particles per tray	40
Batch	6157-12-0100
Type	TRISO $UC_{0.2}O_{1.8}$
Enrichment	> 93% (HEU)
Mean kernel diameter	213 μm
Mean kernel density	10.6 g/cm^3
Mean buffer thickness	104 μm
Mean buffer density	1 g/cm^3
Mean IPyC thickness	39.4 μm

Table 1. 1600°C particle pre- and postheating inventories. Activities are in Bq corrected to 5 Feb 1986.

Isotope		Cs-134			Cs-137			Ce-144		
		Post	Pre	Delta	Post	Pre	Delta	Post	Pre	Delta
Particle ID	**Particle**									
H17B-H01	1	1.03E+07	1.03E+07	0.48%	3.85E+06	3.90E+06	-1.33%	1.03E+08	1.00E+08	2.53%
H17B-H02	2	9.62E+06	9.52E+06	1.06%	3.64E+06	3.67E+06	-0.92%	9.50E+07	9.32E+07	1.93%
H17B-H03	3	9.48E+06	9.58E+06	-1.02%	3.67E+06	3.69E+06	-0.63%	9.93E+07	9.49E+07	4.57%
H17B-H04	4	9.63E+06	9.65E+06	-0.20%	3.63E+06	3.67E+06	-0.88%	9.83E+07	9.34E+07	5.28%
H17B-H05	5	1.03E+07	1.02E+07	0.93%	3.82E+06	3.88E+06	-1.52%	1.04E+08	9.94E+07	4.34%
H17B-H06	6	1.02E+07	1.01E+07	0.58%	3.84E+06	3.86E+06	-0.52%	1.01E+08	9.82E+07	2.63%
H17F-H89	7	9.53E+06	9.82E+06	-2.90%	3.59E+06	3.66E+06	-1.78%	9.56E+07	9.21E+07	3.73%
H17F-H90	8	1.02E+07	1.04E+07	-2.18%	3.86E+06	3.93E+06	-1.86%	1.01E+08	1.02E+08	-0.84%
H17B-H09	9	1.02E+07	1.04E+07	-1.15%	3.88E+06	3.94E+06	-1.53%	9.89E+07	9.94E+07	-0.51%
H17B-H10	10	9.64E+06	9.80E+06	-1.59%	3.68E+06	3.72E+06	-1.11%	9.44E+07	9.65E+07	-2.16%
H17B-H11	11	9.80E+06	1.01E+07	-3.18%	3.80E+06	3.85E+06	-1.11%	9.70E+07	9.85E+07	-1.49%
H17B-H12	12	1.00E+07	1.02E+07	-1.58%	3.86E+06	3.88E+06	-0.67%	1.02E+08	9.98E+07	1.93%
H17B-H13	13	9.12E+06	9.17E+06	-0.57%	3.45E+06	3.50E+06	-1.37%	9.28E+07	8.92E+07	4.04%
H17B-H14	14	9.99E+06	1.00E+07	-0.48%	3.81E+06	3.85E+06	-1.08%	1.01E+08	9.96E+07	1.51%
H17B-H15	15	1.01E+07	1.02E+07	-0.70%	3.84E+06	3.91E+06	-1.75%	1.06E+08	1.01E+08	4.31%
H17B-H16	16	9.55E+06	9.47E+06	0.94%	3.65E+06	3.67E+06	-0.57%	9.86E+07	9.37E+07	5.13%
H17B-H17	17	1.00E+07	1.01E+07	-0.27%	3.75E+06	3.80E+06	-1.50%	9.94E+07	9.76E+07	1.83%
H17B-H18	18	9.70E+06	9.69E+06	0.11%	3.68E+06	3.69E+06	-0.23%	9.82E+07	9.38E+07	4.64%
H17B-H19	19	9.27E+06	9.28E+06	-0.09%	3.53E+06	3.59E+06	-1.56%	9.31E+07	9.09E+07	2.39%
H17B-H20	20	9.35E+06	9.52E+06	-1.83%	3.58E+06	3.61E+06	-0.85%	9.53E+07	9.28E+07	2.62%
H17B-H21	21	9.49E+06	9.45E+06	0.43%	3.61E+06	3.63E+06	-0.59%	9.65E+07	9.21E+07	4.77%
H17B-H22	22	9.51E+06	9.58E+06	-0.78%	3.67E+06	3.72E+06	-1.44%	9.71E+07	9.54E+07	1.76%
H17B-H23	23	9.41E+06	9.44E+06	-0.30%	3.62E+06	3.63E+06	-0.16%	9.58E+07	9.26E+07	3.52%
H17B-H24	24	9.40E+06	9.50E+06	-1.08%	3.59E+06	3.62E+06	-0.66%	9.47E+07	9.44E+07	0.32%
H17B-H25	25	9.99E+06	1.00E+07	-0.20%	3.75E+06	3.81E+06	-1.59%	9.87E+07	9.54E+07	3.46%
H17B-H26	26	1.01E+07	1.01E+07	0.28%	3.86E+06	3.87E+06	-0.24%	1.02E+08	9.74E+07	4.30%
H17B-H27	27	9.48E+06	9.60E+06	-1.24%	3.62E+06	3.67E+06	-1.41%	9.66E+07	9.40E+07	2.68%
H17B-H28	28	1.02E+07	1.01E+07	0.76%	3.89E+06	3.90E+06	-0.33%	1.05E+08	9.98E+07	5.65%
H17B-H29	29	9.42E+06	9.57E+06	-1.55%	3.65E+06	3.69E+06	-1.19%	9.75E+07	9.57E+07	1.80%

Table 1 (cont)

Isotope		Cs-134				Cs-137				Ce-144		
		Post	Pre	Delta		Post	Pre	Delta		Post	Pre	Delta
Particle ID	**Particle**											
H17B-H30	30	9.55E+06	9.60E+06	-0.51%		3.65E+06	3.70E+06	-1.37%		9.64E+07	9.69E+07	-0.50%
H17B-H31	31	9.00E+06	8.96E+06	0.44%		3.42E+06	3.44E+06	-0.54%		9.34E+07	8.85E+07	5.57%
H17B-H32	32	9.57E+06	9.49E+06	0.85%		3.61E+06	3.66E+06	-1.43%		9.54E+07	9.62E+07	-0.89%
H17B-H33	33	9.95E+06	1.01E+07	-1.74%		3.79E+06	3.84E+06	-1.25%		1.01E+08	9.83E+07	2.34%
H17B-H34	34	9.55E+06	9.69E+06	-1.41%		3.66E+06	3.72E+06	-1.60%		9.62E+07	9.50E+07	1.22%
H17B-H35	35	9.47E+06	9.32E+06	1.54%		3.57E+06	3.60E+06	-0.72%		9.57E+07	9.45E+07	1.28%
H17B-H36	36	9.38E+06	9.48E+06	-1.07%		3.61E+06	3.65E+06	-0.95%		9.24E+07	9.07E+07	1.91%
H17B-H37	37	9.57E+06	9.43E+06	1.47%		3.54E+06	3.59E+06	-1.44%		9.27E+07	9.16E+07	1.17%
H17B-H38	38	9.57E+06	9.43E+06	1.42%		3.62E+06	3.66E+06	-1.17%		9.38E+07	9.50E+07	-1.29%
H17B-H39	39	1.01E+07	1.02E+07	-0.79%		3.77E+06	3.85E+06	-2.17%		9.96E+07	9.61E+07	3.68%
H17B-H40	40	1.02E+07	1.02E+07	0.04%		3.83E+06	3.85E+06	-0.67%		9.98E+07	9.89E+07	0.92%
H17D-H41	41	9.67E+06	9.65E+06	0.14%		3.58E+06	3.62E+06	-1.15%		9.25E+07	9.37E+07	-1.29%
H17D-H42	42	9.11E+06	9.28E+06	-1.82%		3.47E+06	3.51E+06	-1.28%		8.81E+07	8.73E+07	0.92%
H17D-H43	43	9.38E+06	9.71E+06	-3.39%		3.59E+06	3.64E+06	-1.44%		9.42E+07	9.28E+07	1.52%
H17D-H44	44	1.02E+07	1.03E+07	-0.36%		3.86E+06	3.91E+06	-1.22%		1.01E+08	1.00E+08	0.81%
H17D-H45	45	9.59E+06	9.54E+06	0.53%		3.62E+06	3.68E+06	-1.52%		9.52E+07	9.26E+07	2.78%
H17D-H46	46	1.02E+07	1.00E+07	1.69%		3.78E+06	3.81E+06	-0.87%		1.01E+08	9.93E+07	1.63%
H17D-H47	47	9.58E+06	9.42E+06	1.77%		3.61E+06	3.63E+06	-0.62%		9.35E+07	9.37E+07	-0.24%
H17D-H48	48	1.03E+07	1.01E+07	1.91%		3.83E+06	3.87E+06	-1.19%		1.00E+08	9.98E+07	0.40%
H17D-H49	49	9.74E+06	9.69E+06	0.52%		3.63E+06	3.69E+06	-1.47%		9.53E+07	9.33E+07	2.15%
H17D-H50	50	9.54E+06	9.66E+06	-1.23%		3.61E+06	3.65E+06	-1.10%		9.31E+07	9.56E+07	-2.61%
H17D-H51	51 *****	9.66E+06	9.86E+06	-2.04%	*****	3.64E+06	3.70E+06	-1.56%	*****	9.70E+07	9.43E+07	2.83%
H17D-H52	52	9.57E+06	9.73E+06	-1.64%		3.68E+06	3.70E+06	-0.54%		9.82E+07	9.44E+07	3.98%
H17D-H53	53	1.01E+07	9.81E+06	2.72%		3.76E+06	3.78E+06	-0.56%		9.93E+07	9.58E+07	3.69%
H17D-H54	54	1.02E+07	1.01E+07	0.38%		3.79E+06	3.81E+06	-0.74%		1.00E+08	9.91E+07	1.28%
H17D-H55	55	1.01E+07	1.04E+07	-2.80%		3.85E+06	3.90E+06	-1.23%		9.90E+07	1.00E+08	-0.96%
H17D-H56	56	9.65E+06	9.75E+06	-0.99%		3.65E+06	3.67E+06	-0.50%		9.56E+07	9.33E+07	2.51%
H17D-H57	57	9.12E+06	9.22E+06	-1.08%		3.44E+06	3.50E+06	-1.54%		9.04E+07	9.02E+07	0.19%
H17D-H58	58	9.36E+06	9.57E+06	-2.21%		3.53E+06	3.60E+06	-1.87%		9.40E+07	9.32E+07	0.82%

Table 1 (cont)

Isotope		Cs-134				Cs-137				Ce-144		
		Post	Pre	Delta		Post	Pre	Delta		Post	Pre	Delta
Particle ID	**Particle**											
H17D-H59	59	1.00E+07	1.01E+07	-0.49%		3.79E+06	3.86E+06	-1.67%		1.01E+08	9.73E+07	3.69%
H17D-H60	60	9.53E+06	9.67E+06	-1.39%		3.62E+06	3.67E+06	-1.34%		9.66E+07	9.35E+07	3.29%
H17D-H61	61 *****	9.75E+06	1.03E+07	-5.11%	*****	3.65E+06	3.90E+06	-6.34%	*****	9.68E+07	1.00E+08	-3.65%
H17D-H62	62 *****	3.95E+06	9.56E+06	-58.70%	*****	1.46E+06	3.64E+06	-59.94%	*****	9.71E+07	9.37E+07	3.59%
H17D-H63	63	1.00E+07	1.00E+07	-0.17%		3.80E+06	3.83E+06	-0.74%		9.95E+07	9.92E+07	0.31%
H17D-H64	64	9.79E+06	9.76E+06	0.29%		3.66E+06	3.72E+06	-1.55%		9.41E+07	9.62E+07	-2.20%
H17D-H65	65	9.65E+06	9.57E+06	0.87%		3.65E+06	3.69E+06	-1.10%		9.60E+07	9.30E+07	3.23%
H17D-H66	66	8.97E+06	8.94E+06	0.37%		3.39E+06	3.43E+06	-1.19%		8.79E+07	8.80E+07	-0.14%
H17D-H67	67	9.84E+06	1.01E+07	-2.42%		3.73E+06	3.79E+06	-1.62%		9.70E+07	9.80E+07	-1.09%
H17D-H68	68	9.52E+06	9.69E+06	-1.74%		3.58E+06	3.65E+06	-1.86%		9.17E+07	9.34E+07	-1.77%
H17D-H69	69	9.45E+06	9.62E+06	-1.82%		3.62E+06	3.64E+06	-0.67%		9.49E+07	9.39E+07	1.03%
H17F-R05	70	9.80E+06	9.88E+06	-0.78%		3.68E+06	3.74E+06	-1.66%		9.58E+07	9.55E+07	0.26%
H17F-H71	71	9.87E+06	9.74E+06	1.34%		3.64E+06	3.69E+06	-1.46%		9.67E+07	9.59E+07	0.88%
H17F-H72	72	9.34E+06	9.45E+06	-1.25%		3.52E+06	3.54E+06	-0.80%		9.22E+07	9.11E+07	1.28%
H17F-H73	73	9.49E+06	9.75E+06	-2.68%		3.59E+06	3.65E+06	-1.59%		9.33E+07	9.21E+07	1.33%
H17F-H74	74	9.76E+06	9.85E+06	-0.99%		3.62E+06	3.68E+06	-1.75%		9.65E+07	9.45E+07	2.12%
H17F-H75	75	9.75E+06	9.79E+06	-0.32%		3.67E+06	3.74E+06	-1.89%		9.45E+07	9.52E+07	-0.76%
H17F-H76	76 *****	6.30E+06	9.73E+06	-35.18%	*****	2.42E+06	3.71E+06	-34.84%	*****	9.89E+07	9.26E+07	6.81%
H17F-H77	77	9.09E+06	9.32E+06	-2.41%		3.42E+06	3.51E+06	-2.34%		8.96E+07	8.74E+07	2.56%
H17F-H78	78	9.92E+06	9.95E+06	-0.25%		3.67E+06	3.74E+06	-1.93%		9.69E+07	9.43E+07	2.85%
H17F-H79	79	9.81E+06	9.88E+06	-0.72%		3.61E+06	3.70E+06	-2.50%		9.72E+07	9.34E+07	4.03%
H17F-H80	80	9.48E+06	9.58E+06	-0.96%		3.53E+06	3.63E+06	-2.64%		9.30E+07	9.25E+07	0.58%
Total Test Particles (80)												
Column Average		9.59E+06	9.76E+06	-1.74E-02		3.62E+06	3.72E+06	-2.44E-02		9.67E+07	9.51E+07	1.76E-02
Standard Deviation		8.15E+05	3.32E+05	7.64E-02		3.06E+05	1.21E+05	7.55E-02		3.58E+06	3.36E+06	2.16E-02
Delta based on Pre and Post averages				-1.74E-02				-2.43E-02				1.74E-02
Lower two sigma limit				-17.03%				-17.55%				-2.57%

Table 1 (cont)

Isotope	Cs-134 Post	Cs-134 Pre	Cs-134 Delta	Cs-137 Post	Cs-137 Pre	Cs-137 Delta	Ce-144 Post	Ce-144 Pre	Ce-144 Delta
Average (μCi)	2.59E+02	2.64E+02	-4.58	9.80E+01	1.00E+02	-2.44	2.61E+03	2.57E+03	44.75
Total diff (μCi)			-366.08			-195.27			3580.19
Non-releasing Particles (76)									
Average	9.70E+06	9.75E+06	-5.06E-03	3.67E+06	3.71E+06	-1.22E-02	9.67E+07	9.51E+07	1.73E-02
Standard Deviation	3.43E+05	3.35E+05	1.30E-02	1.22E+05	1.22E+05	5.35E-03	3.66E+06	3.38E+06	2.03E-02
Difference based on Pre and Post averages			-5.11E-03			-1.22E-02			1.71E-02
Lower two sigma limit			-3.11%			-2.29%			-2.34%
Releasing Particles (4)									
Average	7.49E+06	9.80E+06	-2.40E-01	2.83E+06	3.72E+06	-2.43E-01	9.81E+07	9.50E+07	3.39E-02
Standard Deviation	4.18E+06	4.39E+06	2.66E-01	1.59E+06	1.66E+06	2.70E-01	4.39E+07	4.25E+07	2.77E-02
Difference based on Pre and Post averages			-2.36E-01			-2.39E-01			3.33E-02
Lower two sigma limit			-77.32%			-78.35%			-2.15%
Total Corrected for Cerium Balance (80)									
Average (μCi)	2.55E+02	2.64E+02	-9.01	9.63E+01	1.00E+02	-4.12	2.57E+03	2.57E+03	0.00
Total diff (μCi)			-721.02			-329.44			0.00
Non-releasing Particles Corrected for Cerium Balance (76)									
Average (μCi)	2.58E+02	2.64E+02	-5.77	9.75E+01	1.00E+02	-2.90	2.57E+03	2.57E+03	0.00
Total diff (μCi)			-438.15			-220.08			0.00
Releasing Corrected for Cerium Balance (4)									
Average	1.96E+02	2.65E+02	-69.02	7.40E+01	1.01E+02	-26.52	2.57E+03	2.57E+03	0.00
Total diff (μCi)			-276.08			-106.08			0.00

Table 1 (cont)

Isotope		Eu-154			Eu-155			Ru-106		
		Post	Pre	Delta	Post	Pre	Delta	Post	Pre	Delta
Particle ID	**Particle**									
H17B-H01	1	1.54E+05	1.52E+05	1.06%	1.19E+05	9.59E+04	23.99%	8.05E+06	6.48E+06	24.18%
H17B-H02	2	1.42E+05	1.37E+05	3.46%	1.05E+05	1.10E+05	-5.35%	6.63E+06	5.78E+06	14.83%
H17B-H03	3	1.43E+05	1.37E+05	4.80%	1.09E+05	1.09E+05	-0.15%	6.75E+06	6.66E+06	1.29%
H17B-H04	4	1.42E+05	1.37E+05	3.64%	1.18E+05	8.86E+04	33.27%	7.29E+06	7.04E+06	3.51%
H17B-H05	5	1.46E+05	1.50E+05	-2.83%	1.19E+05	1.07E+05	11.46%	7.04E+06	7.16E+06	-1.71%
H17B-H06	6	1.51E+05	1.44E+05	5.45%	1.14E+05	1.17E+05	-2.22%	8.03E+06	6.33E+06	26.96%
H17F-H89	7	1.39E+05	1.38E+05	0.70%	1.07E+05	9.67E+04	10.76%	7.92E+06	6.12E+06	29.43%
H17F-H90	8	1.54E+05	1.43E+05	7.22%	1.22E+05	1.04E+05	17.07%	8.15E+06	7.35E+06	10.81%
H17B-H09	9	1.53E+05	1.50E+05	2.10%	1.24E+05	1.05E+05	17.67%	7.24E+06	7.55E+06	-4.12%
H17B-H10	10	1.44E+05	1.47E+05	-1.81%	1.10E+05	1.07E+05	3.02%	7.85E+06	6.89E+06	13.82%
H17B-H11	11	1.52E+05	1.39E+05	9.02%	1.04E+05	1.09E+05	-4.74%	6.39E+06	7.11E+06	-10.16%
H17B-H12	12	1.49E+05	1.48E+05	0.89%	1.17E+05	1.09E+05	7.84%	6.86E+06	7.23E+06	-5.04%
H17B-H13	13	1.35E+05	1.35E+05	0.10%	9.09E+04	1.07E+05	-15.47%	6.86E+06	6.45E+06	6.35%
H17B-H14	14	1.48E+05	1.45E+05	1.87%	1.20E+05	9.93E+04	20.47%	7.00E+06	6.57E+06	6.51%
H17B-H15	15	1.48E+05	1.49E+05	-0.66%	1.12E+05	1.17E+05	-4.21%	8.05E+06	6.49E+06	24.09%
H17B-H16	16	1.39E+05	1.39E+05	0.38%	1.05E+05	1.03E+05	1.50%	6.95E+06	7.17E+06	-3.00%
H17B-H17	17	1.44E+05	1.43E+05	0.34%	1.07E+05	1.12E+05	-4.62%	6.40E+06	6.05E+06	5.79%
H17B-H18	18	1.44E+05	1.39E+05	3.69%	1.02E+05	1.02E+05	0.67%	7.22E+06	7.14E+06	1.19%
H17B-H19	19	1.35E+05	1.38E+05	-2.52%	1.15E+05	8.94E+04	28.43%	5.88E+06	5.93E+06	-0.86%
H17B-H20	20	1.36E+05	1.32E+05	3.27%	1.17E+05	1.06E+05	9.73%	6.96E+06	6.36E+06	9.41%
H17B-H21	21	1.41E+05	1.37E+05	2.42%	1.10E+05	9.56E+04	15.43%	7.10E+06	6.10E+06	16.29%
H17B-H22	22	1.45E+05	1.34E+05	8.49%	1.03E+05	1.00E+05	2.73%	7.21E+06	5.80E+06	24.44%
H17B-H23	23	1.40E+05	1.33E+05	4.96%	9.47E+04	1.06E+05	-11.01%	7.02E+06	6.88E+06	2.14%
H17B-H24	24	1.37E+05	1.40E+05	-1.58%	1.12E+05	9.09E+04	23.60%	7.19E+06	6.97E+06	3.20%
H17B-H25	25	1.44E+05	1.46E+05	-1.11%	1.10E+05	8.93E+04	22.68%	6.79E+06	6.83E+06	-0.57%
H17B-H26	26	1.45E+05	1.47E+05	-0.97%	9.70E+04	1.04E+05	-6.91%	7.42E+06	6.98E+06	6.42%
H17B-H27	27	1.37E+05	1.36E+05	0.83%	1.04E+05	1.07E+05	-2.16%	6.79E+06	6.24E+06	8.83%
H17B-H28	28	1.52E+05	1.45E+05	4.76%	9.47E+04	8.97E+04	5.65%	7.18E+06	7.11E+06	0.99%
H17B-H29	29	1.36E+05	1.35E+05	0.87%	1.07E+05	1.01E+05	5.61%	7.07E+06	6.44E+06	9.71%

Table 1 (cont)

Isotope		Eu-154				Eu-155				Ru-106		
		Post	Pre	Delta		Post	Pre	Delta		Post	Pre	Delta
Particle ID	**Particle**											
H17B-H30	30	1.45E+05	1.41E+05	2.36%		1.03E+05	1.04E+05	-0.04%		6.94E+06	6.64E+06	4.53%
H17B-H31	31	1.34E+05	1.31E+05	2.26%		8.97E+04	1.00E+05	-10.49%		6.04E+06	6.64E+06	-9.13%
H17B-H32	32	1.39E+05	1.36E+05	2.19%		1.08E+05	1.04E+05	3.38%		7.37E+06	6.96E+06	5.86%
H17B-H33	33	1.45E+05	1.44E+05	0.49%		1.06E+05	9.56E+04	10.82%		7.91E+06	7.24E+06	9.23%
H17B-H34	34	1.43E+05	1.38E+05	3.25%		1.06E+05	9.94E+04	6.39%		6.80E+06	7.04E+06	-3.41%
H17B-H35	35	1.38E+05	1.45E+05	-5.15%		1.05E+05	1.05E+05	0.23%		6.62E+06	6.58E+06	0.63%
H17B-H36	36	1.41E+05	1.35E+05	4.41%		1.13E+05	1.06E+05	7.23%		7.17E+06	6.48E+06	10.65%
H17B-H37	37	1.41E+05	1.36E+05	3.83%		1.08E+05	1.02E+05	5.90%		6.07E+06	6.96E+06	-12.76%
H17B-H38	38	1.42E+05	1.36E+05	3.99%		1.03E+05	9.47E+04	8.90%		6.46E+06	6.52E+06	-0.91%
H17B-H39	39	1.45E+05	1.42E+05	2.22%		1.10E+05	9.47E+04	16.28%		6.48E+06	6.79E+06	-4.47%
H17B-H40	40	1.48E+05	1.44E+05	3.09%		1.03E+05	1.16E+05	-11.11%		7.04E+06	6.77E+06	4.05%
H17D-H41	41	1.33E+05	1.38E+05	-3.97%		1.00E+05	9.25E+04	8.64%		6.26E+06	7.33E+06	-14.65%
H17D-H42	42	1.34E+05	1.34E+05	0.43%		1.07E+05	1.07E+05	0.23%		6.79E+06	6.47E+06	5.01%
H17D-H43	43	1.45E+05	1.40E+05	3.05%		1.04E+05	1.04E+05	-0.04%		6.90E+06	6.38E+06	8.20%
H17D-H44	44	1.51E+05	1.50E+05	0.77%		1.02E+05	1.14E+05	-10.24%		7.57E+06	7.77E+06	-2.65%
H17D-H45	45	1.43E+05	1.38E+05	3.80%		8.74E+04	8.40E+04	4.13%		7.77E+06	6.86E+06	13.31%
H17D-H46	46	1.45E+05	1.47E+05	-1.55%		1.21E+05	9.77E+04	23.79%		6.85E+06	7.06E+06	-2.85%
H17D-H47	47	1.42E+05	1.39E+05	1.92%		1.01E+05	9.84E+04	2.76%		7.38E+06	6.70E+06	10.23%
H17D-H48	48	1.54E+05	1.42E+05	8.61%		1.20E+05	1.10E+05	9.28%		6.83E+06	7.53E+06	-9.33%
H17D-H49	49	1.45E+05	1.44E+05	0.57%		1.04E+05	9.41E+04	10.15%		6.93E+06	7.14E+06	-2.88%
H17D-H50	50	1.40E+05	1.43E+05	-1.92%		9.26E+04	1.04E+05	-10.94%		6.56E+06	6.63E+06	-1.06%
H17D-H51	51 *****	6.07E+04	1.42E+05	-57.10%	*****	4.97E+04	9.08E+04	-45.29%	*****	7.04E+06	6.41E+06	9.91%
H17D-H52	52	1.42E+05	1.41E+05	0.20%		9.27E+04	9.89E+04	-6.26%		6.54E+06	6.98E+06	-6.31%
H17D-H53	53	1.48E+05	1.44E+05	2.93%		1.21E+05	1.11E+05	8.95%		7.23E+06	6.46E+06	11.96%
H17D-H54	54	1.49E+05	1.42E+05	5.15%		1.05E+05	1.08E+05	-3.20%		6.77E+06	6.67E+06	1.51%
H17D-H55	55	1.48E+05	1.42E+05	4.49%		1.22E+05	1.07E+05	14.56%		6.48E+06	7.10E+06	-8.74%
H17D-H56	56	1.46E+05	1.43E+05	2.11%		1.16E+05	1.17E+05	-0.15%		6.26E+06	6.87E+06	-8.75%
H17D-H57	57	1.35E+05	1.34E+05	0.76%		8.77E+04	9.13E+04	-3.97%		6.09E+06	6.50E+06	-6.40%
H17D-H58	58	1.37E+05	1.36E+05	0.50%		9.28E+04	1.12E+05	-17.14%		6.38E+06	6.48E+06	-1.63%

Table 1 (cont)

Isotope		Eu-154 Post	Eu-154 Pre	Eu-154 Delta		Eu-155 Post	Eu-155 Pre	Eu-155 Delta		Ru-106 Post	Ru-106 Pre	Ru-106 Delta
Particle ID	**Particle**											
H17D-H59	59	1.49E+05	1.42E+05	5.11%		1.08E+05	8.59E+04	26.10%		7.71E+06	7.18E+06	7.31%
H17D-H60	60	1.46E+05	1.40E+05	4.71%		9.48E+04	1.08E+05	-12.41%		6.70E+06	7.20E+06	-6.94%
H17D-H61	61 *****	1.42E+05	1.53E+05	-6.95%	*****	1.17E+05	1.01E+05	15.69%	*****	7.40E+06	6.62E+06	11.75%
H17D-H62	62 *****	1.33E+05	1.39E+05	-4.75%	*****	9.91E+04	1.09E+05	-8.86%	*****	7.09E+06	6.52E+06	8.67%
H17D-H63	63	1.50E+05	1.43E+05	5.43%		1.08E+05	1.10E+05	-1.20%		7.14E+06	6.97E+06	2.52%
H17D-H64	64	1.48E+05	1.41E+05	4.40%		9.37E+04	8.94E+04	4.81%		7.34E+06	7.21E+06	1.76%
H17D-H65	65	1.38E+05	1.41E+05	-2.01%		1.06E+05	1.18E+05	-10.20%		6.86E+06	6.91E+06	-0.74%
H17D-H66	66	1.36E+05	1.31E+05	3.43%		1.01E+05	9.79E+04	2.97%		5.88E+06	5.86E+06	0.38%
H17D-H67	67	1.41E+05	1.43E+05	-1.12%		1.19E+05	9.52E+04	24.97%		6.87E+06	6.92E+06	-0.71%
H17D-H68	68	1.44E+05	1.32E+05	8.85%		1.13E+05	1.01E+05	12.17%		5.99E+06	6.27E+06	-4.39%
H17D-H69	69	1.41E+05	1.38E+05	1.96%		1.09E+05	1.16E+05	-6.05%		6.13E+06	6.42E+06	-4.56%
H17F-R05	70	1.39E+05	1.37E+05	1.58%		1.07E+05	1.09E+05	-1.98%		6.95E+06	7.34E+06	-5.25%
H17F-H71	71	1.39E+05	1.38E+05	1.18%		1.21E+05	9.55E+04	26.87%		7.10E+06	6.95E+06	2.08%
H17F-H72	72	1.36E+05	1.36E+05	-0.08%		1.14E+05	9.04E+04	25.89%		5.76E+06	5.87E+06	-1.80%
H17F-H73	73	1.39E+05	1.34E+05	3.41%		9.54E+04	1.08E+05	-12.01%		6.15E+06	6.31E+06	-2.57%
H17F-H74	74	1.38E+05	1.39E+05	-0.44%		9.46E+04	9.16E+04	3.21%		6.55E+06	6.64E+06	-1.28%
H17F-H75	75	1.44E+05	1.39E+05	3.26%		1.09E+05	1.17E+05	-7.27%		6.87E+06	6.15E+06	11.74%
H17F-H76	76 *****	1.72E+03	1.37E+05	-98.74%	*****	0.00E+00	9.35E+04	-100.00%	*****	7.19E+06	6.44E+06	11.70%
H17F-H77	77	1.37E+05	1.31E+05	4.14%		1.02E+05	8.24E+04	23.41%		6.50E+06	5.98E+06	8.70%
H17F-H78	78	1.45E+05	1.39E+05	4.26%		1.16E+05	1.04E+05	11.48%		7.15E+06	6.59E+06	8.56%
H17F-H79	79	1.45E+05	1.39E+05	4.12%		9.51E+04	1.02E+05	-6.79%		7.25E+06	6.91E+06	5.05%
H17F-H80	80	1.38E+05	1.32E+05	4.72%		9.48E+04	9.07E+04	4.57%		6.20E+06	7.02E+06	-11.69%
Total Test Particles (80)												
Average		1.40E+05	1.40E+05	-1.26E-04		1.05E+05	1.02E+05	3.04E-02		6.92E+06	6.72E+06	3.30E-02
Standard Deviation		1.89E+04	5.10E+03	1.33E-01		1.63E+04	8.68E+03	1.75E-01		5.48E+05	4.36E+05	9.15E-02
Difference based on Pre and Post averages				-3.28E-04				2.59E-02				3.02E-02
Lower two sigma limit				-26.71%				-31.93%				-14.99%

Table 1 (cont)

Isotope	Eu-154 Post	Eu-154 Pre	Eu-154 Delta	Eu-155 Post	Eu-155 Pre	Eu-155 Delta	Ru-106 Post	Ru-106 Pre	Ru-106 Delta
Average (μCi)	3.78E+00	3.79E+00	0.00	2.83E+00	2.76E+00	0.07	1.87E+02	1.82E+02	5.48
Total diff (μCi)			-0.10			5.72			438.05
Non-releasing Particles (76)									
Average	1.43E+05	1.40E+05	2.19E-02	1.07E+05	1.02E+05	5.02E-02	6.91E+06	6.73E+06	2.92E-02
Standard Deviation	5.39E+03	5.00E+03	2.90E-02	9.28E+03	8.72E+03	1.19E-01	5.58E+05	4.44E+05	9.23E-02
Difference based on Pre and Post averages			2.16E-02			4.38E-02			2.64E-02
Lower two sigma limit			-3.61%			-18.76%			-15.53%
Releasing Particles (4)									
Average	8.64E+04	1.40E+05	-3.88E-01	6.43E+04	1.01E+05	-3.88E-01	7.11E+06	6.58E+06	8.20E-02
Standard Deviation	7.08E+04	6.27E+04	4.54E-01	5.20E+04	4.59E+04	4.27E-01	3.18E+06	2.95E+06	5.03E-02
Difference based on Pre and Post averages			-3.83E-01			-3.61E-01			8.08E-02
Lower two sigma limit			-129.61%			-124.30%			-1.87%
Total Corrected for Cerium Balance (80)									
Average (μCi)	3.72E+00	3.79E+00	-0.07	2.78E+00	2.76E+00	0.02	1.84E+02	1.82E+02	2.27
Total diff (μCi)			-5.28			1.85			181.90
Non-releasing Particles Corrected for Cerium Balance (76)									
Average (μCi)	3.80E+00	3.78E+00	0.02	2.83E+00	2.76E+00	0.07	1.84E+02	1.82E+02	1.65
Total diff (μCi)			1.26			5.50			125.26
Releasing Corrected for Cerium Balance (4)									
Average	2.26E+00	3.79E+00	-1.53	1.68E+00	2.72E+00	-1.04	1.86E+02	1.78E+02	8.18
Total diff (μCi)			-6.11			-4.16			32.72

Table 2. 1400°C particle pre- and postheating inventories. Activities are in Bq corrected to 5 Feb 1986.

Isotope		Cs-134			Cs-137			Ce-144		
		Post	Pre	Delta	Post	Pre	Delta	Post	Pre	Delta
Particle ID	**Particle**									
H18B-H01	1	9.29E+06	9.69E+06	-4.06%	3.71E+06	3.79E+06	-2.04%	9.74E+07	9.75E+07	-0.10%
H18B-H02	2	8.72E+06	8.73E+06	-0.12%	3.38E+06	3.43E+06	-1.40%	8.64E+07	8.97E+07	-3.70%
H18B-H03	3	9.80E+06	1.02E+07	-3.51%	3.87E+06	3.97E+06	-2.45%	1.01E+08	9.99E+07	1.46%
H18B-H04	4	9.10E+06	9.39E+06	-3.08%	3.57E+06	3.66E+06	-2.48%	9.45E+07	9.39E+07	0.61%
H18B-H05	5	9.09E+06	9.31E+06	-2.29%	3.56E+06	3.66E+06	-2.61%	9.73E+07	9.37E+07	3.80%
H18B-H06	6	9.24E+06	9.65E+06	-4.24%	3.69E+06	3.79E+06	-2.75%	9.68E+07	9.69E+07	-0.06%
H18B-H07	7	8.62E+06	8.80E+06	-2.10%	3.38E+06	3.45E+06	-1.93%	9.00E+07	9.10E+07	-1.10%
H18B-H08	8	8.62E+06	8.82E+06	-2.30%	3.35E+06	3.45E+06	-2.97%	8.86E+07	8.91E+07	-0.65%
H18B-H09	9	8.86E+06	9.12E+06	-2.85%	3.49E+06	3.56E+06	-1.97%	9.41E+07	9.19E+07	2.42%
H18B-H10	10	9.63E+06	9.97E+06	-3.49%	3.83E+06	3.92E+06	-2.15%	1.03E+08	1.03E+08	0.41%
H18B-H11	11	9.02E+06	9.36E+06	-3.61%	3.55E+06	3.66E+06	-3.07%	9.32E+07	9.33E+07	-0.15%
H18B-H12	12	8.36E+06	8.53E+06	-1.95%	3.30E+06	3.36E+06	-1.53%	9.06E+07	8.80E+07	2.87%
H18B-H13	13	9.36E+06	9.48E+06	-1.35%	3.63E+06	3.70E+06	-2.11%	9.56E+07	9.55E+07	0.04%
H18B-H14	14	9.78E+06	1.01E+07	-3.09%	3.86E+06	3.95E+06	-2.11%	1.05E+08	1.01E+08	4.43%
H18B-H15	15	9.68E+06	9.91E+06	-2.29%	3.80E+06	3.88E+06	-2.07%	1.01E+08	1.00E+08	0.98%
H18B-H16	16	8.94E+06	9.04E+06	-1.05%	3.52E+06	3.60E+06	-2.15%	9.28E+07	9.35E+07	-0.79%
H18B-H17	17	9.34E+06	9.38E+06	-0.36%	3.64E+06	3.71E+06	-1.96%	9.74E+07	9.58E+07	1.73%
H18B-H18	18	9.71E+06	9.93E+06	-2.22%	3.87E+06	3.95E+06	-2.07%	1.01E+08	1.01E+08	-0.29%
H18F-H21	19	1.01E+07	1.02E+07	-0.89%	3.80E+06	3.91E+06	-2.84%	9.99E+07	1.01E+08	-0.94%
H18F-H22	20	9.42E+06	9.45E+06	-0.35%	3.56E+06	3.65E+06	-2.65%	9.68E+07	9.39E+07	3.12%
H18F-H23	21	1.01E+07	1.05E+07	-4.15%	3.83E+06	4.01E+06	-4.49%	1.01E+08	1.03E+08	-2.21%
H18F-H24	22	9.54E+06	9.80E+06	-2.69%	3.65E+06	3.76E+06	-2.97%	9.81E+07	9.47E+07	3.56%
H18F-H25	23	9.39E+06	9.38E+06	0.15%	3.60E+06	3.69E+06	-2.42%	9.42E+07	9.56E+07	-1.56%
H18F-H26	24	9.28E+06	9.57E+06	-3.00%	3.61E+06	3.67E+06	-1.74%	9.69E+07	9.59E+07	1.08%
H18F-H27	25	9.38E+06	9.70E+06	-3.26%	3.62E+06	3.71E+06	-2.28%	9.63E+07	9.77E+07	-1.48%
H18F-H28	26	9.41E+06	9.63E+06	-2.32%	3.60E+06	3.74E+06	-3.72%	9.57E+07	9.22E+07	3.79%
H18F-H29	27	9.40E+06	9.63E+06	-2.45%	3.60E+06	3.72E+06	-3.13%	9.45E+07	9.55E+07	-1.07%
H18F-H30	28	9.95E+06	1.03E+07	-3.23%	3.83E+06	3.97E+06	-3.63%	1.01E+08	9.99E+07	1.15%
H18F-H31	29	8.85E+06	9.07E+06	-2.36%	3.41E+06	3.52E+06	-3.23%	8.88E+07	8.83E+07	0.58%

Table 2 (cont)

Isotope		Cs-134			Cs-137			Ce-144		
		Post	Pre	Delta	Post	Pre	Delta	Post	Pre	Delta
Particle ID	**Particle**									
H18F-H32	30	9.27E+06	9.53E+06	-2.66%	3.54E+06	3.66E+06	-3.39%	9.33E+07	9.35E+07	-0.17%
H18D-H41	31	9.33E+06	9.54E+06	-2.25%	3.61E+06	3.74E+06	-3.38%	9.77E+07	9.44E+07	3.50%
H18D-H42	32	9.20E+06	9.35E+06	-1.67%	3.56E+06	3.66E+06	-2.72%	9.47E+07	9.34E+07	1.48%
H18D-H43	33	9.80E+06	1.02E+07	-3.50%	3.84E+06	3.94E+06	-2.56%	1.01E+08	1.00E+08	1.28%
H18D-H44	34	9.69E+06	9.91E+06	-2.23%	3.79E+06	3.86E+06	-1.92%	1.03E+08	1.00E+08	2.92%
H18D-H45	35	9.65E+06	1.00E+07	-3.71%	3.77E+06	3.85E+06	-2.07%	9.91E+07	9.89E+07	0.25%
H18D-H46	36	9.86E+06	1.01E+07	-2.43%	3.82E+06	3.93E+06	-2.75%	1.02E+08	1.01E+08	0.55%
H18D-H47	37	9.53E+06	9.66E+06	-1.37%	3.64E+06	3.71E+06	-2.01%	9.72E+07	9.63E+07	0.95%
H18D-H48	38	9.20E+06	9.57E+06	-3.93%	3.63E+06	3.72E+06	-2.56%	9.50E+07	9.61E+07	-1.13%
H18D-H49	39	8.76E+06	9.20E+06	-4.76%	3.46E+06	3.55E+06	-2.53%	9.21E+07	9.20E+07	0.08%
H18D-H50	40	9.25E+06	9.39E+06	-1.55%	3.55E+06	3.67E+06	-3.20%	9.60E+07	9.44E+07	1.73%
H18D-H51	41	9.21E+06	9.42E+06	-2.24%	3.55E+06	3.66E+06	-2.90%	9.23E+07	9.42E+07	-2.01%
H18D-H52	42	9.25E+06	9.63E+06	-3.94%	3.66E+06	3.70E+06	-1.26%	9.87E+07	9.63E+07	2.54%
H18D-H53	43	9.44E+06	9.46E+06	-0.24%	3.62E+06	3.67E+06	-1.34%	9.57E+07	9.48E+07	0.88%
H18D-H54	44	9.17E+06	9.24E+06	-0.72%	3.52E+06	3.57E+06	-1.31%	9.31E+07	9.14E+07	1.88%
H18D-H55	45	9.46E+06	9.56E+06	-1.07%	3.65E+06	3.73E+06	-2.04%	9.37E+07	9.48E+07	-1.10%
H18D-H56	46	9.82E+06	1.00E+07	-1.88%	3.82E+06	3.93E+06	-2.90%	1.00E+08	9.97E+07	0.73%
H18D-H57	47	9.84E+06	9.93E+06	-0.96%	3.81E+06	3.87E+06	-1.40%	9.97E+07	1.02E+08	-2.62%
H18D-H58	48	9.73E+06	9.88E+06	-1.58%	3.82E+06	3.90E+06	-2.03%	1.01E+08	1.01E+08	0.72%
H18D-H59	49	9.28E+06	9.45E+06	-1.75%	3.59E+06	3.65E+06	-1.69%	9.50E+07	9.33E+07	1.80%
H18D-H60	50	9.64E+06	9.91E+06	-2.73%	3.78E+06	3.86E+06	-2.19%	1.01E+08	9.85E+07	2.64%
H18D-H61	51	8.76E+06	8.73E+06	0.26%	3.38E+06	3.44E+06	-1.59%	9.07E+07	8.99E+07	0.92%
H18D-H62	52	9.66E+06	9.60E+06	0.56%	3.64E+06	3.73E+06	-2.59%	9.79E+07	9.59E+07	2.05%
H18D-H63	53	9.26E+06	9.55E+06	-3.00%	3.63E+06	3.72E+06	-2.40%	9.52E+07	9.54E+07	-0.13%
H18D-H64	54	9.10E+06	9.41E+06	-3.21%	3.54E+06	3.62E+06	-2.05%	9.32E+07	9.35E+07	-0.41%
H18D-H65	55	9.55E+06	9.56E+06	-0.11%	3.63E+06	3.73E+06	-2.66%	9.58E+07	9.38E+07	2.13%
H18D-H66	56	9.18E+06	9.38E+06	-2.10%	3.60E+06	3.69E+06	-2.53%	9.55E+07	9.31E+07	2.54%
H18D-H67	57	9.66E+06	1.00E+07	-3.82%	3.80E+06	3.91E+06	-3.04%	1.02E+08	1.00E+08	1.62%
H18D-H68	58	9.28E+06	9.58E+06	-3.06%	3.60E+06	3.71E+06	-3.01%	9.38E+07	9.39E+07	-0.16%

Table 2 (cont)

Isotope		Cs-134			Cs-137			Ce-144		
		Post	Pre	Delta	Post	Pre	Delta	Post	Pre	Delta
Particle ID	**Particle**									
H18D-H69	59	9.53E+06	9.52E+06	0.04%	3.64E+06	3.71E+06	-1.90%	9.67E+07	9.58E+07	0.98%
H18D-H70	60	9.64E+06	9.70E+06	-0.64%	3.75E+06	3.84E+06	-2.16%	9.83E+07	9.77E+07	0.69%
H18F-H71	61	9.71E+06	9.64E+06	0.76%	3.66E+06	3.77E+06	-2.84%	9.82E+07	9.74E+07	0.87%
H18F-H72	62	9.99E+06	1.03E+07	-3.12%	3.85E+06	3.95E+06	-2.66%	1.02E+08	1.01E+08	1.53%
H18F-H73	63	9.56E+06	9.75E+06	-1.90%	3.65E+06	3.77E+06	-3.15%	9.70E+07	9.48E+07	2.29%
H18F-H74	64	9.32E+06	9.55E+06	-2.43%	3.59E+06	3.67E+06	-2.21%	9.25E+07	9.44E+07	-1.94%
H18F-H75	65	9.41E+06	9.54E+06	-1.35%	3.57E+06	3.68E+06	-3.03%	9.52E+07	9.59E+07	-0.82%
H18F-H76	66	9.57E+06	9.72E+06	-1.55%	3.65E+06	3.75E+06	-2.43%	9.39E+07	9.78E+07	-3.93%
H18F-H77	67	9.98E+06	9.95E+06	0.30%	3.79E+06	3.87E+06	-2.21%	1.00E+08	1.02E+08	-1.05%
H18F-H78	68	9.67E+06	9.90E+06	-2.30%	3.67E+06	3.79E+06	-2.97%	9.76E+07	1.00E+08	-2.87%
H18F-H79	69	9.92E+06	1.01E+07	-2.04%	3.86E+06	3.96E+06	-2.46%	1.02E+08	1.03E+08	-1.63%
H18F-H80	70	9.41E+06	9.42E+06	-0.08%	3.59E+06	3.69E+06	-2.86%	9.65E+07	9.66E+07	-0.08%
H18F-H81	71	9.88E+06	1.03E+07	-3.94%	3.79E+06	3.93E+06	-3.50%	9.97E+07	9.93E+07	0.42%
H18F-H82	72	9.46E+06	9.68E+06	-2.29%	3.64E+06	3.75E+06	-2.87%	9.58E+07	9.62E+07	-0.39%
H18F-H83	73	9.83E+06	1.02E+07	-3.41%	3.83E+06	3.98E+06	-3.80%	1.01E+08	1.01E+08	-0.63%
H18F-H84	74	9.62E+06	9.64E+06	-0.13%	3.63E+06	3.74E+06	-2.82%	9.81E+07	9.79E+07	0.19%
H18F-H85	75	9.58E+06	9.85E+06	-2.77%	3.70E+06	3.83E+06	-3.40%	9.70E+07	9.61E+07	0.90%
H18F-H86	76	9.24E+06	9.51E+06	-2.84%	3.58E+06	3.68E+06	-2.84%	9.44E+07	9.38E+07	0.61%
H18F-H87	77	9.30E+06	9.52E+06	-2.30%	3.57E+06	3.70E+06	-3.57%	9.53E+07	9.31E+07	2.37%
H18F-H88	78	9.34E+06	9.60E+06	-2.73%	3.58E+06	3.70E+06	-3.19%	9.68E+07	9.49E+07	1.91%
H18F-H89	79	1.00E+07	1.01E+07	-0.11%	3.78E+06	3.91E+06	-3.28%	1.01E+08	1.01E+08	-0.16%
H18F-H90	80	9.44E+06	9.72E+06	-2.89%	3.62E+06	3.72E+06	-2.55%	9.66E+07	9.49E+07	1.80%
Total Test Particles (80)										
Column Average		9.43E+06	9.63E+06	-2.10E-02	3.65E+06	3.75E+06	-2.55E-02	9.68E+07	9.62E+07	5.55E-03
Standard Deviation		3.61E+05	3.86E+05	1.31E-02	1.34E+05	1.43E+05	6.44E-03	3.70E+06	3.62E+06	1.73E-02
Delta based on Pre and Post averages				-2.11E-02			-2.55E-02			5.44E-03
Lower two sigma limit				-4.73%			-3.83%			-2.91%

Table 2 (cont)

Isotope	Cs-134			Cs-137			Ce-144		
	Post	Pre	Delta	Post	Pre	Delta	Post	Pre	Delta
Average (μCi)	2.55E+02	2.60E+02	-5.50	9.86E+01	1.01E+02	-2.58	2.62E+03	2.60E+03	14.14
Total diff (μCi)			-440.04			-206.73			1131.00
Total Corrected for Cerium Balance (80)									
Average (μCi)	2.53E+02	2.60E+02	6.88	9.81E+01	1.01E+02	3.12	2.60E+03	2.60E+03	0.00
Total diff (μCi)			550.24			249.39			0.00

Table 2 (cont)

Isotope		Eu-154			Eu-155			Ru-106		
		Post	Pre	Delta	Post	Pre	Delta	Post	Pre	Delta
Particle ID	**Particle**									
H18B-H01	1	1.43E+05	1.42E+05	0.88%	1.03E+05	1.05E+05	-2.41%	7.18E+06	6.63E+06	8.39%
H18B-H02	2	1.34E+05	1.27E+05	5.30%	9.32E+04	9.97E+04	-6.56%	6.64E+06	5.88E+06	12.86%
H18B-H03	3	1.48E+05	1.53E+05	-3.09%	1.18E+05	1.09E+05	8.76%	7.34E+06	6.42E+06	14.28%
H18B-H04	4	1.38E+05	1.42E+05	-3.06%	1.05E+05	8.16E+04	28.84%	6.87E+06	5.48E+06	25.36%
H18B-H05	5	1.41E+05	1.32E+05	6.36%	1.01E+05	9.49E+04	6.00%	5.97E+06	6.28E+06	-4.89%
H18B-H06	6	1.43E+05	1.37E+05	4.29%	9.93E+04	9.54E+04	4.05%	6.93E+06	6.48E+06	7.04%
H18B-H07	7	1.31E+05	1.27E+05	2.58%	8.96E+04	1.06E+05	-15.52%	6.85E+06	5.97E+06	14.79%
H18B-H08	8	1.33E+05	1.27E+05	4.93%	9.21E+04	9.51E+04	-3.12%	6.49E+06	5.59E+06	16.09%
H18B-H09	9	1.38E+05	1.32E+05	4.45%	9.68E+04	9.57E+04	1.17%	6.72E+06	6.28E+06	6.93%
H18B-H10	10	1.48E+05	1.45E+05	2.62%	1.09E+05	1.12E+05	-3.16%	6.48E+06	6.73E+06	-3.69%
H18B-H11	11	1.42E+05	1.34E+05	5.57%	1.14E+05	9.54E+04	19.95%	7.07E+06	6.27E+06	12.74%
H18B-H12	12	1.34E+05	1.27E+05	5.69%	1.05E+05	9.74E+04	7.57%	6.41E+06	6.02E+06	6.43%
H18B-H13	13	1.42E+05	1.37E+05	3.77%	9.94E+04	9.21E+04	7.89%	7.14E+06	6.85E+06	4.26%
H18B-H14	14	1.50E+05	1.41E+05	5.95%	1.05E+05	9.62E+04	9.43%	7.01E+06	7.17E+06	-2.21%
H18B-H15	15	1.46E+05	1.47E+05	-0.82%	1.14E+05	9.92E+04	14.69%	6.76E+06	7.14E+06	-5.37%
H18B-H16	16	1.39E+05	1.32E+05	4.96%	9.70E+04	1.02E+05	-4.79%	6.24E+06	6.46E+06	-3.31%
H18B-H17	17	1.44E+05	1.37E+05	5.19%	1.00E+05	9.10E+04	9.80%	7.16E+06	6.66E+06	7.61%
H18B-H18	18	1.49E+05	1.48E+05	0.32%	1.04E+05	1.02E+05	1.81%	7.87E+06	6.77E+06	16.30%
H18F-H21	19	1.43E+05	1.45E+05	-1.47%	9.68E+04	1.09E+05	-10.99%	6.99E+06	7.01E+06	-0.34%
H18F-H22	20	1.38E+05	1.34E+05	3.09%	1.01E+05	1.07E+05	-5.55%	6.45E+06	6.77E+06	-4.74%
H18F-H23	21	1.54E+05	1.42E+05	8.99%	1.13E+05	1.01E+05	12.31%	6.98E+06	6.29E+06	11.02%
H18F-H24	22	1.41E+05	1.41E+05	0.02%	9.66E+04	9.82E+04	-1.68%	7.20E+06	6.23E+06	15.52%
H18F-H25	23	1.39E+05	1.36E+05	2.35%	1.06E+05	1.06E+05	-0.59%	6.51E+06	6.46E+06	0.77%
H18F-H26	24	1.39E+05	1.37E+05	1.37%	1.04E+05	1.08E+05	-4.39%	6.65E+06	7.12E+06	-6.53%
H18F-H27	25	1.40E+05	1.41E+05	-0.75%	1.02E+05	1.04E+05	-1.30%	6.88E+06	6.49E+06	6.04%
H18F-H28	26	1.40E+05	1.38E+05	1.33%	9.92E+04	1.02E+05	-2.77%	6.62E+06	6.34E+06	4.49%
H18F-H29	27	1.45E+05	1.36E+05	6.10%	9.39E+04	1.00E+05	-6.15%	5.90E+06	6.81E+06	-13.36%
H18F-H30	28	1.52E+05	1.45E+05	4.80%	1.01E+05	1.12E+05	-9.15%	7.44E+06	6.86E+06	8.50%
H18F-H31	29	1.32E+05	1.29E+05	2.32%	9.25E+04	9.66E+04	-4.20%	7.34E+06	6.11E+06	20.14%

Table 2 (cont)

Isotope		Eu-154			Eu-155			Ru-106		
		Post	Pre	Delta	Post	Pre	Delta	Post	Pre	Delta
Particle ID	**Particle**									
H18F-H32	30	1.37E+05	1.36E+05	0.86%	9.79E+04	9.45E+04	3.59%	7.27E+06	6.43E+06	13.08%
H18D-H41	31	1.40E+05	1.41E+05	-1.16%	9.41E+04	9.14E+04	2.96%	6.79E+06	6.46E+06	5.17%
H18D-H42	32	1.38E+05	1.41E+05	-1.82%	1.27E+05	8.09E+04	57.45%	6.92E+06	6.74E+06	2.63%
H18D-H43	33	1.47E+05	1.43E+05	2.96%	1.17E+05	1.10E+05	5.74%	8.06E+06	6.47E+06	24.56%
H18D-H44	34	1.46E+05	1.41E+05	3.51%	1.06E+05	1.17E+05	-8.68%	7.10E+06	7.05E+06	0.76%
H18D-H45	35	1.46E+05	1.47E+05	-0.72%	1.14E+05	9.97E+04	13.96%	7.12E+06	6.78E+06	4.98%
H18D-H46	36	1.51E+05	1.43E+05	6.05%	1.06E+05	1.06E+05	0.21%	7.00E+06	6.77E+06	3.28%
H18D-H47	37	1.39E+05	1.43E+05	-3.19%	1.18E+05	1.07E+05	10.96%	7.27E+06	6.40E+06	13.51%
H18D-H48	38	1.44E+05	1.35E+05	6.29%	1.17E+05	1.04E+05	13.26%	7.22E+06	6.07E+06	18.96%
H18D-H49	39	1.32E+05	1.33E+05	-0.53%	1.05E+05	8.71E+04	20.44%	6.27E+06	6.58E+06	-4.70%
H18D-H50	40	1.41E+05	1.34E+05	4.99%	9.66E+04	9.66E+04	-0.01%	7.07E+06	7.11E+06	-0.54%
H18D-H51	41	1.41E+05	1.33E+05	6.13%	1.05E+05	9.37E+04	11.83%	7.39E+06	6.39E+06	15.60%
H18D-H52	42	1.43E+05	1.33E+05	7.43%	1.19E+05	9.48E+04	25.93%	6.33E+06	6.87E+06	-7.88%
H18D-H53	43	1.38E+05	1.35E+05	1.91%	1.07E+05	1.06E+05	0.40%	7.65E+06	6.79E+06	12.64%
H18D-H54	44	1.38E+05	1.35E+05	2.30%	1.03E+05	9.99E+04	3.49%	5.97E+06	6.43E+06	-7.07%
H18D-H55	45	1.42E+05	1.41E+05	0.82%	1.01E+05	1.01E+05	0.04%	6.22E+06	6.40E+06	-2.77%
H18D-H56	46	1.45E+05	1.47E+05	-1.02%	1.09E+05	1.32E+05	-17.25%	6.68E+06	6.78E+06	-1.45%
H18D-H57	47	1.48E+05	1.45E+05	1.69%	1.07E+05	1.16E+05	-7.09%	7.32E+06	7.18E+06	1.99%
H18D-H58	48	1.51E+05	1.48E+05	2.37%	1.07E+05	1.09E+05	-1.87%	6.93E+06	7.51E+06	-7.67%
H18D-H59	49	1.40E+05	1.43E+05	-1.86%	1.04E+05	9.89E+04	5.34%	7.24E+06	6.22E+06	16.36%
H18D-H60	50	1.45E+05	1.40E+05	3.58%	1.09E+05	1.12E+05	-3.20%	7.32E+06	6.99E+06	4.75%
H18D-H61	51	1.27E+05	1.27E+05	0.38%	1.03E+05	8.62E+04	19.90%	6.42E+06	5.59E+06	14.88%
H18D-H62	52	1.43E+05	1.44E+05	-0.34%	1.22E+05	1.17E+05	4.17%	7.25E+06	6.14E+06	17.97%
H18D-H63	53	1.38E+05	1.39E+05	-1.06%	1.09E+05	9.86E+04	10.68%	6.94E+06	6.24E+06	11.14%
H18D-H64	54	1.38E+05	1.34E+05	2.43%	1.11E+05	9.45E+04	17.39%	6.39E+06	6.35E+06	0.72%
H18D-H65	55	1.41E+05	1.42E+05	-0.93%	1.13E+05	1.15E+05	-1.81%	6.91E+06	7.31E+06	-5.37%
H18D-H66	56	1.39E+05	1.41E+05	-1.29%	9.99E+04	1.05E+05	-4.77%	6.45E+06	6.25E+06	3.24%
H18D-H67	57	1.46E+05	1.47E+05	-0.85%	1.30E+05	1.08E+05	19.98%	7.71E+06	6.61E+06	16.70%
H18D-H68	58	1.42E+05	1.37E+05	3.20%	1.10E+05	9.50E+04	16.23%	7.07E+06	6.36E+06	11.14%

Table 2 (cont)

Isotope		Eu-154			Eu-155			Ru-106		
		Post	Pre	Delta	Post	Pre	Delta	Post	Pre	Delta
Particle ID	**Particle**									
H18D-H69	59	1.41E+05	1.36E+05	4.02%	1.08E+05	1.04E+05	3.84%	6.71E+06	6.79E+06	-1.19%
H18D-H70	60	1.49E+05	1.43E+05	4.55%	1.04E+05	1.26E+05	-17.56%	6.82E+06	6.76E+06	0.91%
H18F-H71	61	1.42E+05	1.33E+05	6.68%	9.86E+04	9.30E+04	6.03%	7.31E+06	7.02E+06	4.10%
H18F-H72	62	1.50E+05	1.41E+05	6.39%	1.10E+05	9.72E+04	13.57%	7.14E+06	6.75E+06	5.81%
H18F-H73	63	1.41E+05	1.38E+05	1.72%	1.02E+05	1.16E+05	-12.17%	7.36E+06	6.35E+06	15.97%
H18F-H74	64	1.42E+05	1.38E+05	3.32%	1.06E+05	1.07E+05	-1.15%	6.71E+06	6.65E+06	0.88%
H18F-H75	65	1.41E+05	1.34E+05	4.82%	1.01E+05	1.02E+05	-0.36%	6.37E+06	6.59E+06	-3.21%
H18F-H76	66	1.40E+05	1.41E+05	-0.72%	1.04E+05	8.64E+04	20.36%	6.80E+06	6.98E+06	-2.59%
H18F-H77	67	1.46E+05	1.52E+05	-4.11%	1.07E+05	1.12E+05	-5.16%	6.90E+06	7.47E+06	-7.72%
H18F-H78	68	1.46E+05	1.37E+05	6.72%	1.24E+05	9.82E+04	26.11%	6.08E+06	6.65E+06	-8.57%
H18F-H79	69	1.49E+05	1.45E+05	3.40%	1.05E+05	1.07E+05	-1.81%	7.85E+06	7.28E+06	7.90%
H18F-H80	70	1.39E+05	1.39E+05	-0.45%	9.98E+04	1.12E+05	-11.00%	6.68E+06	6.21E+06	7.66%
H18F-H81	71	1.48E+05	1.47E+05	0.89%	1.11E+05	1.03E+05	7.20%	7.93E+06	6.93E+06	14.41%
H18F-H82	72	1.43E+05	1.52E+05	-6.12%	9.97E+04	1.09E+05	-8.84%	6.91E+06	7.52E+06	-8.20%
H18F-H83	73	1.51E+05	1.48E+05	2.18%	1.10E+05	1.21E+05	-8.96%	7.05E+06	6.92E+06	1.94%
H18F-H84	74	1.36E+05	1.39E+05	-2.48%	1.03E+05	1.04E+05	-0.76%	7.39E+06	6.42E+06	15.16%
H18F-H85	75	1.45E+05	1.38E+05	4.76%	1.06E+05	1.03E+05	2.72%	7.45E+06	6.28E+06	18.56%
H18F-H86	76	1.46E+05	1.34E+05	9.04%	1.15E+05	9.51E+04	20.89%	6.54E+06	6.36E+06	2.70%
H18F-H87	77	1.39E+05	1.35E+05	2.72%	1.16E+05	1.01E+05	14.93%	6.00E+06	5.74E+06	4.46%
H18F-H88	78	1.42E+05	1.33E+05	6.84%	1.09E+05	1.01E+05	8.41%	7.10E+06	6.55E+06	8.53%
H18F-H89	79	1.49E+05	1.49E+05	0.55%	1.11E+05	1.20E+05	-7.90%	7.57E+06	7.40E+06	2.22%
H18F-H90	80	1.42E+05	1.36E+05	4.03%	1.03E+05	9.99E+04	2.61%	7.72E+06	6.92E+06	11.45%
Total Test Particles (80)										
Average		1.42E+05	1.39E+05	2.31E-02	1.06E+05	1.03E+05	4.00E-02	6.93E+06	6.59E+06	5.54E-02
Standard Deviation		5.33E+03	6.14E+03	3.21E-02	8.07E+03	9.40E+03	1.20E-01	4.80E+05	4.38E+05	8.74E-02
Difference based on Pre and Post averages				2.23E-02			3.23E-02			5.20E-02
Lower two sigma limit				-4.11%			-20.06%			-11.95%

Table 2 (cont)

Isotope	Eu-154			Eu-155			Ru-106		
	Post	Pre	Delta	Post	Pre	Delta	Post	Pre	Delta
	3.84E+00	3.76E+00	0.08	2.86E+00	2.77E+00	0.09	1.87E+02	1.78E+02	9.26
Total diff (μCi)			6.72			7.16			740.81
Total Corrected for Cerium Balance (80)									
Average (μCi)	3.82E+00	3.76E+00	-0.06	2.85E+00	2.77E+00	-0.07			
Total diff (μCi)			-5.06			-5.92			

Mean IPyC density	1.89 g/cm^3
Mean SiC thickness	33.8 μm
Mean SiC density	3.19 g/cm^3
Mean OPyC thickness	40.2 μm
Mean OPyC density	1.85 g/cm^3
Mean total diameter	639 μm
TRIGA FGR ^{85}Kr at 1100°C	2.6 x 10^{-7} R/B (before irradiation)
Burnup fissions per initial metal atom (FIMA)	67%
Average irradiation temp	809°C
Fast fluence	4.2 x 10^{25} n/m^2

The burnup was calculated initially as 78% FIMA.[7] A more accurate measurement was made by a gamma spectrometric analysis leading to a value of 67% FIMA. See Sect. 3.2.

The CCCTF particle holder for each test was composed of four separate particle trays stacked vertically and firmly held to the graphite fuel holder by a graphite retaining nut. The entire unit was held in the isothermal zone of the furnace for the test by a graphite support as shown in Fig. 4.

3.2 BURNUP ANALYSIS

The test plan originally called for burnup analysis by radiochemical methods. Because of funding limitations, the burnup was calculated by using the results of the postheating particle gamma spectrometry and comparing them to the expected fission yields. The burnup, 67% FIMA, is about 14% lower than first estimated. This analysis is detailed in Appendix A.

3.3 METALLOGRAPHY

Pretest metallography was performed on the HRB-17/-18 particles at GA. Particle appearance was as expected, with the particle coatings showing good structure. The results of this work are shown in Figs. 5 and 6.

ORNL-DWG-92-5160

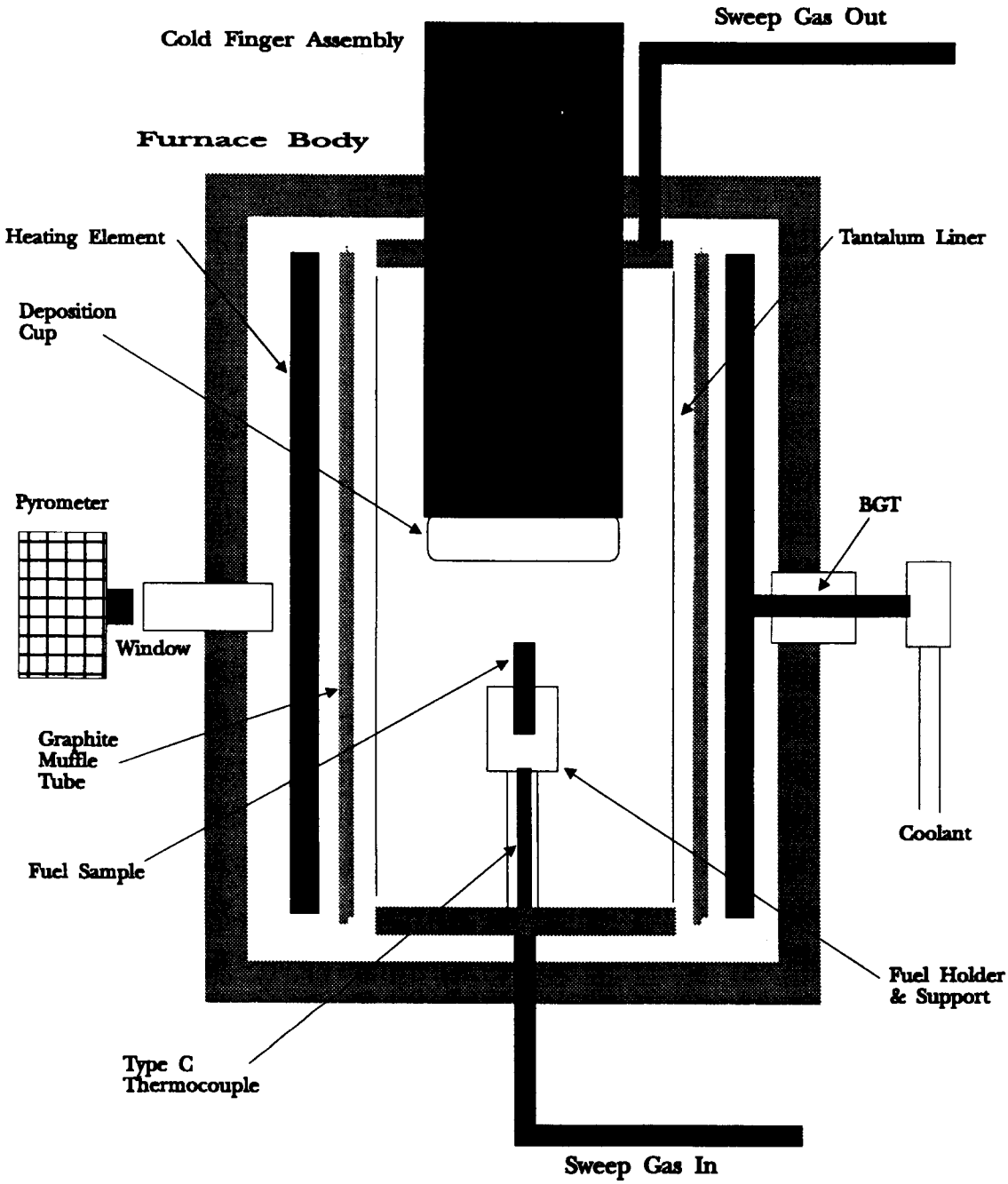

Fig. 4. Furnace internal geometry.

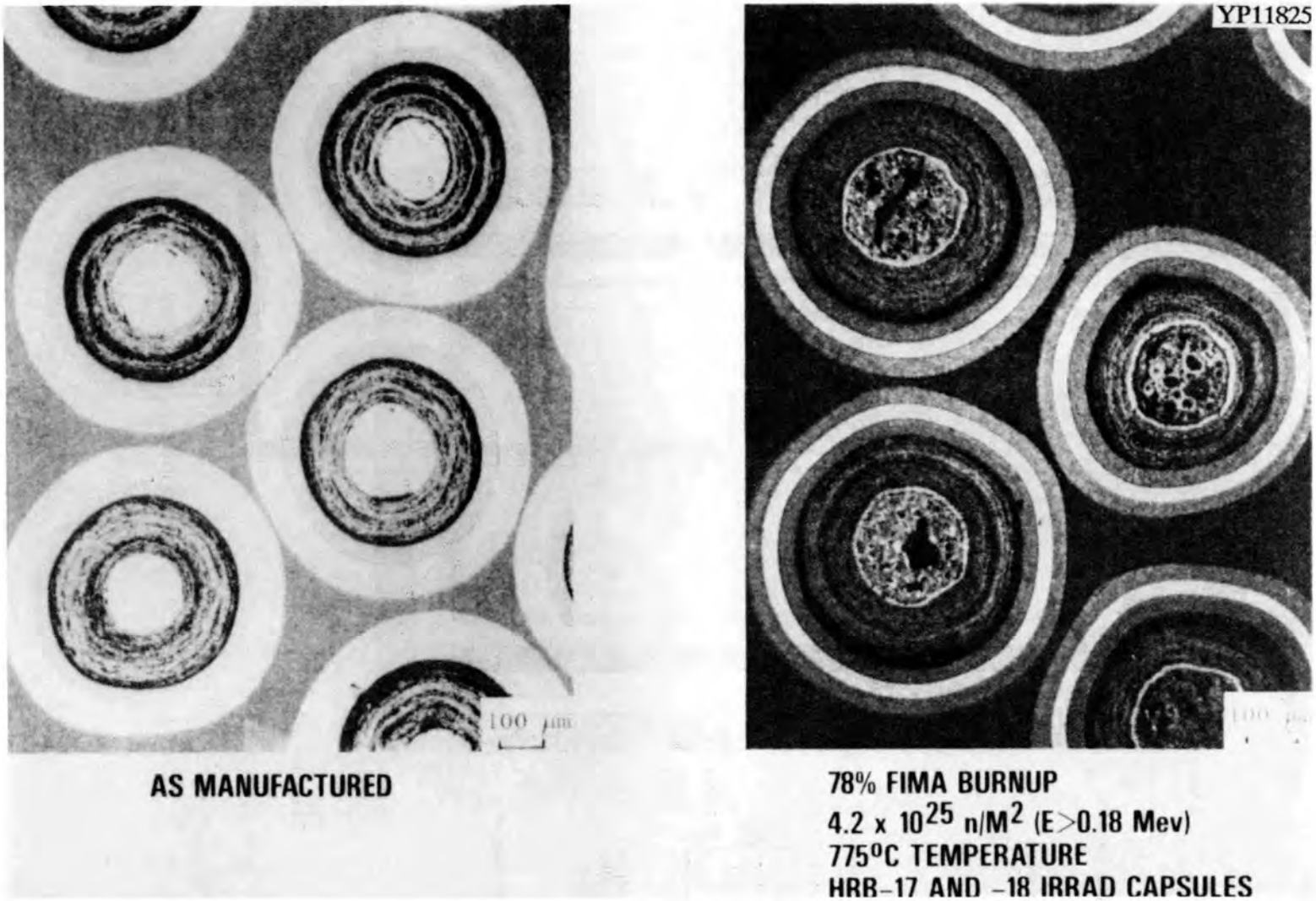

Fig. 5. HRB-17/-18 particle pretest metallography. This work was done at GA. Recent calculations indicate burnup was 68% rather than the initial estimate of 78%.

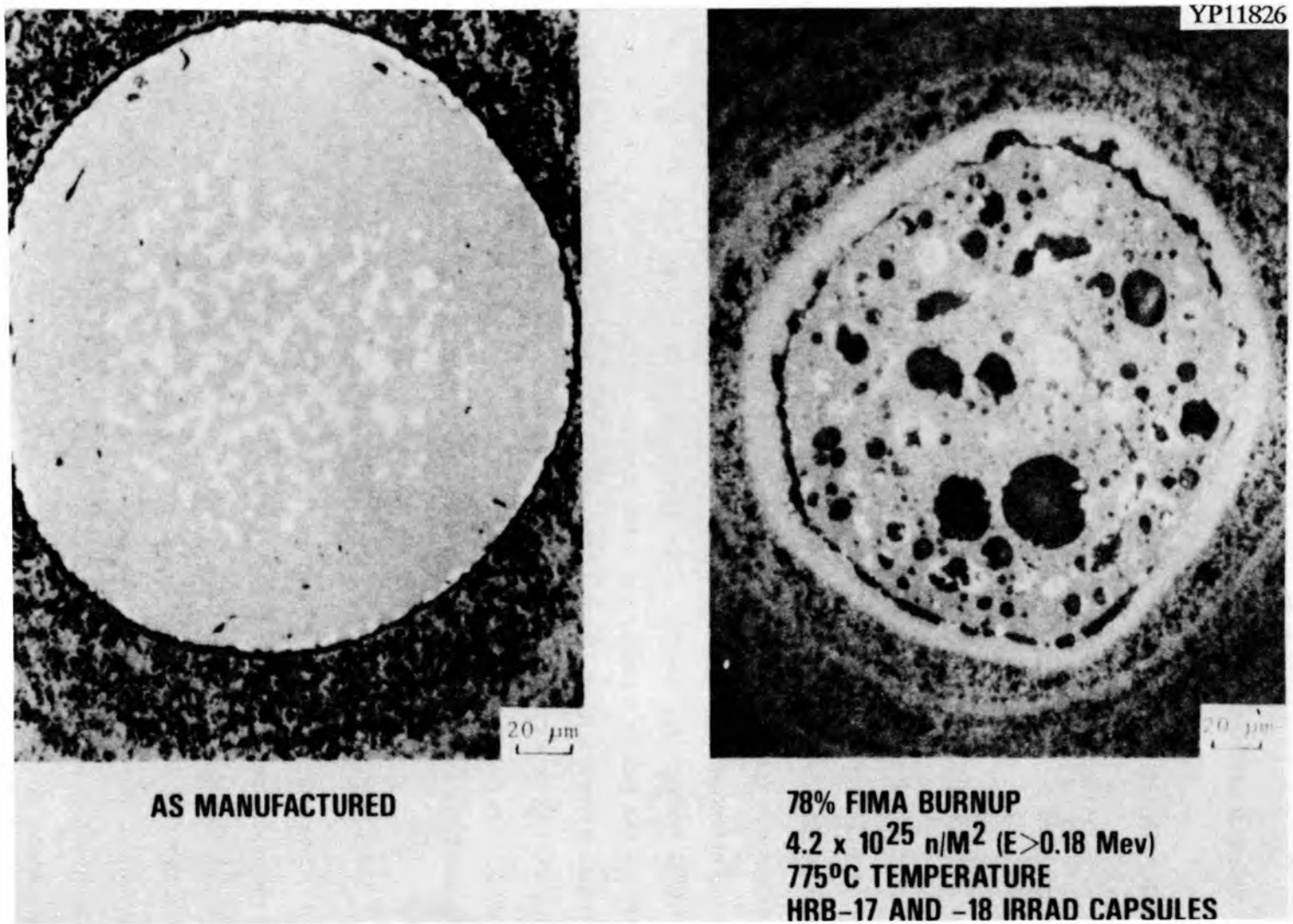

Fig. 6. HRB-17/-18 kernel pretest metallography. This work was done at GA. Recent calculations indicate burnup was 68% rather than the initial estimate of 78%.

3.4 SEM AND MICROPROBE ANALYSIS

Due to equipment and personnel unavailability, this work was not performed on the heated or unheated particles.

3.5 RADIOGRAPHY

Due to equipment and personnel unavailability, this work was not performed on the heated or unheated particles.

3.6 HRB-17 PREHEATING RADIOCHEMISTRY ANALYSIS

Five unheated particles were selected for destructive analysis. The particles were analyzed for the following radionuclides: ^{134}Cs, ^{137}Cs, ^{90}Sr, ^{144}Ce, ^{154}Eu, and ^{155}Eu. Of these five particles, all five yielded useable results. The average radiochemical results agreed with the average gamma spectrometry results within 9% for the following radionuclides: ^{144}Ce, ^{154}Eu, and ^{155}Eu. The results agreed within 5% for the average ^{90}Sr inventory when using the predicted inventory based on 67% burnup (see above). Poor agreement, greater than 35% difference, was obtained between the gamma scanning and radiochemistry results for the ^{134}Cs and ^{137}Cs measurements. No reason was determined for this discrepancy. The radiochemistry results for cesium cannot be supported by predictions for expected fission yields. Because of this discrepancy, the gamma spectrometry results have been used as the reference inventories for ^{134}Cs and ^{137}Cs. The average ^{90}Sr inventory was 94 μCi. The uncertainty (first standard deviation) may be approximated as 9%.

3.7 HRB-18 PREHEATING RADIOCHEMISTRY ANALYSIS

Five unheated particles were selected for destructive analysis. The particles were analyzed in the same manner as the HRB-17 particles for the following radionuclides: ^{134}Cs, ^{137}Cs, ^{90}Sr, ^{144}Ce, ^{154}Eu, and ^{155}Eu. Of these five particles, all five yielded useable results. The average radiochemical results agreed with the average gamma spectrometry results within 10% for the following radionuclides: ^{144}Ce, ^{154}Eu, and ^{155}Eu. The results agreed within 13% for the average ^{90}Sr inventory when using the predicted inventory based on 67% burnup (see above). Poor agreement, greater than 40% difference, was obtained between the gamma scanning and radiochemistry results for the ^{134}Cs and ^{137}Cs measurements. Again, the gamma scanning results

have been used as the reference inventories for ^{134}Cs and ^{137}Cs. The average ^{90}Sr inventory was 86 μCi. The uncertainty (first standard deviation) may be approximated as 10%.

4.0 EXPERIMENTAL CONDITIONS

This section describes the temperature history, the furnace sweep gas flow and monitoring, the cold trap performance, the detector performance, and the furnace postheating examination for both tests. Key test personnel are also identified.

4.1 1600°C TEST TEMPERATURE HISTORY

The heatup of the HRB-17 particles at 1600° C went as planned. The furnace temperature as a function of time is shown in Fig. 7. The furnace temperature was monitored by three temperature sensors. A tantalum-clad Type C thermocouple with hafnia insulation was located near the fuel specimen, just under the fuel holder, and served to monitor the fuel temperature. A boron graphite thermocouple (BGT) was located outside the muffle tube region of the furnace. It normally operates at a temperature as much as 60° C higher than the test specimen. In practice, this means that the furnace control temperature is set to a point slightly above the specimen target temperature. The BGT is preferred for control because its output is very stable and free of electrical noise. The final temperature sensor is an optical pyrometer. The optical pyrometer focuses on the outside of the muffle tube through a window in the furnace. The pyrometer normally indicates a temperature slightly below the specimen temperature because of local cooling of the muffle tube surface by the helium purge gas from the sight window housing and by local heat loss resulting from radiation through the window.

The initial selection for the control temperature was slightly low, and minor corrections were made to bring the specimen temperature to 1600° C as indicated by the Type C thermocouple near the specimen. This fine tuning was only necessary during the initial ramp to temperature, and no adjustments were necessary once 1600° C was achieved. The agreement between the temperature sensors remained excellent throughout the experiment (within 5° C), indicating drift was not a problem, and individual sensor calibration was maintained. The removal of the cold finger for deposition cup changing resulted in no measurable temperature perturbations to the specimen. This is in contrast to the 1400° C test (detailed below) and is probably due to the cold finger being located further from the sample in the 1600° C test.

ORNL-DWG-92-5161

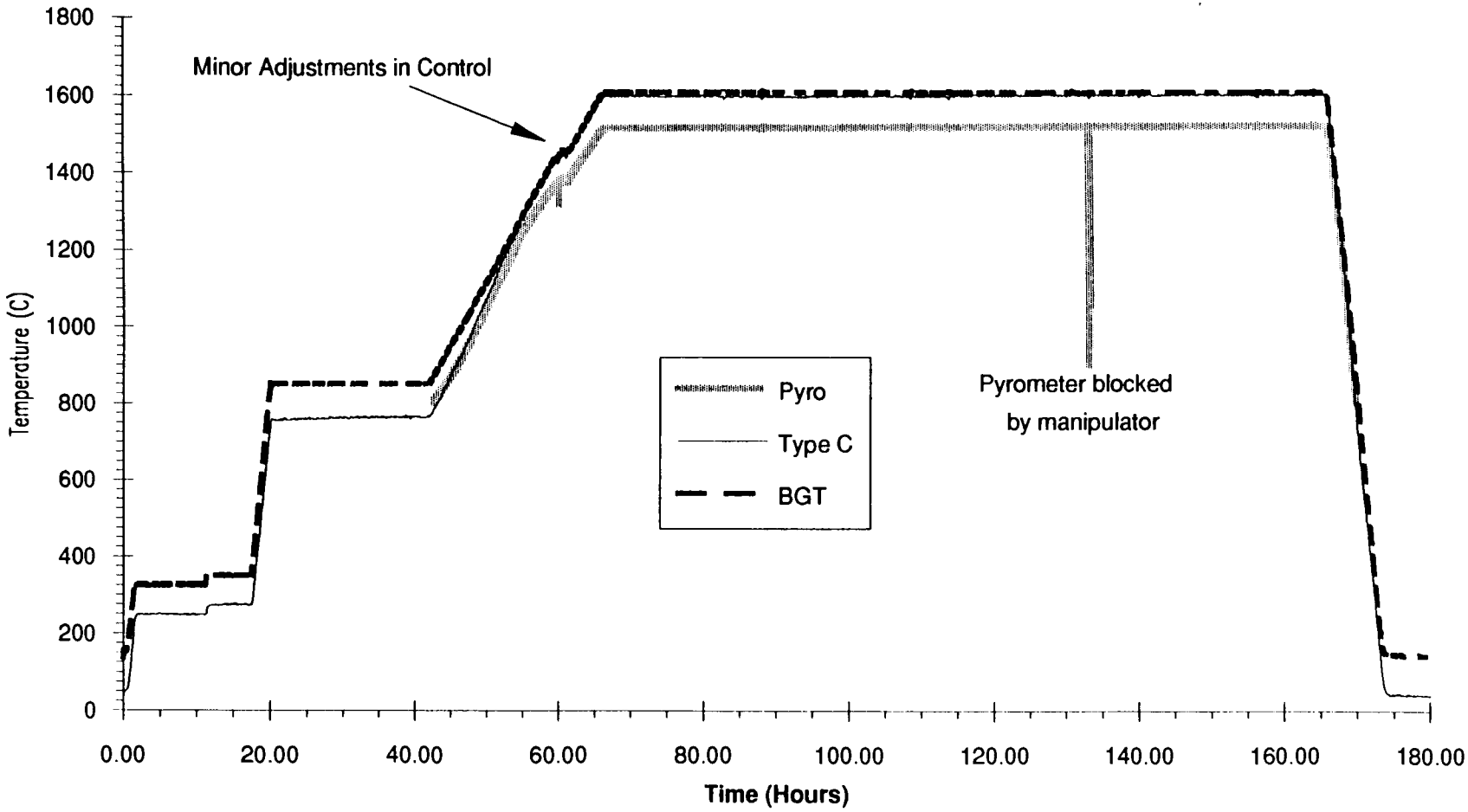

Fig. 7. Furnace temperature history as measured by the pyrometer, BGT, and Type C thermocouple for the HRB-17 test.

4.2 1400° C TEST TEMPERATURE HISTORY

The heatup of the particles at 1400° C went largely as planned with the exception of two problems, one minor and one major. The furnace temperature as a function of time is shown in Fig. 8. The thermocouple arrangement was the same as the 1600° C test.

Again, the initial selection for the control temperature was slightly low, and minor corrections were made to bring the specimen temperature to 1400° C as indicated by the Type C thermocouple near the specimen. This fine tuning increased the average temperature of the specimen by about 15° C over a period of several days. The agreement between the temperature sensors also remained excellent throughout the experiment indicating drift was not a problem and individual sensor calibration was maintained.

Small transients in the Type C thermocouple history were noted and can be seen in Fig. 8. These transients are due to changing the deposition cup. The deposition cup functions as a reflective cover on the furnace isothermal zone, and its removal from the furnace for replacement results in a measurable temperature perturbation to the specimen. This temperature perturbation is a 15 to 20° C temperature drop when the furnace is at 1400° C. This perturbation was not observed in the BGT output. No attempt was made to mitigate this minor temperature drop by using the Type C thermocouple as a control sensor. No change was made because the furnace temperature controller could not respond on a time scale short enough to be useful.

Other than the above minor points, the furnace temperature was held at the desired level by the control program with little operator intervention. Late into the heating program, the coolant flow switch malfunctioned resulting in the shutdown of the power supply and an uncontrolled rapid furnace cooling.

At hour 319.5, the power supply cooling flow interlock switch either malfunctioned or became temporarily blocked by debris, resulting in a shutdown of the power supply. The furnace immediately began to cool and did not recover. This effectively terminated the experiment. Restart of the experiment was not attempted because of concerns that furnace damage might have occurred during the rapid cooling. Of particular concern was the possible cracking of the tantalum muffle tube liner, embrittled by the high-temperature exposure, from thermal shock during the rapid cooldown. Later examination of the furnace and liner showed no damage. Fortunately, 259.5 h of the planned 300 h at temperature had been completed, and the cesium release rate had settled down to low levels by then, well past the transient phase.

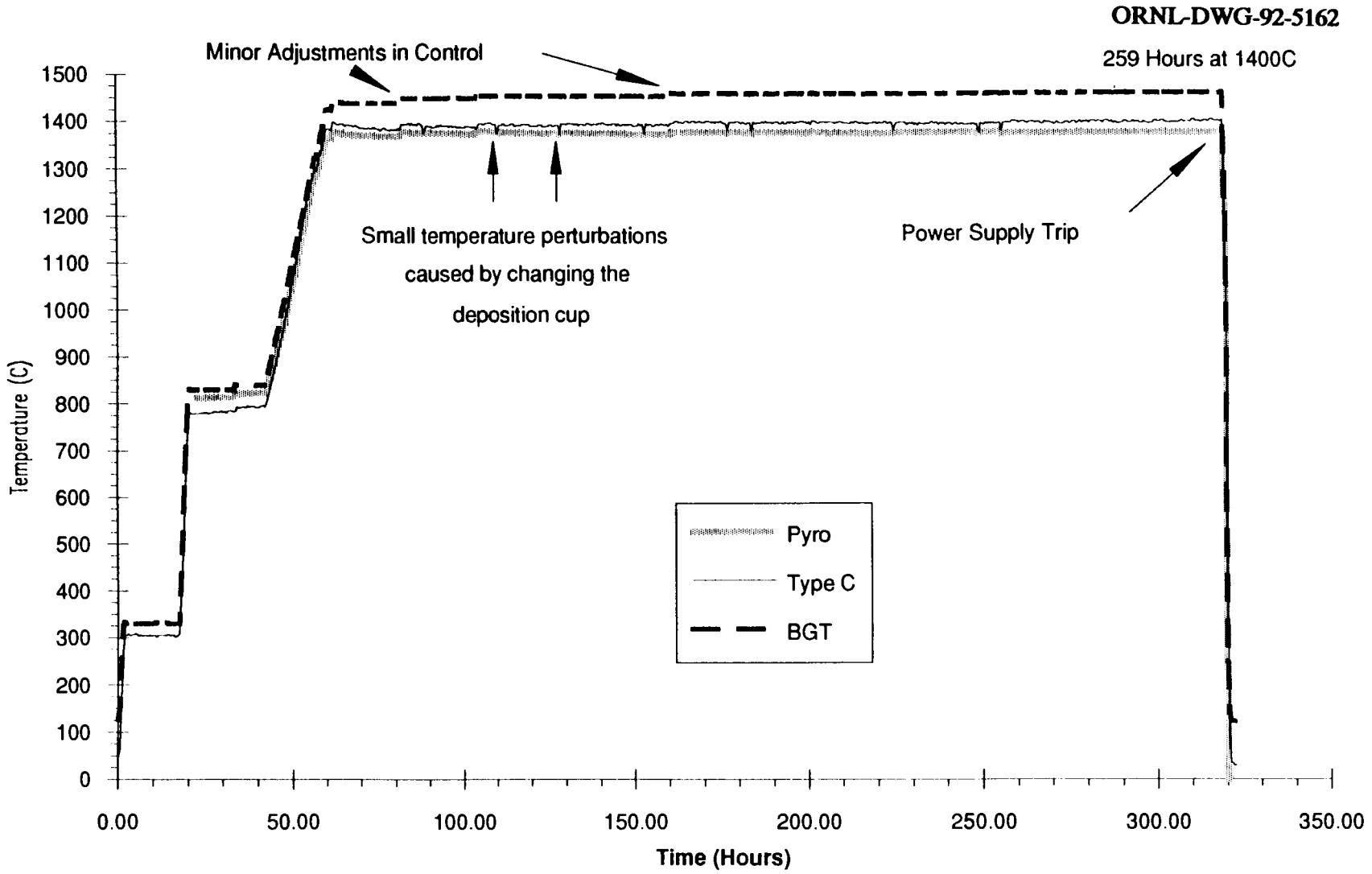

Fig. 8. Furnace temperature history as measured by the pyrometer, BGT, and Type C thermocouple for the HRB-18 test.

4.3 1600° C TEST FURNACE SWEEP GAS AND FLOWS

The furnace sweep gas was high-purity, less than 1 PPM O_2 or H_2O, helium that flowed for the duration of the experiment.[1-4] Exhaust from the internal region of the furnace was monitored twice a day by an RGA to provide an indication of any large changes in the furnace atmosphere. No significant changes in the impurity level of the furnace exhaust gas were observed during the duration of the test.

The history of the furnace gas flow during this test is shown in Fig. 9. The curves, which indicate the gas flow, exhibit two main characteristics. The first set are of the disruptions in the gas flow history. These spikes occur whenever the cold finger is withdrawn from or inserted into the furnace. The second characteristic is a slow drift in the flow rate that was corrected by manual flow adjustments. The major reason for this drift is thought to be the sensitivity of the gas regulators to the ambient temperature and the regulators' response to the cold finger movement. Because the regulators are operated at the lower end of their pressure range, there is a small amount of hysteresis in the regulator action, which does not allow a full return to the preset value after a pressure disturbance. Flow adjustments were made as necessary; furnace performance was insensitive to minor changes in the flow rate.

The furnace system was leak checked both before and after the heating test. The leak rate of the furnace at the end of the test was small but higher than the near-zero level expected. It is not clear if the small leak developed during the experimental run or is an artifact of the testing, which subjects the furnace to a pressure differential of 3 to 4 times the normal operating pressure differential (between the furnace interior and the hot cell). This possible leak was estimated to be $< 5\%$ of total purge gas flow, so that the effect on krypton collection efficiency is small if the leak existed during the test.

4.4 1400° C TEST FURNACE SWEEP GAS AND FLOWS

The furnace sweep gas flow for the 1400° C test was similar to that detailed above, and it was also monitored twice a day by an RGA to provide an indication of major changes in the furnace atmosphere. No significant change in the impurity level of the furnace exhaust gas was observed during the duration of the test.

The history of the furnace gas flow during this test is shown in Fig. 10. The interpretation is the same as was described above for the 1600° C test except for the trap plugging.

ORNL-DWG-92-5163

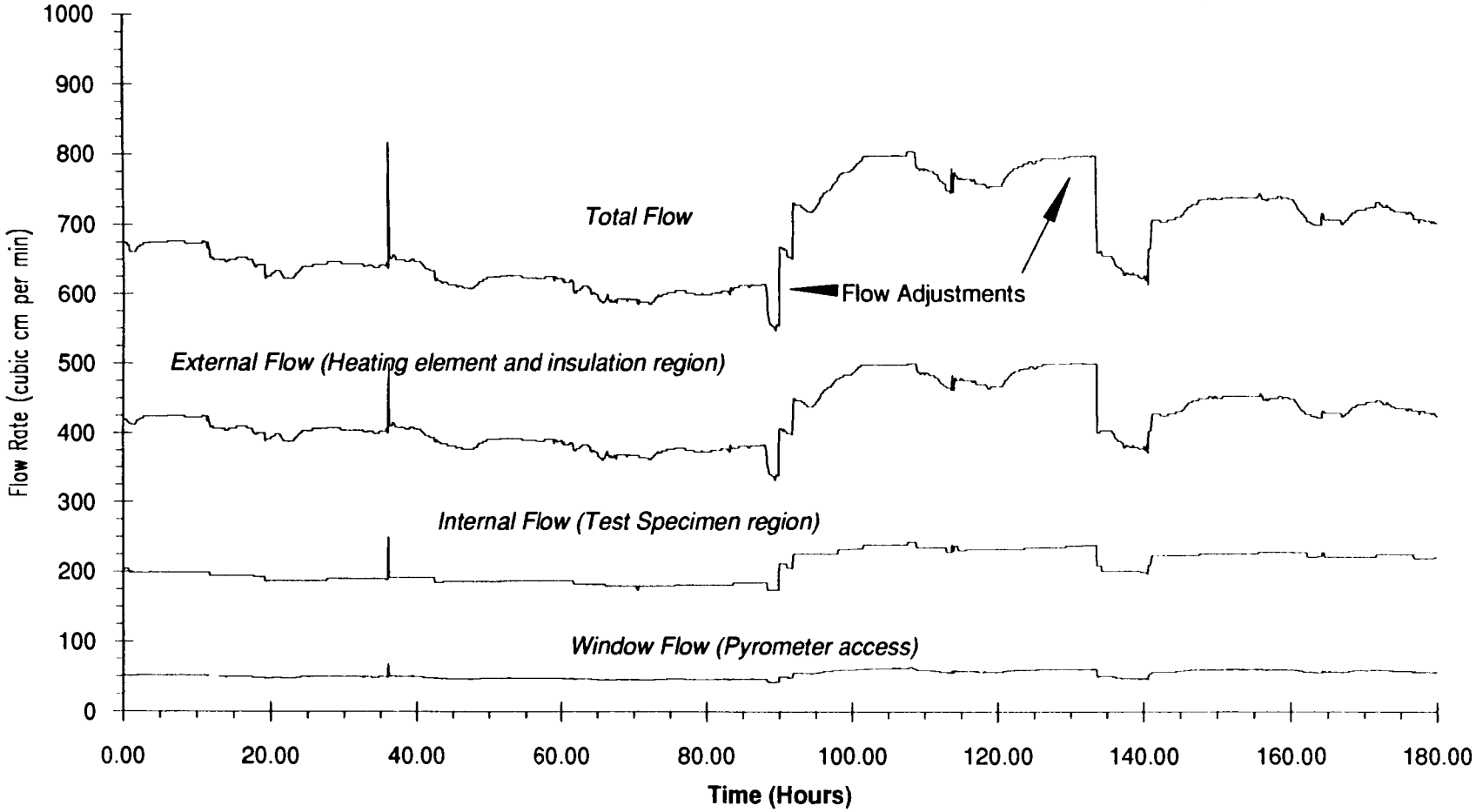

Fig. 9. Furnace sweep gas flow history for each region showing the flow spikes and drift for the 1600°C test.

ORNL-DWG-92-5164

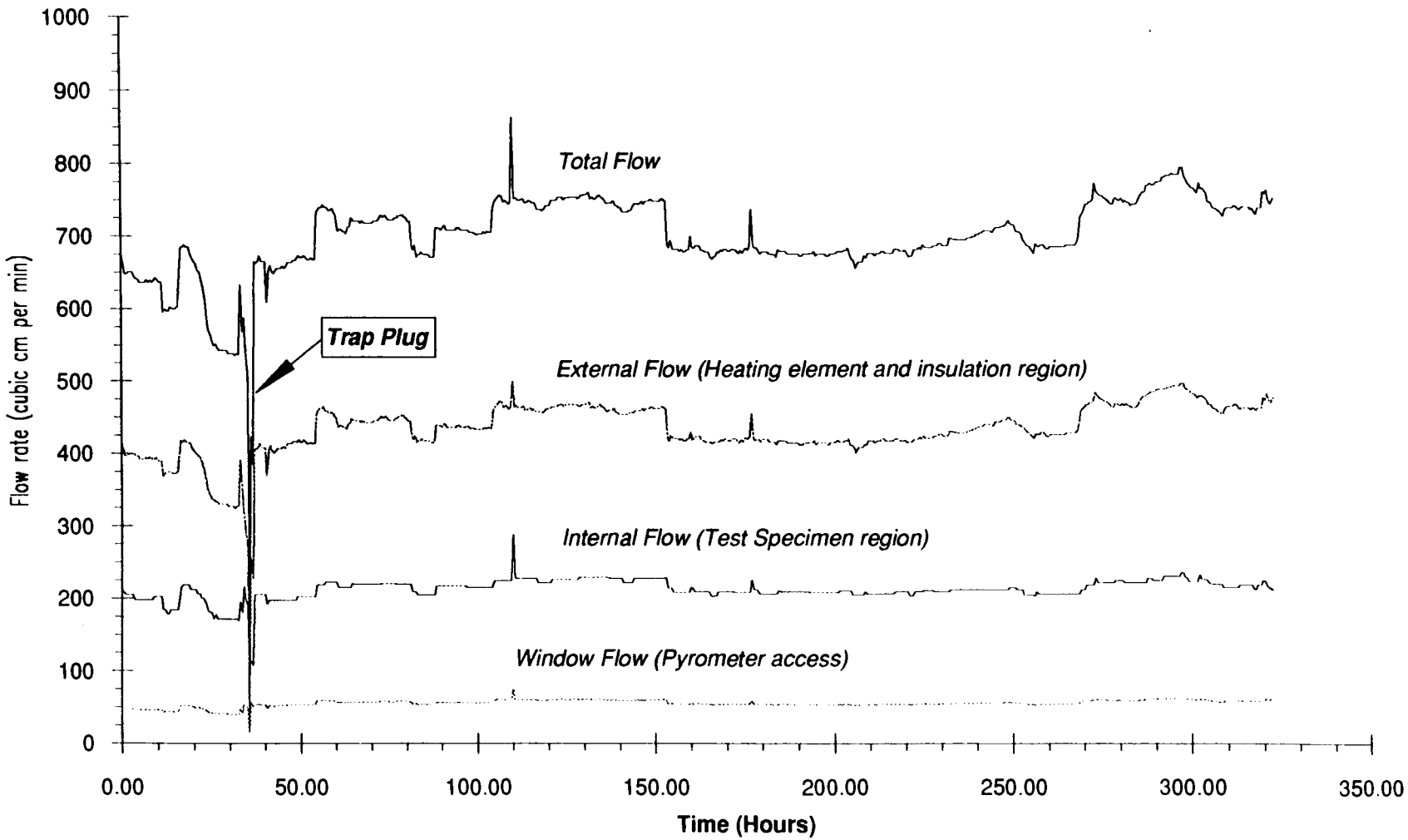

Fig. 10. Furnace sweep gas flow history for each region showing the trap blockage, flow spikes, and drift for the 1400°C test.

During the 800°C heating plateau phase, at approximately hour 35, the flow through the trap system dropped to low levels indicating a blockage. The details of this flow reduction and blockage are shown in Fig. 11. Flow adjustments were not successful in increasing the flow or freeing the blockage. The first cold trap was then slowly warmed in an effort to melt/remove the blockage and restore flow. Because of previous experience, the first trap was considered the most likely candidate as the source of the problem. No krypton activity had been detected up to this time in either trap. While the first trap was being warmed up, the second trap was held at its nominal temperature as a backup, should a sudden release of krypton take place.

At a temperature of approximately -145°C, flow was suddenly restored, and the cooling to trap 1 was then immediately restarted. The trap temperature history for this period of time is shown in Fig. 12. Normal CCCTF function was quickly resumed, and no problems were noted for the balance of the experiment. After completion of the heating, the contents of the trap system were examined using the RGA. The examination indicated the presence of CO and CO_2. The most probable cause of the trap plugging was the buildup of frozen CO_2 in the inlet line to the first trap. Even though the sweep gas is routed through a water condenser, which operates below the freezing point of CO_2, before it enters the cold trap system, the vapor pressure of solid CO_2 is still high enough for it to move slowly through the condenser and into the trap system, which has a small and easily plugged inlet line. Since the fuel holder and fuel holder support had been exposed to air for an extended period of time, it is possible that they may have been a source of the CO_2.

The gas flow from the internal region of the furnace was periodically monitored by the RGA and no abnormal conditions recorded. The detailed monitoring of the furnace gas composition was beyond the capabilities of the RGA because of the very low level of impurities and the large background of helium. In most cases, the signals of interest were at the electronic noise level, and quantitative data were not readily obtainable. A qualitative time history of mass 18 (water) and mass 28 (CO or N_2) is shown in Fig. 13. These data have a large and not easily quantified error, so conclusions regarding relative magnitudes cannot be drawn. These data are included for completeness and to indicate that no large changes took place in the furnace atmosphere during the heating cycle. No clear CO_2 signal was observed during the experiment that could be correlated with the plugging of trap 1. This is not unexpected because the instrument does not have the sensitivity to reliably perform the desired low-level measurements.

ORNL-DWG-92-5165

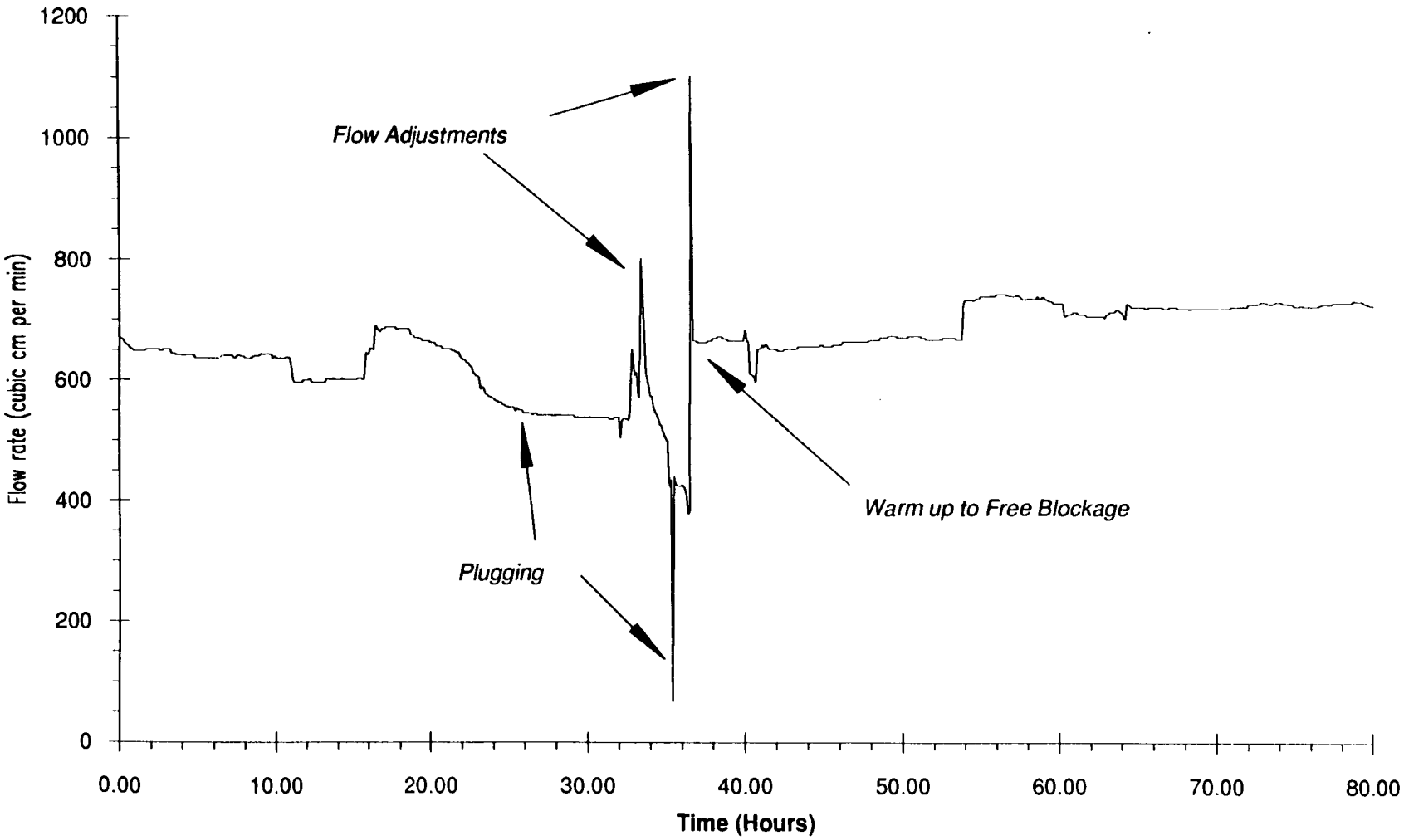

Fig. 11. Sweep gas flow history during trap blockage, trap warmup, and flow restoration for the 1400°C test.

ORNL-DWG-92-5166

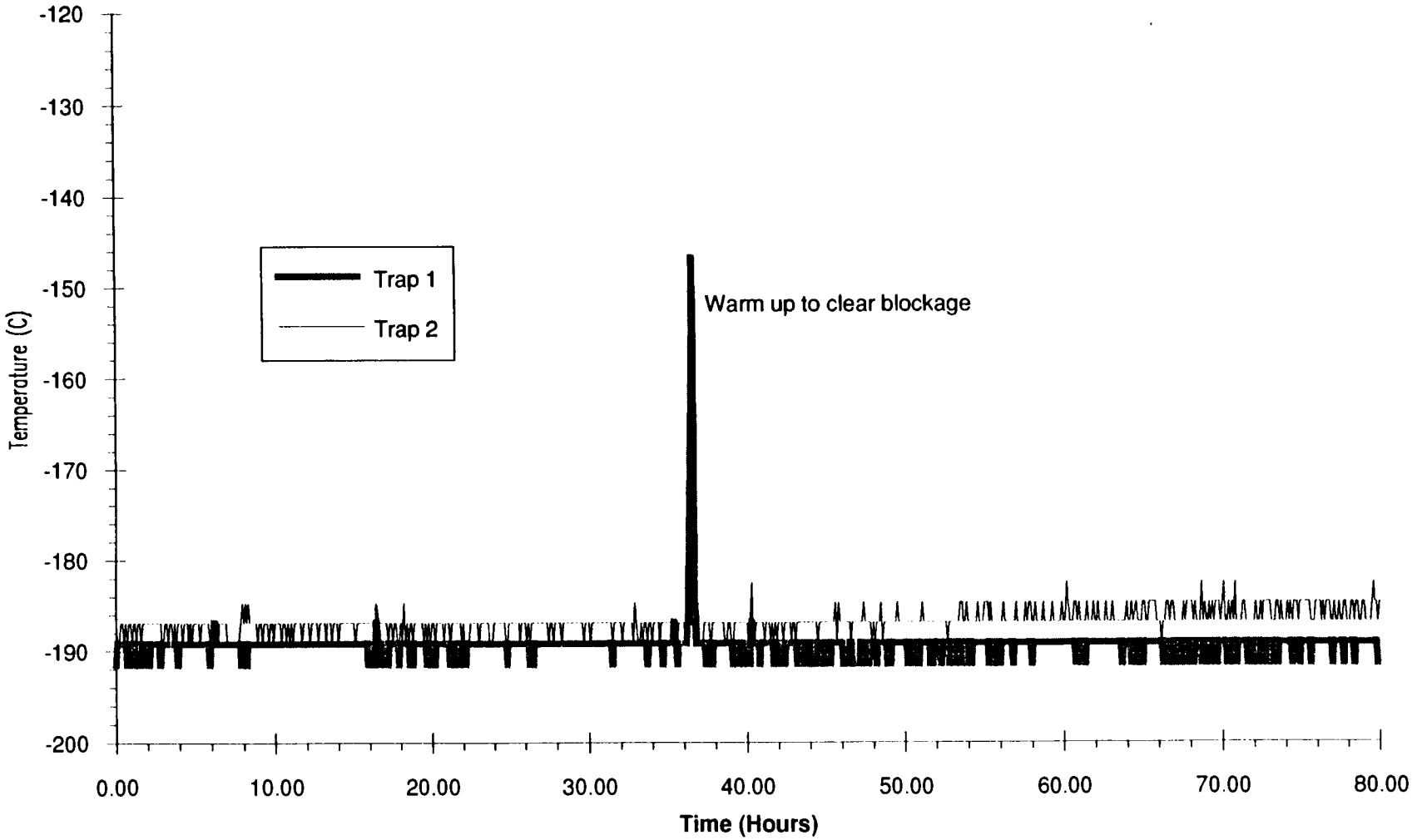

Fig. 12. Trap temperature histories during trap blockage, trap warmup, and flow restoration for the 1400°C test.

ORNL-DWG-92-5167

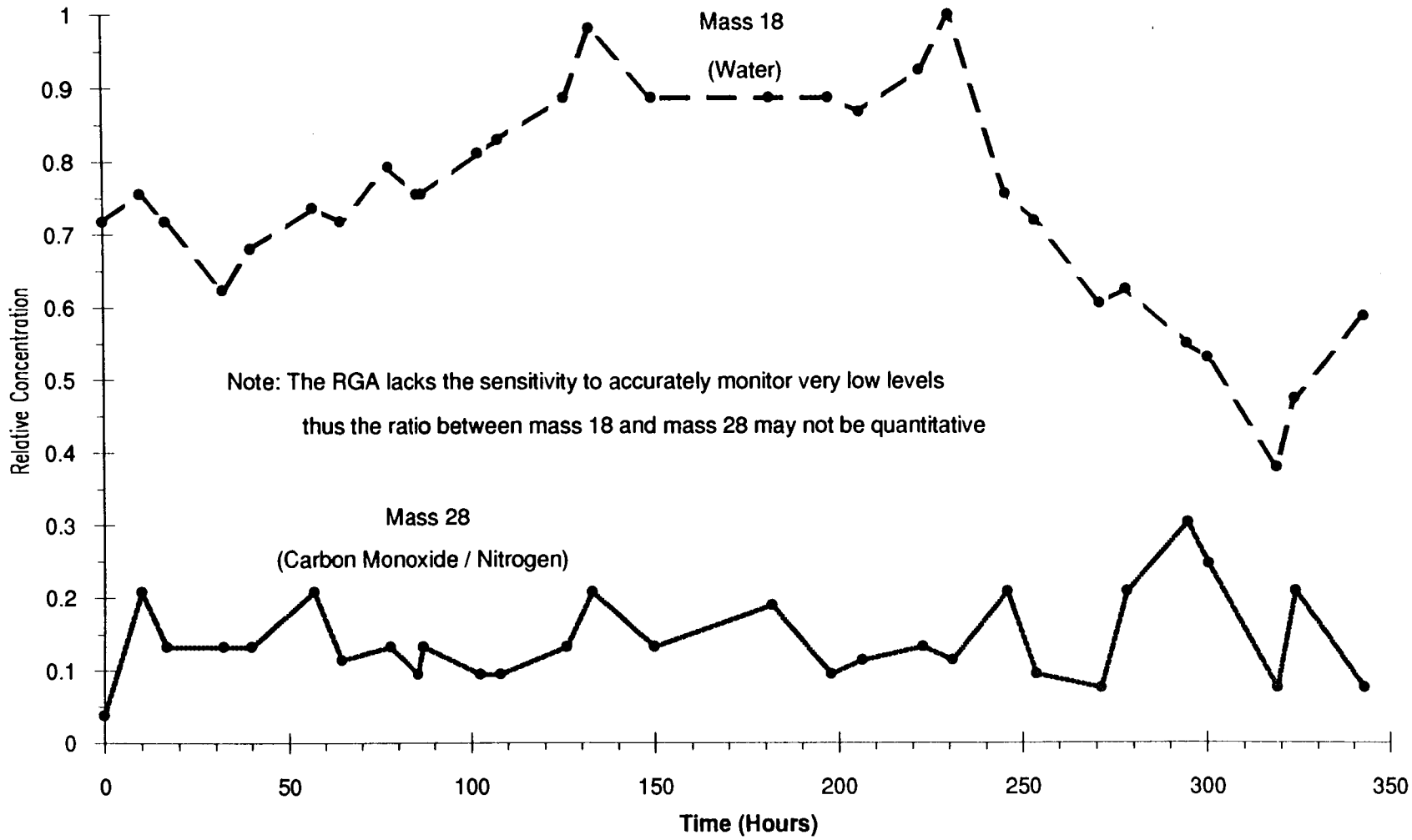

Fig. 13. History of RGA monitoring of mass 18/28 impurities in the furnace internal region for the 1400°C test. These data are only qualitative in nature.

4.5 CCCTF COMPONENTS

After termination of both the 1600 and 1400°C heating experiments, the furnace was disassembled and the internal components examined. In general, the furnace components all appeared to be in good condition. In the 1400°C heating test, there was no observable damage from the sudden cooldown. Some white deposits were observed on the middle of the Type C thermocouple sheath used in the 1400°C test. These deposits have not been analyzed.

Results indicate that only the furnace components exposed in the internal region of the furnace were contaminated with condensible fission products. The muffle tube liner, the fuel holder, the fuel holder support, the Type C thermocouple, the furnace bottom flange, the upper cooling collar, the gate valve, and the cold finger all had detectable cesium inventories. Measurements indicated that the cesium inventories of these components were below the inventories of the most active deposition cups, except for the muffle tube liner and fuel holder, which appeared to have inventories at least comparable to a deposition cup. The graphite muffle tube had only a slight amount of contamination, and the remainder of the furnace, such as the heating elements and insulation, had no measurable contamination.

The other furnace control and flow functions appeared to be normal and performed as expected except for the binding of the deposition cup drive motor in the 1600°C test and the flow switch in the 1400°C test. The liquid nitrogen supply and control system for the cold traps performed well.

Good time-dependent agreement between the furnace temperature sensors throughout both tests (within 5°C) indicated that little, if any, drift was present in the temperature measurements. The power input to the furnace was steady during the test temperature (1600 and 1400°C) phase of the heating program, providing further indication that no furnace temperature drift was occurring.

4.6 PERSONNEL

The following people were actively involved with the test or its support activities: C. A. Baldwin and T. L. Collins provided support for the gamma counting and loading of the fuel particles; J. L. Collins and C. S. Webster assisted in the gamma counting of the furnace components and furnace preparation; R. T. Pack and J. L. Botts performed the radiochemical analysis; J. R. Travis assisted in general hot cell operations and deposition cup changing; and W. A. Gabbard, C. M. Malone, R. N. Morris, J. C. Whitson, and J. L. Wright were involved with general CCCTF preparation and operation.

5.0 EXPERIMENTAL HEATING RESULTS

This section details the fission product releases and compares the results of the 1400° C test with that of the 1600° C test. It also estimates the amount of cesium surface contamination on the particles.

5.1 GAMMA-EMITTING FISSION PRODUCT RELEASE AT 1600° C

5.1.1 Metallic Fission Products

During the heating program, the deposition cups were changed twice a day with at least 4.2 h between changes. During the course of the experiment, at hour 60, the drive motor mechanism operating the deposition cup attachment screw bound up and had to be repaired. This occurred when the furnace was at 1440° C in its final temperature ramp to 1600° C. Visual inspection revealed that the fault was due to a misalignment of the drive motor. Fortunately, the mounting screws for the motor were accessible, and the screws were loosened with the use of the manipulators and the motor realigned. The drive motor then performed normally without further problems for the balance of the experiment.

The integral cesium collected on the deposition cups is shown in Fig. 14 and Table 3. For analysis purposes, the time assigned to a deposition cup is the time it is withdrawn from the furnace. The maximum time a cup was in the furnace was 20.3 h; the minimum, 4.2 h. Thus, the time resolution is of the order of a few hours. There was one cup change during the ramp from 800 to 1400° C, so the time and temperature of the beginning of the release can only be approximately determined; however, a clear release trend is evident. The cesium collection rate for the deposition cups is shown in Fig. 15. The rate is defined to be the cup activity divided by the time the cup was in the furnace. The time assignment is the average of the cup in-time and cup out-time. As can be seen, after an initial release lasting roughly 40 h, the release rate drops to a lower level for approximately 30 h and then increases by about a factor of two. It then gradually tapers off until the termination of the test. The first peak in the release rate is due to contamination that the particles received during irradiation, while the second peak is due to particle releases.

Gamma spectrometric examination of the particles on an individual basis indicates that four particles released a large fraction of their cesium and/or europium inventory. The following fission products were measured, both before and after heating: ^{134}Cs, ^{137}Cs, ^{144}Ce, ^{106}Ru, ^{154}Eu,

ORNL-DWG-92-5168

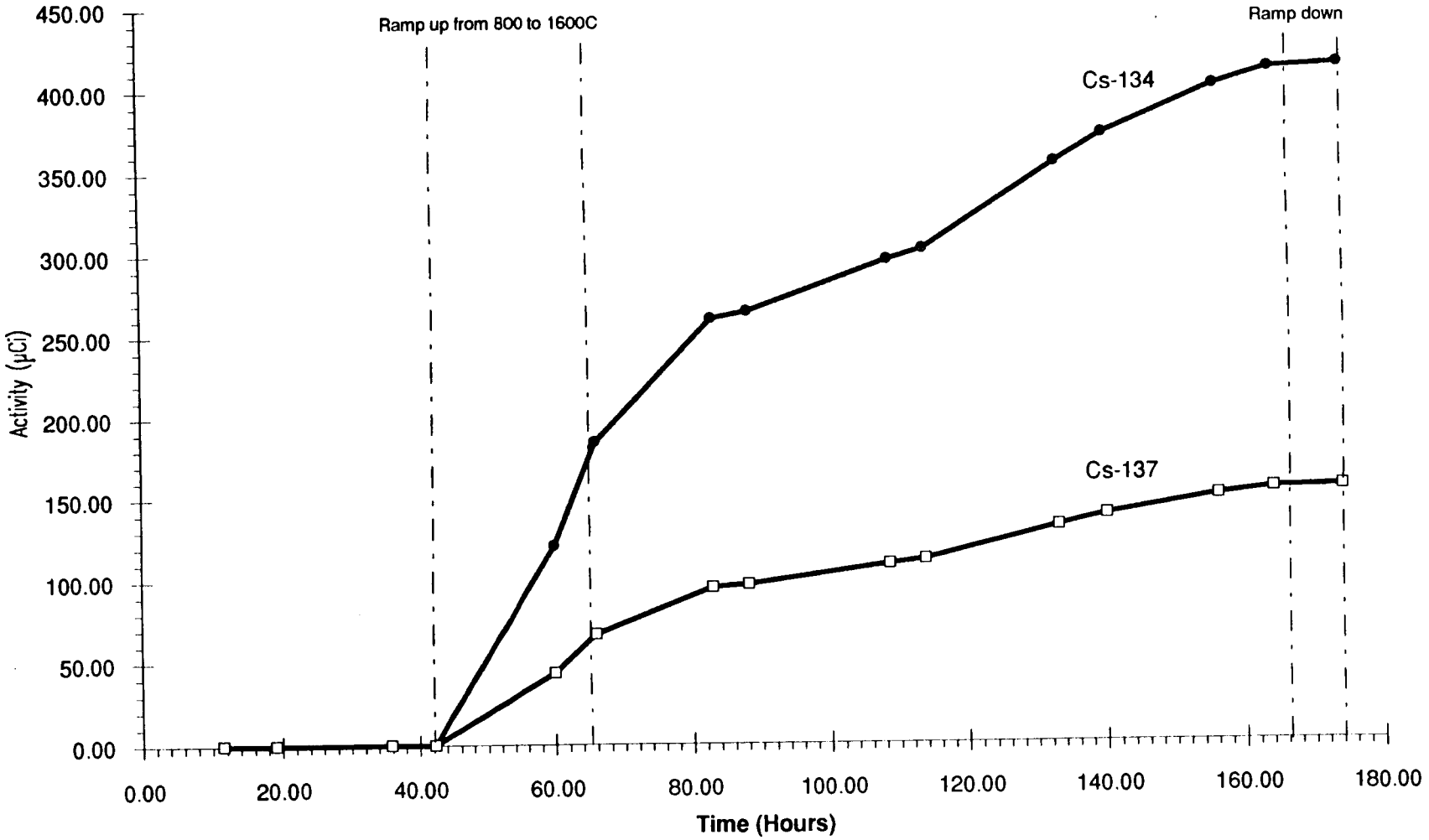

Fig. 14. Integrated deposition cup cesium collection as a function of time for the 1600°C test. Corrected to 5 Feb 1986.

Table 3. 1600°C deposition cup cesium data. Corrected to 5 Feb 1986.

1600°C (HRB-17) Deposition Cup Results

Cup	Experimental Time (h)	Rate Time (h)	Date In	Time In	Temperature In (C)	Date Out	Time Out	Temperature Out (C)	Elapsed Time (h)	Measured Cs-134 (µCi)	Cs-134 Rate (µCi/h)	Total Cs-134 (µCi)	Measured Cs-137 (µCi)	Cs-137 Rate (µCi/h)	Total Cs-137 (µCi)
32	11.48	5.74	22/10/91	20:19	25	23/10/91	7:48	300	11.48	0.00	0.00	0.00	0.00	0.00	0.00
33	19.05	15.37	23/10/91	8:01	300	23/10/91	15:22	641	7.35	0.00	0.00	0.00	0.00	0.00	0.00
34	35.87	27.57	23/10/91	15:35	641	24/10/91	8:11	850	16.60	0.04	0.00	0.04	0.02	0.00	0.02
35	42.27	39.18	24/10/91	8:25	850	24/10/91	14:35	858	6.17	0.03	0.00	0.07	0.01	0.00	0.03
36	60.00	51.13	24/10/91	14:35	858	25/10/91	8:19	1437	17.73	121.00	6.82	121.07	43.60	2.46	43.63
37	65.93	63.82	25/10/91	10:01	1437	25/10/91	14:15	1600	4.23	63.40	14.98	184.47	23.60	5.57	67.23
38	82.93	74.55	25/10/91	14:29	1600	26/10/91	7:15	1600	16.77	75.47	4.50	259.94	28.13	1.68	95.36
39	88.07	85.62	26/10/91	7:29	1600	26/10/91	12:23	1600	4.90	4.24	0.87	264.18	1.62	0.33	96.97
40	108.63	98.47	26/10/91	12:38	1600	27/10/91	8:57	1600	20.32	31.40	1.55	295.58	12.03	0.59	109.00
41	113.77	111.30	27/10/91	9:09	1600	27/10/91	14:05	1600	4.93	6.36	1.29	301.93	2.44	0.49	111.44
42	133.08	123.54	27/10/91	14:19	1600	28/10/91	9:24	1600	19.08	52.25	2.74	354.18	20.02	1.05	131.46
43	140.12	136.79	28/10/91	9:47	1600	28/10/91	16:26	1600	6.65	17.44	2.62	371.62	6.79	1.02	138.25
44	156.17	148.32	28/10/91	16:48	1600	29/10/91	8:29	1600	15.68	28.69	1.83	400.31	11.13	0.71	149.38
45	164.02	160.31	29/10/91	8:55	1600	29/10/91	16:20	1600	7.42	9.92	1.34	410.23	3.88	0.52	153.26
46	174.02	169.13	29/10/91	16:34	1600	30/10/91	2:20	25	9.77	2.54	0.26	412.77	0.98	0.10	154.24

ORNL-DWG-92-5169

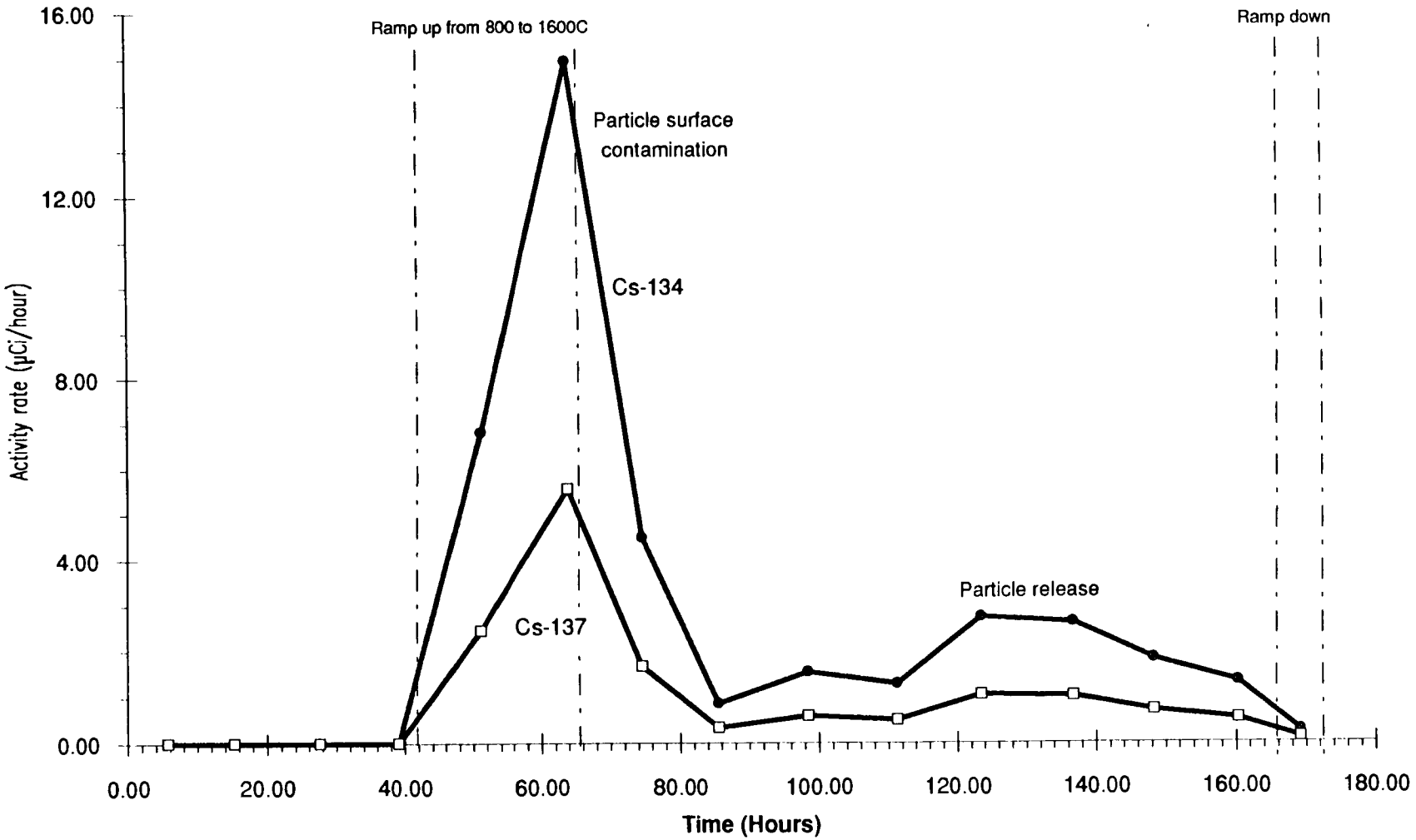

Fig. 15. Deposition cup cesium collection rate as a function of time for the 1600°C test. Corrected to 5 Feb 1986.

and ^{155}Eu. The measured differences between the preheating and postheating particle inventories are near the repeatability limit of the gamma spectrometry equipment, and it is difficult to accurately quantify the relative inventory changes in a particular particle, except for the four previously mentioned particles. The only cesium loss expected was that due to contamination, and the overall data trend indicates that, a significant fraction, 5%, lost ^{134}Cs and ^{137}Cs during the heating. This result is supported by the deposition cup record and by examination of the furnace internal components. In addition, ^{154}Eu was found in the furnace graphite components. The ratio between the average postheating particle inventory and the average preheating inventory for the above radionuclides is:

Radionuclide	Post/Preheating
^{134}Cs	0.98 ± 0.02
^{137}Cs	0.98 ± 0.01
^{106}Ru	1.03 ± 0.09
^{144}Ce	1.02 ± 0.02
^{154}Eu	1.00 ± 0.03
^{155}Eu	1.03 ± 0.12

Note that the given uncertainty (first standard deviation) is the repeatability of the measurement–not its absolute accuracy, which has a greater uncertainty. Only ^{134}Cs and ^{137}Cs had a predominately lower average postheating than preheating inventory. Of the six measured radionuclides, only four have uncertainty limits that are of the same magnitude as the estimated inventory changes. Because of this, the following discussion will be restricted to ^{134}Cs, ^{137}Cs, ^{144}Ce, and ^{154}Eu. The percent change in particle inventory for ^{134}Cs, ^{137}Cs, ^{144}Ce, and ^{154}Eu on a per-particle basis is shown in Figs. 16 through 19. Note that ^{137}Cs, Fig. 17, shows a net decrease for almost all the particles while ^{144}Ce, Fig. 18, shows the expected random differential measurement increase and decrease on a per-particle basis, although the average has been shifted upward from the baseline a small amount. Cerium forms an extremely stable oxide (Ce_2O_3) in the kernel, which has low mobility at 1600°C for the times of interest. Cerium, therefore, provides a convenient internal reference for comparison with more mobile fission products such as cesium. The results for ^{134}Cs, Fig. 16, and ^{154}Eu, Fig. 19, are less clear, their behavior dominated by the releasing particles and the relatively large uncertainty.

ORNL-DWG-92-5170

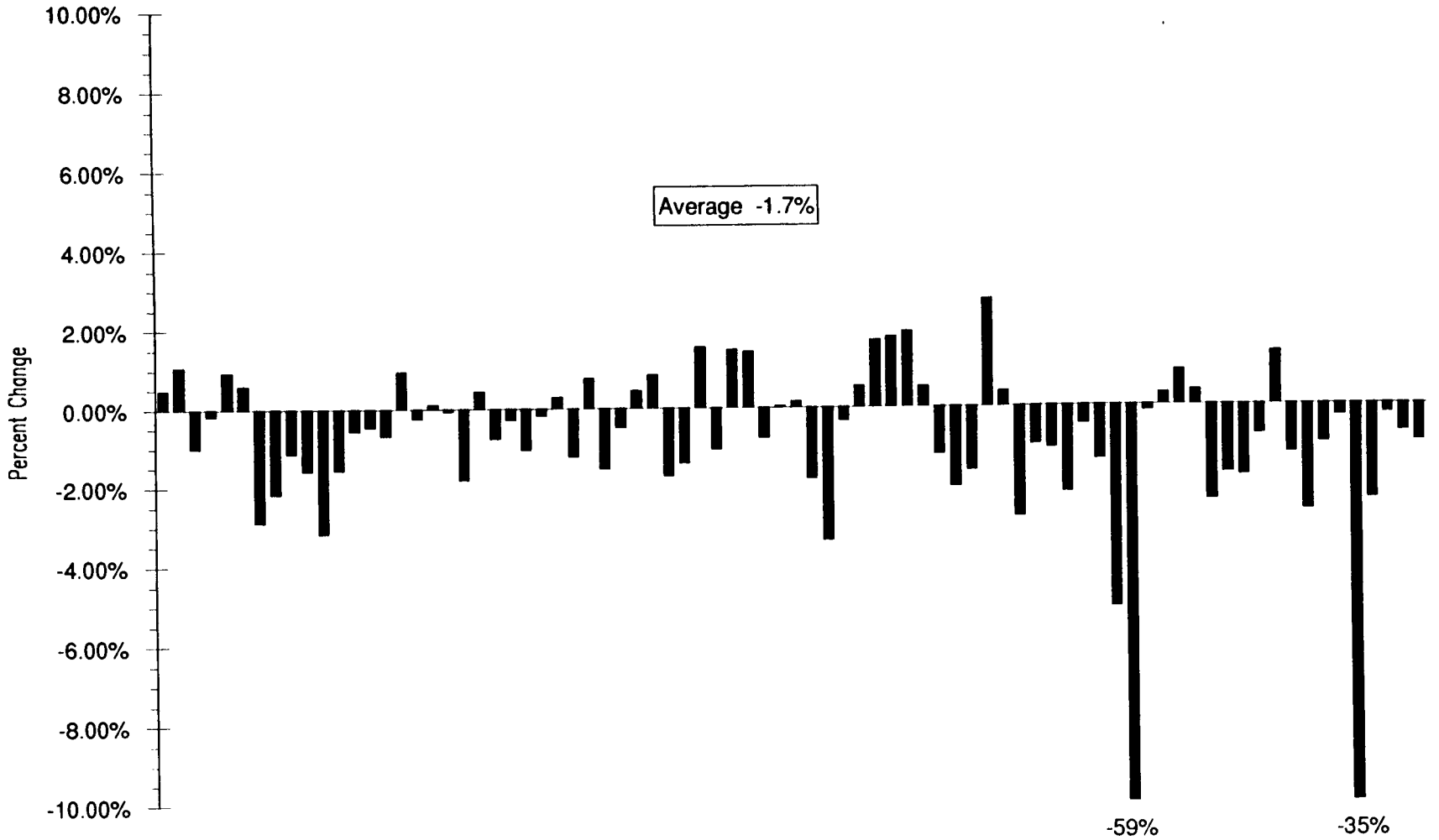

Fig. 16. Measured change in particle Cs-134 inventory on a particle-by-particle basis for the 1600°C test. Note indicated losses.

ORNL-DWG-92-5171

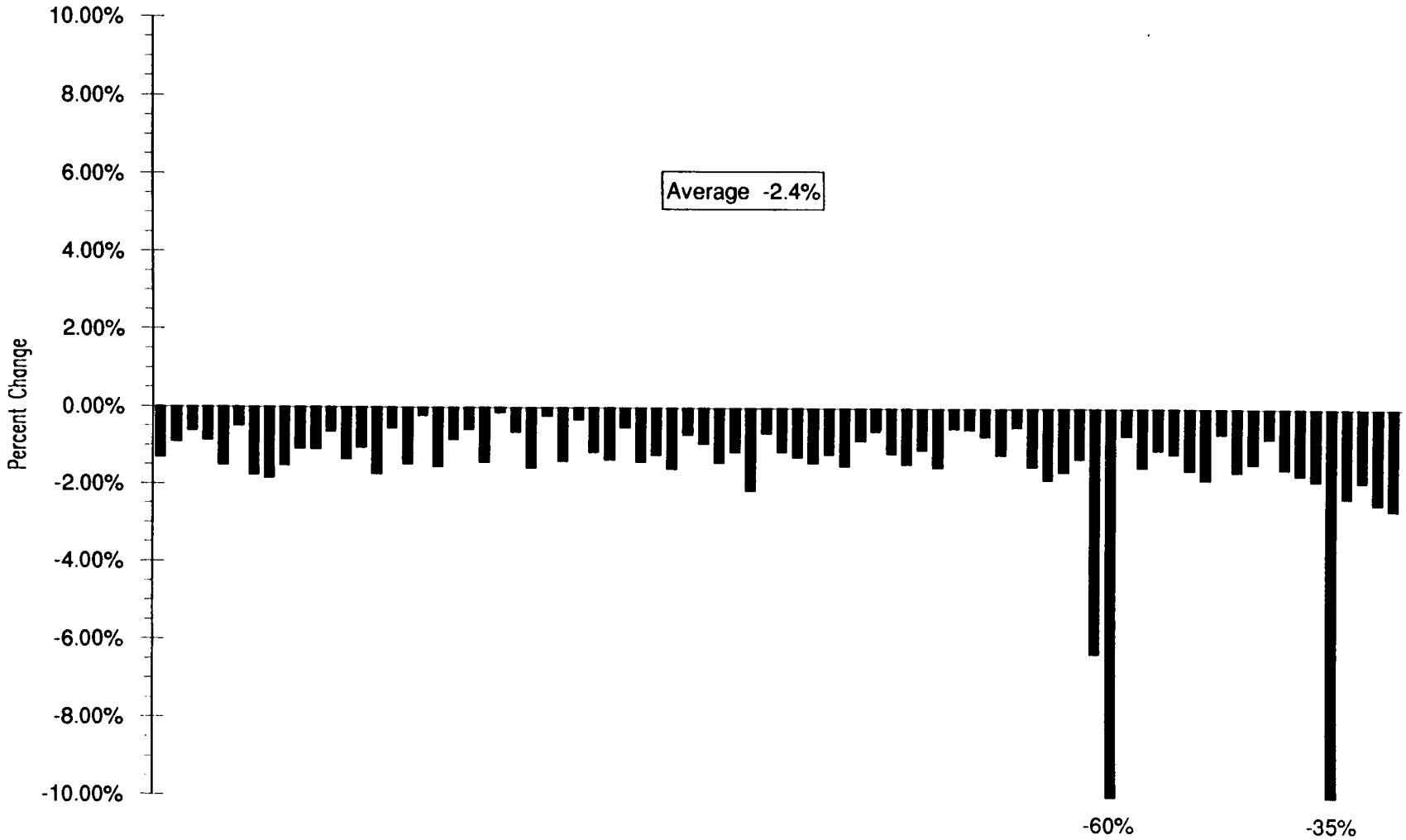

Fig. 17. Measured change in particle Cs-137 inventory on a particle-by-particle basis for the 1600°C test. Note indicated losses and downward trend.

ORNL-DWG-92-5172

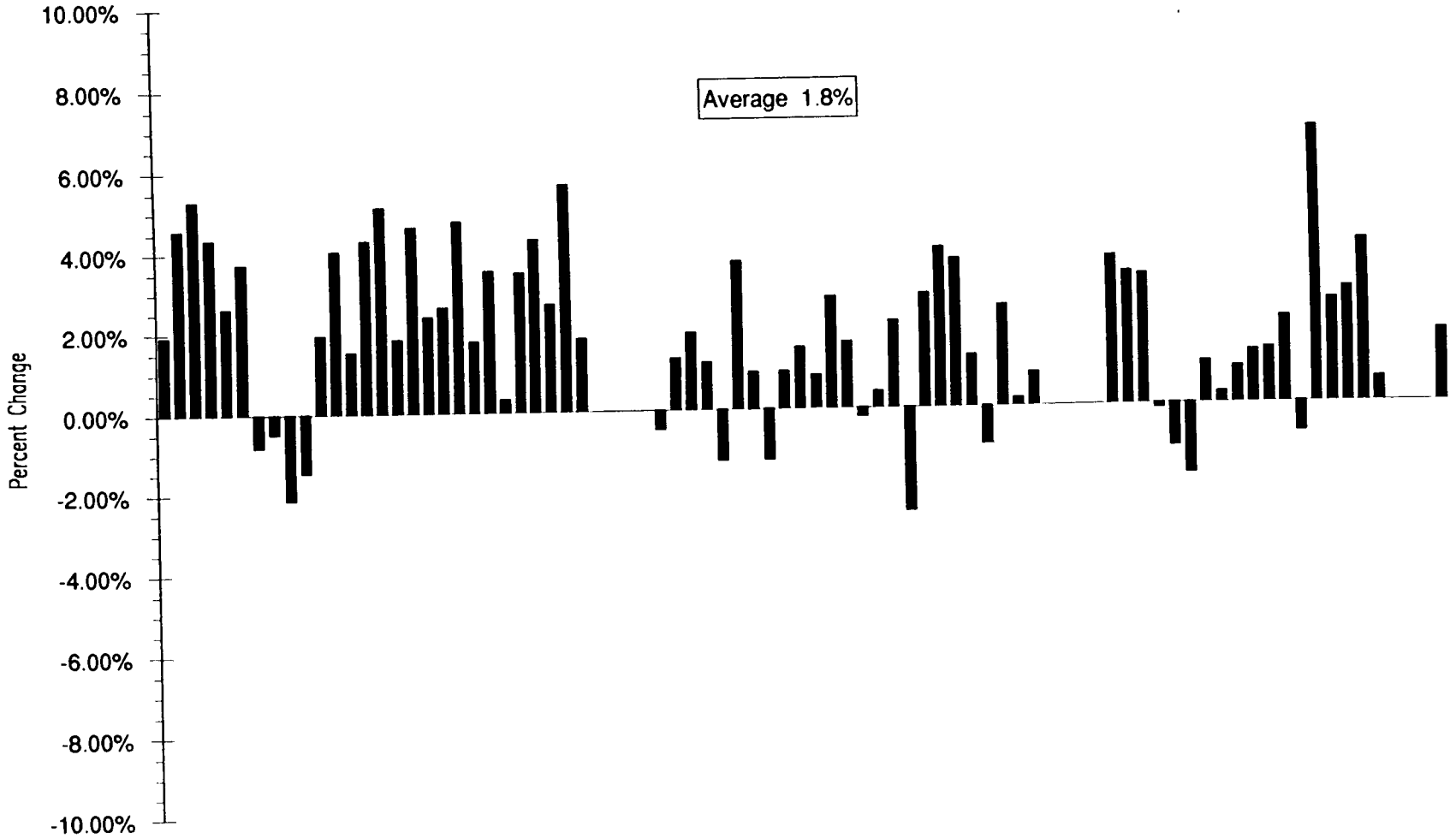

Fig. 18. Measured change in particle Ce-144 inventory on a particle-by-particle basis for the 1600°C test.

ORNL-DWG-92-5173

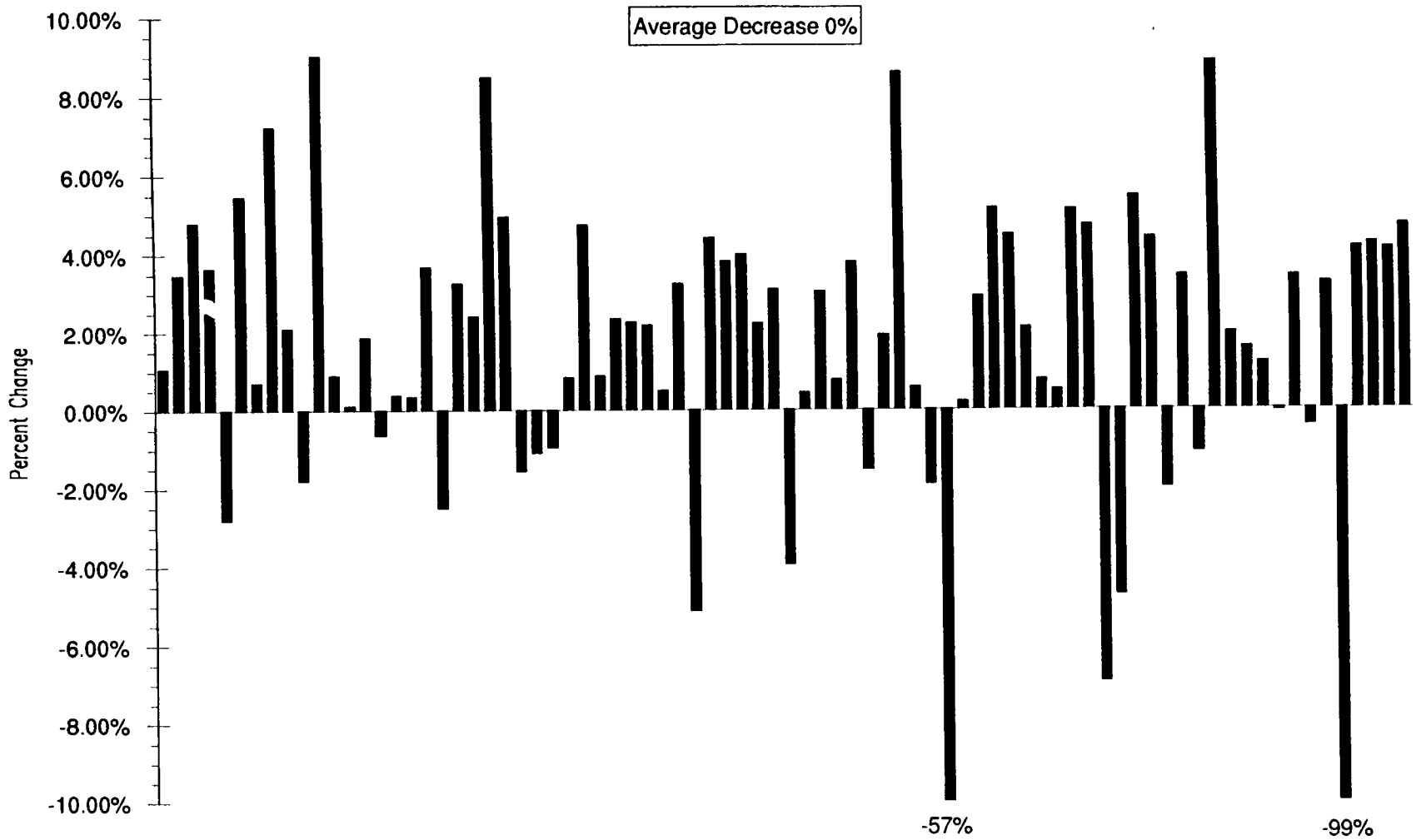

Fig. 19. Measured change in particule Eu-154 inventory on a particle-by-particle basis for the 1600°C test. Note indicated losses.

Note that one particle lost 2% of its cesium but 57% of its europium; another lost 6% of its cesium and 7% of its europium; a third lost 60% of its cesium but only 5% of its europium; and finally, a fourth particle lost 35% of its cesium and 99% of its europium. The wide variation in the released cesium/europium ratio between particles may be due to differences in kernel composition due to large variations in the uranium oxide/carbide mix. Statistics for kernel composition are not available, so this possibility cannot be easily investigated. Detailed particle inventories of ^{134}Cs, ^{137}Cs, ^{144}Ce, ^{154}Eu, ^{155}Eu, and ^{106}Ru, both before and after heating, are tabulated in Table 1.

Except for the four releasing particles, the changes in particle inventory are small and at the repeatability limit of the equipment; it is, therefore, difficult to draw unambiguous and quantifiable conclusions from this single piece of data for the small average cesium decrease for the non-releasing particles. Because the non-releasing particles were contaminated during irradiation from neighboring designed-to-fail (DTF) particles, their small average cesium loss of approximately 0.5% for ^{134}Cs and 1.2% for ^{137}Cs is likely to be due to this contamination. This conclusion is supported by the deposition cup record, which shows a cesium collection peak during and just after the ramp up to test temperature. This small average loss and collection rate peak during and just after the ramp up to test temperature (Fig. 15) is similar to that seen during the HRB-18 unbonded particle test. The HRB-18 particles had also been near DTF particles during irradiation, and unlike this test, no particles suffered large releases during their heating test (see Sect. 5.2).

The later, second peak in the deposition cup collection rate history (Fig. 15) is likely due to the three particles that released cesium above the contamination level, the contamination having long since left the particles in the ramp up to temperature. Together, the concept of initial batch particle contamination and later, large releases from three particles support the deposition cup cesium record for both experiments.

Small releases cannot be reliably determined solely by use of particle inventory measurements because of the uncertainty inherent in the pre- and postheating comparison. The deposition cup aggregate inventory and the furnace component inventory provide additional data about the fuel releases. The deposition cup activity has been described above; the furnace inventory is as follows (in μCi, corrected to end-of-irradiation, 5 Feb 1986):

Item	Activity (μCi) ^{134}Cs	^{137}Cs	^{154}Eu	Uncertainty
Fuel support holder	59.0	22.0	0.9	50%
Bottom door and thermocouple	7.9	3.0	0	50%
Tantalum shield	0.2	0.1	0	50%
Spool piece	1.9	0.9	0	50%
Debris at furnace bottom	0.7	0.1	0	50%
Debris from muffle tube and liner	1.3	0.4	0	50%
Gate valve	4.5	1.8	0	50%
Tantalum liner	158.0	57.0	0	50%
Fuel holder parts	3.3	1.3	5.4	6%
Furnace total	237.0	86.0	6.3	50%

The rather large uncertainty is due to the difficulty of gamma counting the large, odd-sized parts.

Using all of the collected data, the release fraction can be computed using information with less uncertainty. The respective inventories in μCi (decayed to 5 Feb 1986) are:

Item	Activity (μCi) ^{134}Cs	^{137}Cs	^{154}Eu	Uncertainty
HRB-17 all furnace parts	237	86	6.3	50%
HRB-17 deposition cups	413	154	0	6%
HRB-17 total	650	240	6.3	19%
HRB-17 measured particle release	250	96	5.8	7%
HRB-17 difference	400	144	0.5	31%
HRB-17 preheat inventory	21,120	8000	303.0	6%
Total fractional loss	3.1%	3.0%	2.1%	21%
Contamination loss	1.9%	1.8%	0.0%	32%
Release loss	1.2%	1.2%	2.1%	9%

The total fractional loss is the total release divided by the total preheating inventory. The release loss is the release by the four "leaking" particles divided by the total preheating inventory.

The contamination loss is the difference between the total release and the release by the four "leaking" particles divided by the total preheating inventory. Note that when the analysis includes the deposition cup and furnace component data, as well as the particle data, the loss for ^{134}Cs and ^{137}Cs is the same, which is what one would expect. This result is within the uncertainty limits of the particle data.

5.1.2 Gaseous Fission Products

During the heating, the furnace effluent was monitored for ^{85}Kr released from the particles. As of this date, the krypton inventory of a representative particle has not been measured because the low activity of the contained ^{85}Kr is masked by the activity of radionuclides such as ^{134}Cs, ^{137}Cs, ^{106}Ru, and ^{144}Ce making in situ particle measurements impossible. No indication of krypton release was observed. The detector history for both traps is shown in Fig. 20. At approximately hour 60, the detector background appeared to increase as indicated by the ratemeters. The ratemeters measure the activity in a broad energy band centered around the ^{85}Kr peak and provide an approximate indication of the trap activity and local background. The result of this shift in background level was an occasional, spurious signal and an increase in the minimum detectable krypton level. The direct cause of the background shift was determined to be contaminated dust that was trapped in a filter near the detectors. It is not clear how much the minimum detectable activity level had been increased due to the apparent change in the background; no spurious signal was greater than 6% of a single-particle krypton inventory. The average of the signals was approximately 1% of a single-particle inventory. Thus, the best estimate of the detector system data is that any krypton release was less than 1% of a single-particle inventory with no strong evidence for any release. See the discussion in the next section for more details about the expected krypton behavior.

The calibration of the detector system was checked both before and after the test. The detector peak location was also checked after the test and before the traps were warmed up and found to be acceptable. The agreement of the detector system with the calibration source was within 2% before the test and 1% after the test. The change in the detector system's response over the course of the test was $\leq$ 1%.

5.2 GAMMA-EMITTING FISSION PRODUCT RELEASE AT 1400° C

5.2.1 Metallic Fission Products

During the course of the heating, the deposition cups were changed twice a day with at least 3.7 h between changes. The handling and analysis of the deposition cups was the same as

ORNL-DWG-92-5174

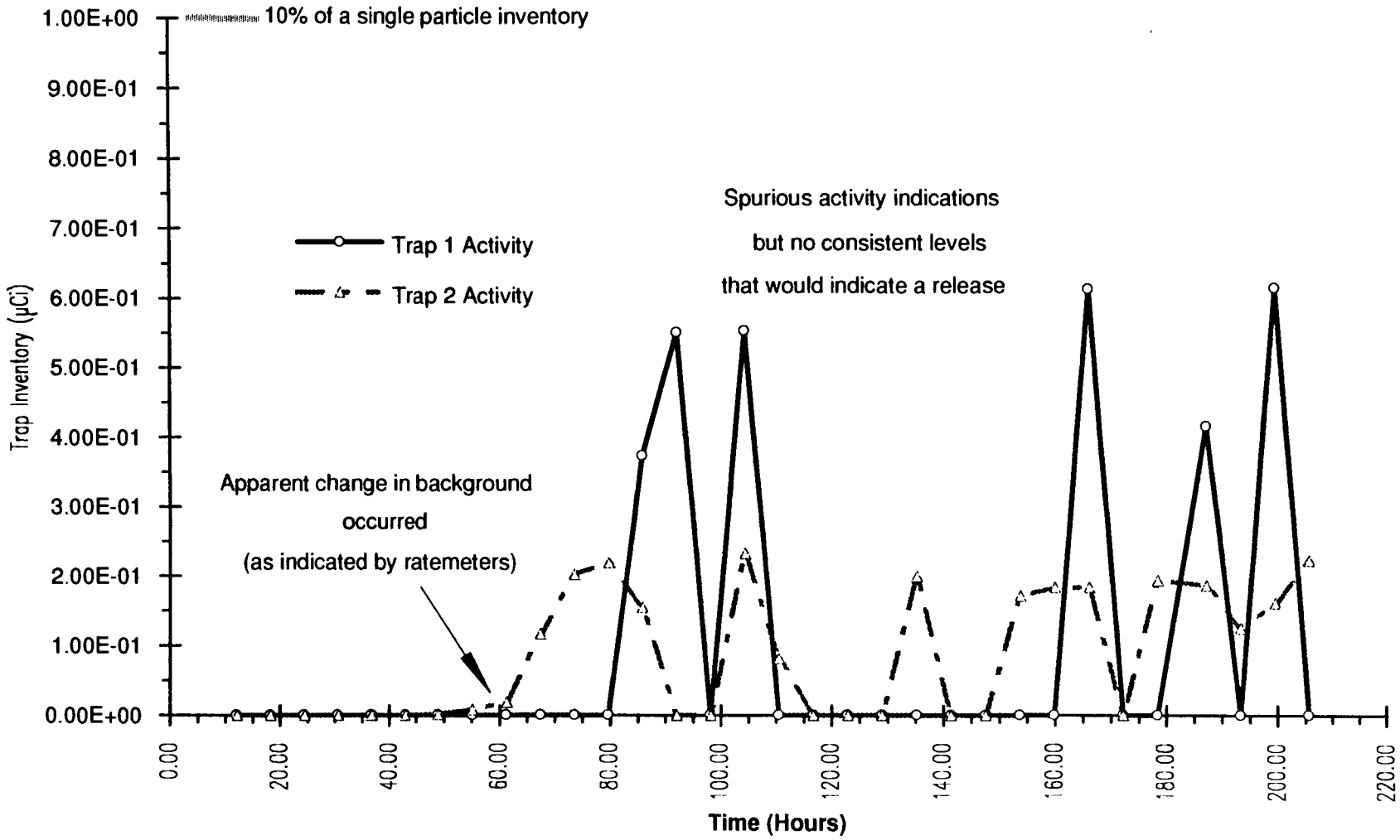

Fig. 20. Cumulative cold trap activities during 1600°C particle heatup test. No krypton release was observed.

that used for the 1600°C experiment. The integral cesium collected on the deposition cups is shown in Fig. 21 and Table 4. The maximum time a cup was in the furnace was 18.3 h; the minimum, 3.7 h. The cesium collection rate for the deposition cups is shown in Fig. 22. As can be seen, after an initial release lasting roughly 60 h, the release rate drops to a low level over a period of 100 h.

The particles were measured in the same way as described in the previous section, and visual and gamma spectrometric examination of the particles on an individual basis indicate that none suffered a coating failure. The overall data trend indicates that, on average, the particles lost ^{134}Cs and ^{137}Cs during the heating as was the case for the particles heated at 1600°C. The ratio between the average postheating particle inventory and the average preheating inventory is:

Radionuclide	Post/Preheating
^{134}Cs	0.98 ± 0.02
^{137}Cs	0.98 ± 0.01
^{106}Ru	1.06 ± 0.09
^{144}Ce	1.01 ± 0.02
^{154}Eu	1.02 ± 0.03
^{155}Eu	1.04 ± 0.12

Again, the two cesium isotopes were the only radionuclides to have a predominately lower average postheating than preheating inventory. As before, only ^{134}Cs, ^{137}Cs, ^{144}Ce, and ^{154}Eu will be considered. The percent change in particle inventory for ^{134}Cs, ^{137}Cs, ^{144}Ce, and ^{154}Eu on a per-particle basis is shown in Figs. 23 through 26. Note that ^{134}Cs and ^{137}Cs, Figs. 23 and 24, respectively, show a net decrease for almost all the particles, while ^{144}Ce shows the expected random differential measurement increase and decrease on a per-particle basis with a small average increase above the baseline. Detailed particle inventories of ^{134}Cs, ^{137}Cs, ^{144}Ce, ^{154}Eu, ^{155}Eu, and ^{106}Ru, both before and after heating, are tabulated in Table 2.

These inventory changes are small and at the repeatability limit of the equipment. Clearly, the cesium loss is supported by the deposition cup record, and the estimated average loss of 2.1% for ^{134}Cs and 2.6% for ^{137}Cs corresponds roughly (within a factor of 2 to 4) with the average estimated loss from the non-releasing particles heated at 1600°C, which were irradiated in capsule HRB-17 under conditions similar to those in capsule HRB-18.

ORNL-DWG-92-5175

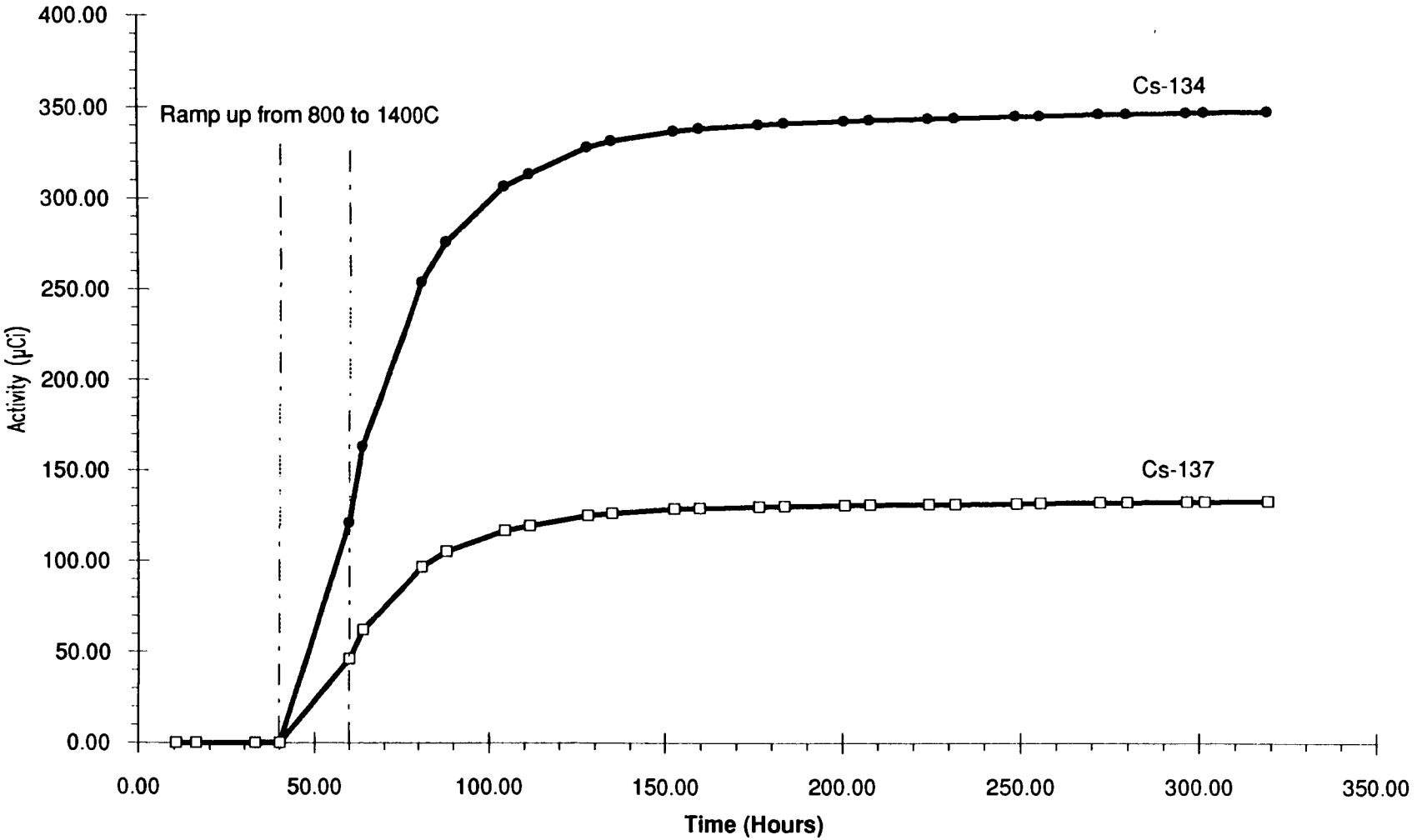

Fig. 21. Integrated deposition cup cesium collection as a function of time for the 1400°C test. Corrected to 5 Feb. 1986.

Table 4. 1400°C deposition cup cesium data. Corrected to 5 Feb 1986.

1400°C (HRB-18) Deposition Cup Results

Cup	Experimental Time (h)	Rate Time (h)	Date In	Time In	Temperature In (C)	Date Out	Time Out	Temperature Out (C)	Elapsed Time (h)	Measured Cs-134 (µCi)	Cs-134 Rate (µCi/h)	Total Cs-134 (µCi)	Measured Cs-137 (µCi)	Cs-137 Rate (µCi/h)	Total Cs-137 (µCi)
1	10.67	5.33	9/9/91	23:30	25	10/9/91	10:10	300	10.67	0.00	0.00	0.00	0.00	0.00	0.00
2	16.20	13.57	10/9/91	10:26	300	10/9/91	15:42	300	5.27	0.00	0.00	0.00	0.00	0.00	0.00
3	33.17	24.75	10/9/91	15:50	300	11/9/91	8:40	800	16.83	0.06	0.00	0.06	0.02	0.00	0.02
4	40.08	36.67	11/9/91	8:45	800	11/9/91	15:35	800	6.83	0.24	0.04	0.30	0.09	0.01	0.11
7	60.00	50.13	11/9/91	15:45	800	12/9/91	11:30	1400	19.75	120.30	6.09	120.60	46.03	2.33	46.14
8	63.92	62.07	12/9/91	11:43	1400	12/9/91	15:25	1400	3.70	42.27	11.42	162.87	15.93	4.31	62.07
9	81.12	72.66	12/9/91	15:42	1400	13/9/91	8:37	1400	16.92	90.96	5.38	253.83	34.32	2.03	96.39
11	88.15	84.66	13/9/91	8:40	1400	13/9/91	15:39	1400	6.98	22.29	3.19	276.12	8.52	1.22	104.91
13	104.55	96.46	13/9/91	15:52	1400	14/9/91	8:03	1400	16.18	30.63	1.89	306.75	11.78	0.73	116.69
14	111.75	108.15	14/9/91	8:03	1400	14/9/91	15:15	1400	7.20	6.79	0.94	313.54	2.56	0.36	119.25
15	128.17	119.02	14/9/91	13:22	1400	15/9/91	7:40	1400	18.30	14.79	0.81	328.33	5.64	0.31	124.89
16	134.98	131.72	15/9/91	7:57	1400	15/9/91	14:29	1400	6.53	3.38	0.52	331.70	1.29	0.20	126.18
17	152.73	143.98	15/9/91	14:44	1400	16/9/91	8:14	1400	17.50	5.48	0.31	337.19	2.08	0.12	128.25
18	159.87	156.44	16/9/91	8:31	1400	16/9/91	15:22	1400	6.85	1.22	0.18	338.40	0.47	0.07	128.73
19	176.55	168.34	16/9/91	15:38	1400	17/9/91	8:03	1400	16.42	2.30	0.14	340.70	0.91	0.06	129.64
20	183.77	180.32	17/9/91	8:22	1400	17/9/91	15:16	1400	6.90	0.67	0.10	341.37	0.26	0.04	129.90
21	200.88	192.46	17/9/91	15:32	1400	18/9/91	8:23	1400	16.85	1.41	0.08	342.78	0.58	0.03	130.48
22	208.02	204.58	18/9/91	8:38	1400	18/9/91	15:31	1400	6.88	0.45	0.07	343.24	0.18	0.03	130.66
23	224.58	216.43	18/9/91	15:46	1400	19/9/91	8:05	1400	16.32	0.76	0.05	343.99	0.30	0.02	130.96
24	231.95	228.46	19/9/91	6:28	1400	19/9/91	15:27	1400	6.98	0.35	0.05	344.35	0.15	0.02	131.11
25	249.15	240.67	19/9/91	15:41	1400	20/9/91	8:39	1400	16.97	0.84	0.05	345.18	0.33	0.02	131.45
26	255.73	252.58	20/9/91	8:55	1400	20/9/91	15:14	1400	6.32	0.27	0.04	345.46	0.11	0.02	131.56
27	272.43	264.20	20/9/91	15:28	1400	21/9/91	7:56	1400	16.47	0.66	0.04	346.11	0.25	0.02	131.81
28	280.05	276.36	21/9/91	8:10	1400	21/9/91	15:33	1400	7.38	0.19	0.03	346.30	0.07	0.01	131.88
29	296.57	288.43	21/9/91	15:48	1400	22/9/91	8:04	1400	16.27	0.58	0.04	346.88	0.23	0.01	132.11
30	301.57	299.18	22/9/91	8:17	1400	22/9/91	13:04	1400	4.78	0.13	0.03	347.02	0.05	0.01	132.17
31	319.33	310.51	22/9/91	13:11	1400	23/9/91	6:50	100	17.65	0.42	0.02	347.44	0.18	0.01	132.35

ORNL-DWG-92-5176

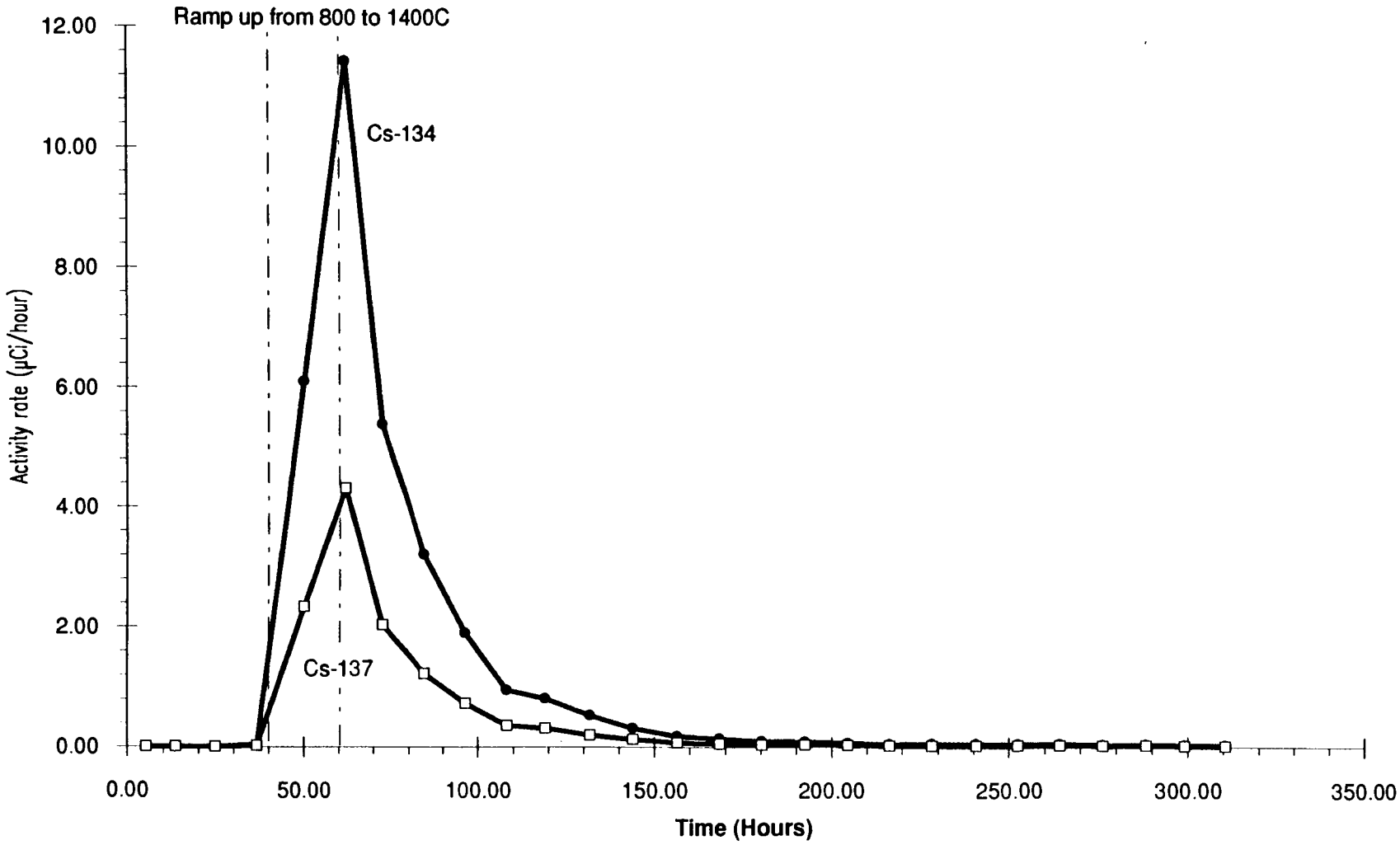

Fig. 22. Deposition cup cesium collection rate as a function of time for the 1400°C test. Corrected to 5 Feb 1986.

ORNL-DWG-92-5177

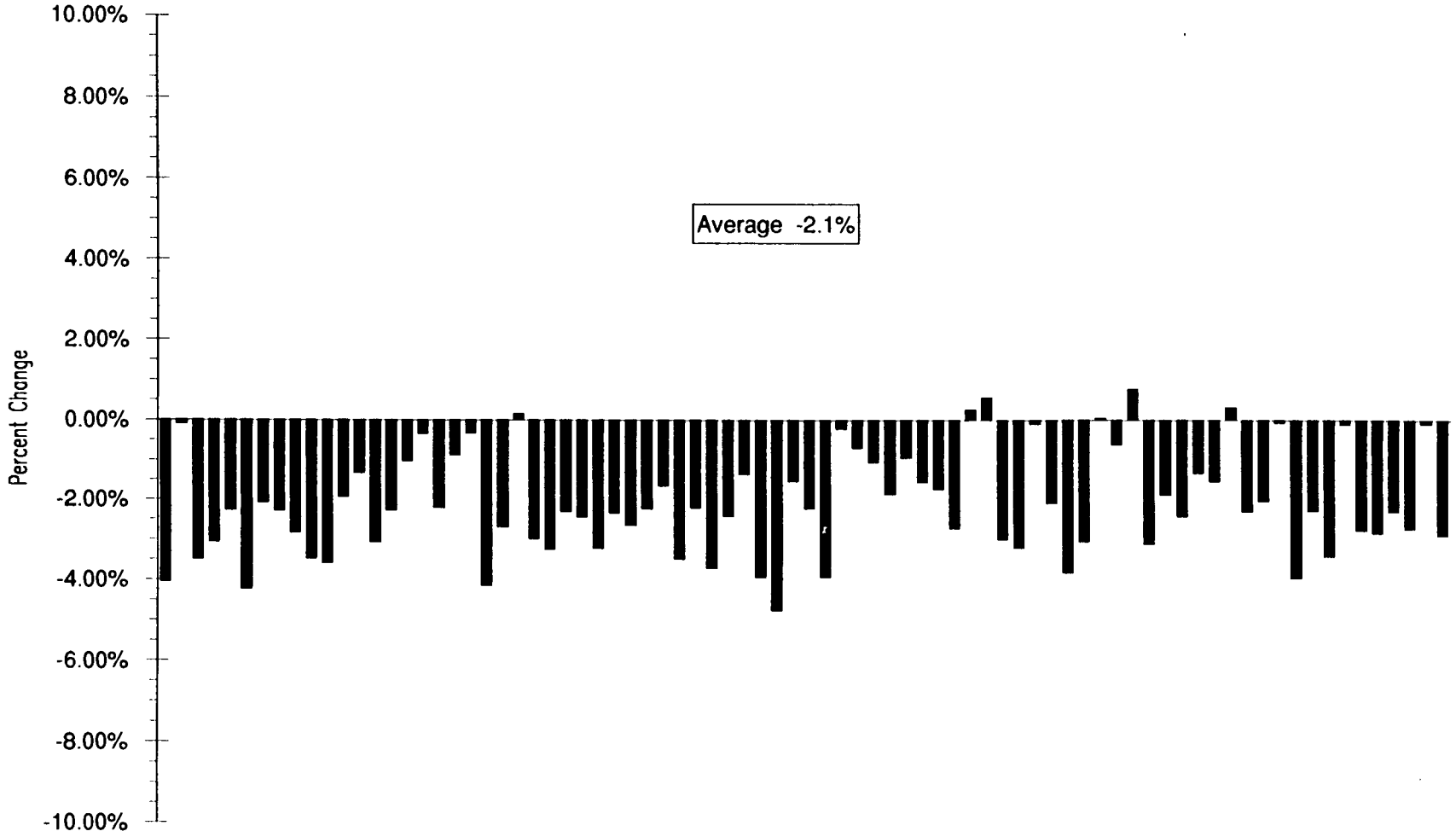

Fig. 23. Measured change in particle Cs-134 inventory on a particle-by-particle basis for the 1400°C test. Note downward trend.

ORNL-DWG-92-5178

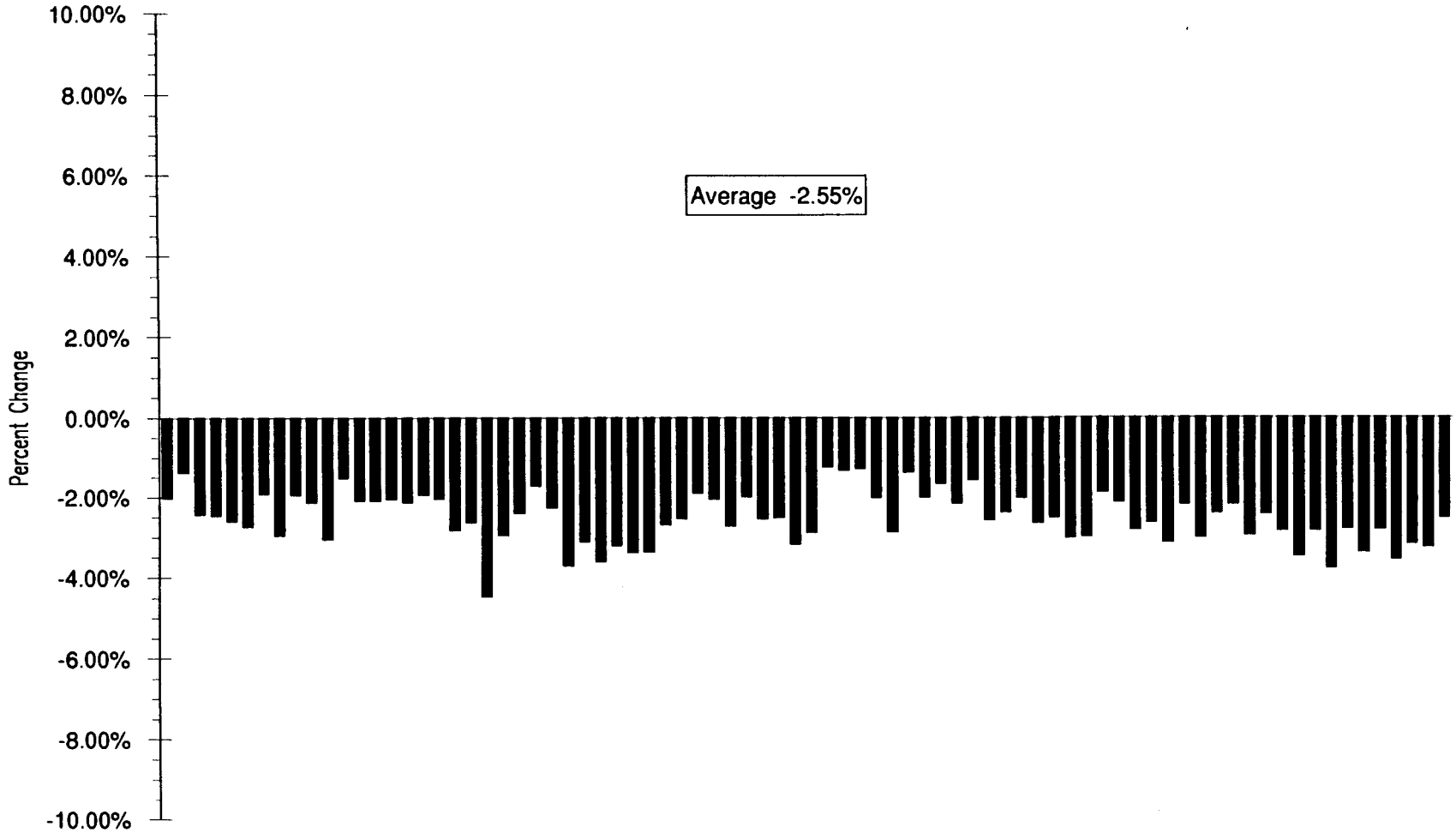

Fig. 24. Measured change in particle Cs-137 inventory on a particle-by-particle basis for the 1400°C test. Note downward trend.

ORNL-DWG-92-5179

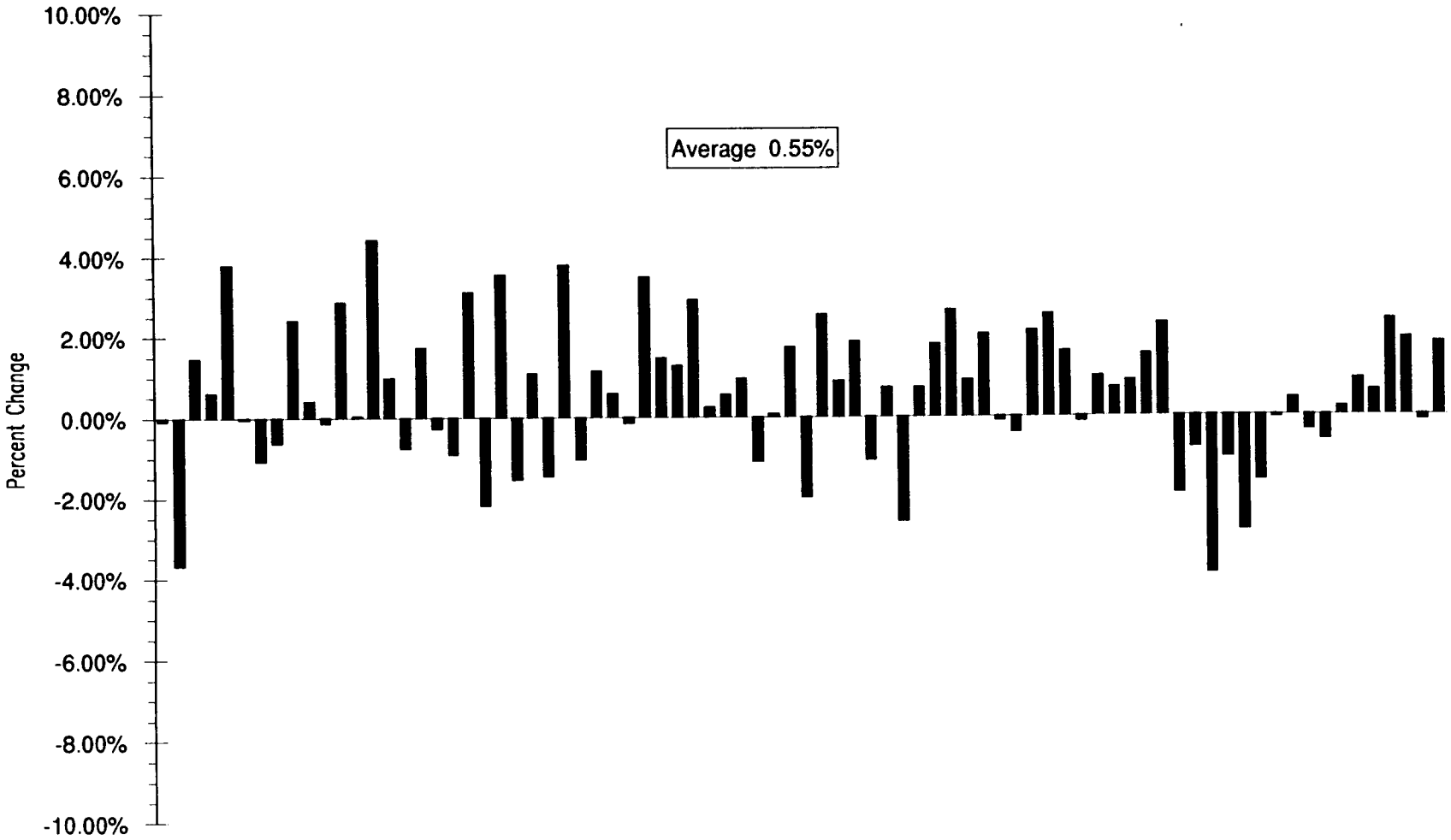

Fig. 25. Measured change in particle Ce-144 inventory on a particle-by-particle basis for the 1400°C test. Note random scatter.

ORNL-DWG-92-5180

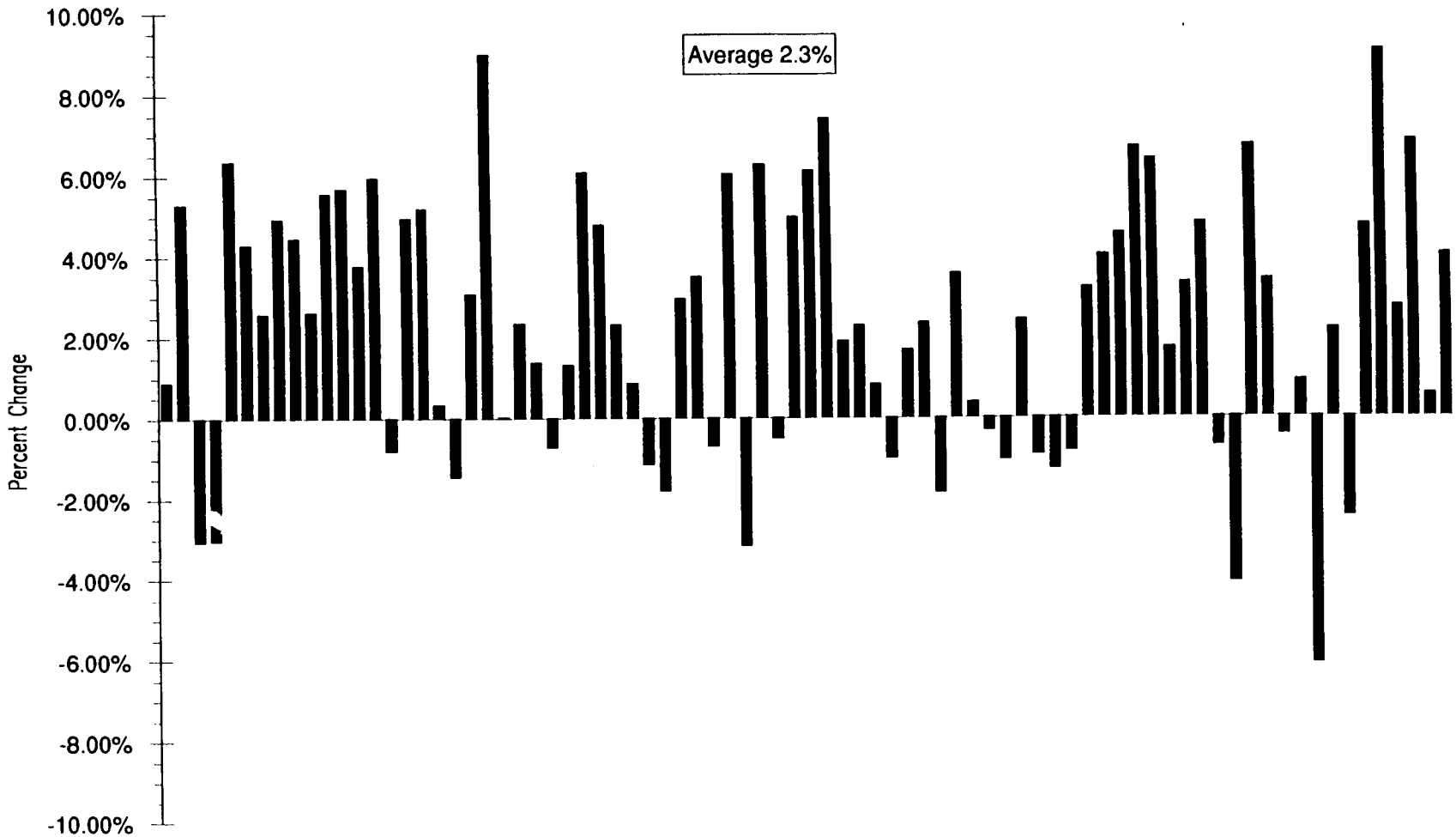

Fig. 26. Measured change in particle Eu-154 inventory on a particle-by-particle basis for the 1400°C test.

As with the HRB-17 heated fuel, small releases in the HRB-18 heated fuel cannot be reliably determined solely by use of particle inventory measurements, and the deposition cup and furnace component inventories must be used to reduce the uncertainties. The deposition cup inventories and the furnace component inventories are (in μCi, corrected to 5 Feb 1986):

	Activity (μCi)			
Item	^{134}Cs	^{137}Cs	^{154}Eu	Uncertainty
Fuel support and tantalum shield	5.5	2.1	0	50%
Bottom door	1.4	0.5	0	50%
Thermocouple	6.4	2.4	0	50%
Spool piece	4.5	1.7	0	50%
Deposits on cold finger	1.7	0.6	0	50%
Gate valve	1.3	0.5	0	50%
Fuel holder parts	0.6	0.5	0	6%
Furnace total	21.0	8.0	0	50%

The furnace parts used in the HRB-18 test furnace inventory total are different than those used in the HRB-17 test inventory because the activity was much lower and distributed in a slightly different fashion.

Using all of the above data, the releases can be computed (in μCi, decayed to 5 Feb 1986) as follows:

	Activity (μCi)			
Item	^{134}Cs	^{137}Cs	^{154}Eu	Uncertainty
HRB-18 all furnace parts	21	8	0	50%
HRB-18 deposition cups	347	132	0	6%
HRB-18 total	368	140	0	6%
HRB-18 preheat inventory	20,800	8080	301	6%
Total fraction loss	1.8%	1.7%	0.0%	9%

Again, note that when the analysis includes the deposition cup and furnace component data, as well as the particle data, the loss for ^{134}Cs and ^{137}Cs is the same, which is what one would expect. This result is within the uncertainty limits of the particle data.

5.2.2 Gaseous Fission Products

During the heating, the furnace effluent was monitored for ^{85}Kr release from the particles. No indication of krypton release was observed. The detector history for both traps is shown in Fig. 27. As can be seen, there is no sustained krypton inventory indicated by the detectors, only random noise peaks. After the power supply failure, the detector system and furnace flow remained in their normal condition for one counting period, 6 h, to determine if any krypton had been released during the rapid cooldown; none was detected. In the shutdown mode, trap 1 was warmed up to allow its contents to transfer to trap 2. Finally, the water condenser was warmed up to allow its contents to travel to trap 2. The purpose of this transfer and warmup was to reconcentrate any krypton that may have migrated within cold trap 1 and to empty the contents of the condenser into cold trap 2 in order to determine if some krypton may have been held up in it. This last operation resulted in the plugging of trap 2, as expected, but since no further flow was required, no problems were created. Other than the spurious signals at or below the detectability limit, no indication of krypton in the traps was observed. After the counting of trap 2 was complete, its contents were examined by the RGA as previously discussed.

The minimum detectable activity level (MDAL) was estimated on the assumption that changes in the background activity level over the time of the experiment are negligible and that electronic drift would also be inconsequential. As shown in Fig. 27, an occasional noise spike can exceed the MDAL. Previous experience with this trap system during ^{85}Kr tracer studies indicated that the krypton can be held for long periods of time with an apparent inventory decay of no more than about 1% per day (due to migration within the trap).[4] Therefore, while rapid increases in trap krypton inventory are possible due to fuel release, the trap krypton decay time would be measured in weeks as long as the trap remained cooled. No behavior of this nature is indicated by Figs. 27 or 20, supporting the conclusion that no measurable krypton was released by the particles in either test.

Again, the calibration of the detector system was checked both before and after the test. The agreement of the detector systems with the calibration source was within 2.5% before the test and 3% after the test. The change in the detector systems' response over the course of the test was $\leq$ 1%.

ORNL-DWG-92-5181

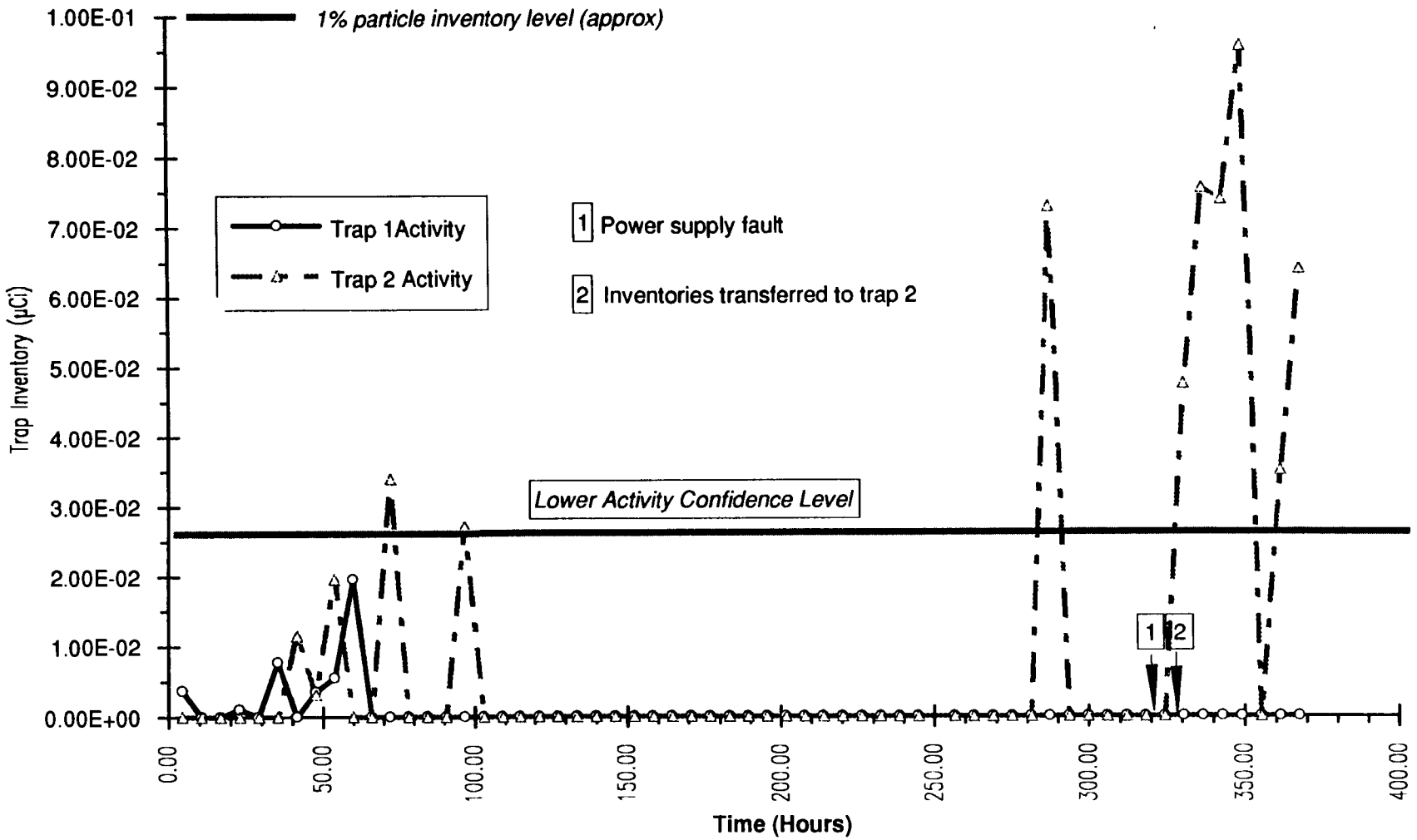

Fig. 27. Cumulative cold trap activities during 1400°C particle heatup test. No krypton-85 release was observed.

5.3 STRONTIUM RELEASE AT 1600° C

The strontium inventory of representative deposition cups, furnace parts, and representative particles was determined by radiochemical methods. The graphite parts were burned and the residual ash used in the analysis. These methods were required because, unlike the other radionuclides of interest, ^{90}Sr emits beta particles rather than the more easily measured gamma rays.

Because the strontium analysis was a destructive technique, a pre- and postheating particle inventory measurement was not possible. However, five unheated and five heated particles were analyzed to obtain representative measurements. The analysis of the five unheated particles was detailed in a previous section. The analysis of five heated particles resulted in four useable inventories. The analysis of one particle yielded results that were several orders of magnitude outside of the others. No reason other than lab error could be determined for this result. The average values of ^{144}Ce and ^{154}Eu were in good agreement with inventories based on the gamma scanning measurements, with a difference of less than 10%. A less favorable agreement, 18% difference, was obtained with ^{155}Eu. As in the preheating work, poor agreement was obtained for ^{134}Cs and ^{137}Cs with an error of 40%. The agreement between the measured ^{90}Sr and its calculated value was 1%. The average ^{90}Sr value was 100 μCi with an uncertainty of 5% (first standard deviation).

Because of the relatively large uncertainties, no information on particle performance could be obtained from the average pre- and postheating ^{90}Sr inventories. A much larger change in the average inventory would have been necessary.

The ^{90}Sr content of the deposition cups was determined by leaching the cups and analyzing the leachant. After the strontium content of the deposition cups had been determined, the process leachant was gamma counted for ^{134}Cs and ^{137}Cs as a consistency check. The aggregate ^{134}Cs and ^{137}Cs activity, as determined by radiochemical methods, was within 16% of the dry gamma-counting result.

The integrated ^{90}Sr deposition cup collection is shown in Fig. 28 and the values tabulated in Table 5. Note that collection begins approximately 15 h after the test temperature is reached and continues throughout the test. The ^{90}Sr collection rate, Fig. 29, starts after the test temperature is reached and increases for approximately 50 h. It stabilizes at this point and remains constant (within the data scatter) until the termination of the experiment.

In an effort to obtain the total ^{90}Sr release, the tantalum liner and the tantalum heat shield were leached and the leachant analyzed for ^{134}Cs, ^{137}Cs, ^{144}Ce, ^{154}Eu, ^{155}Eu, and ^{90}Sr. In addition,

ORNL-DWG-92-5182

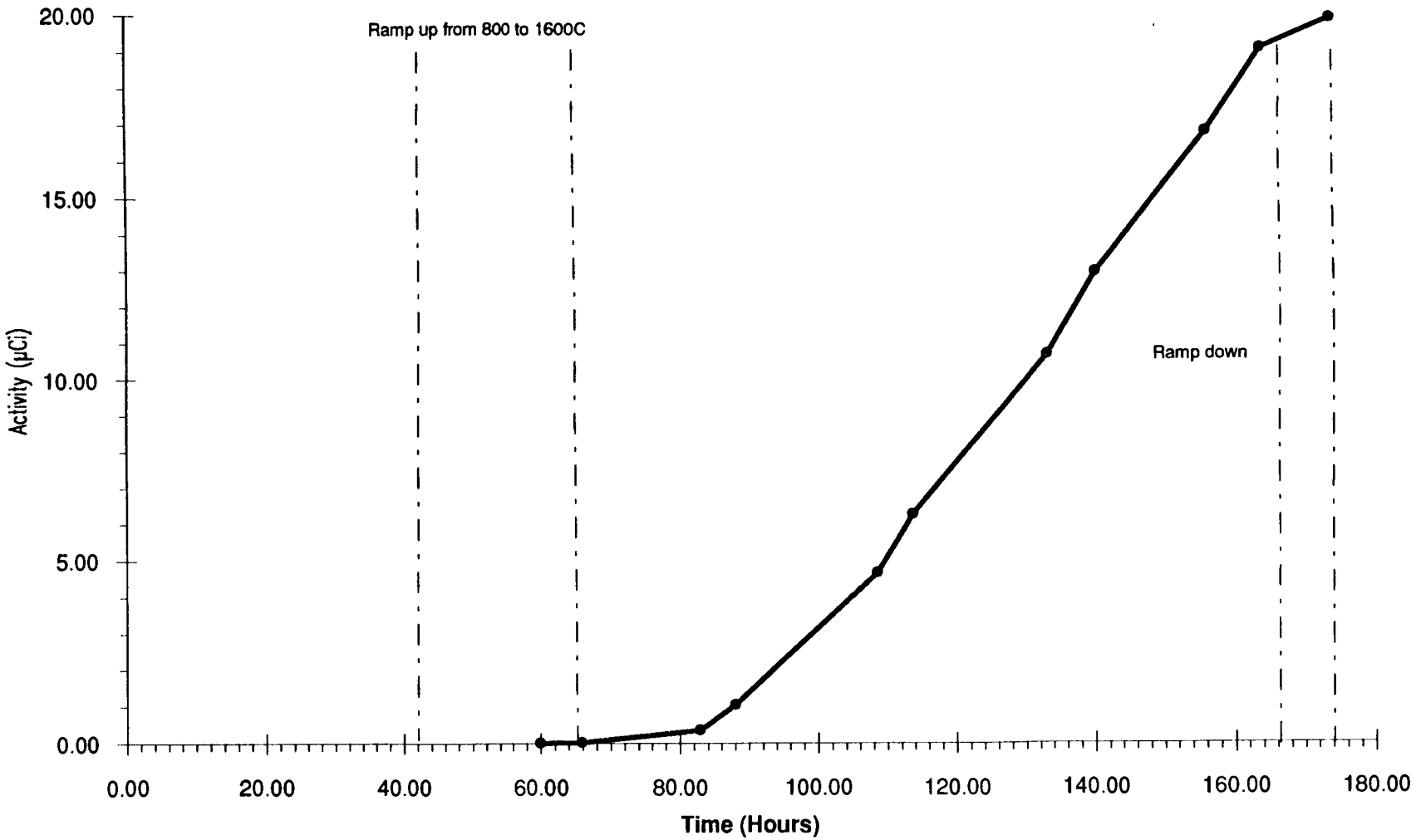

Fig. 28. Integrated deposition cup strontium collection as a function of time for the 1600°C test. Corrected to 5 Feb 1986.

Table 5. 1600°C deposition cup strontium data. Corrected to 5 Feb 1986.

1600°C (HRB-17) Deposition Cup Results

Cup	Experimental Time (h)	Rate Time (h)	Date In	Time In	Temperature In (C)	Date Out	Time Out	Temperature Out (C)	Elaspsed Time (h)	Measured Sr-90 (μCi)	Sr-90 Rate (μCi/h)	Total Sr-90 (μCi)
36	60.00	51.13	24/10/91	14:35	858	25/10/91	8:19	1437	17.73	0.00	0.00	0.00
37	65.93	63.82	25/10/91	10:01	1437	25/10/91	14:15	1600	4.23	0.01	0.00	0.01
38	82.93	74.55	25/10/91	14:29	1600	26/10/91	7:15	1600	16.77	0.35	0.02	0.36
39	88.07	85.62	26/10/91	7:29	1600	26/10/91	12:23	1600	4.90	0.69	0.14	1.05
40	108.63	98.47	26/10/91	12:38	1600	27/10/91	8:57	1600	20.32	3.62	0.18	4.67
41	113.77	111.30	27/10/91	9:09	1600	27/10/91	14:05	1600	4.93	1.58	0.32	6.25
42	133.08	123.54	27/10/91	14:19	1600	28/10/91	9:24	1600	19.08	4.39	0.23	10.64
43	140.12	136.79	28/10/91	9:47	1600	28/10/91	16:26	1600	6.65	2.29	0.34	12.93
44	156.17	148.32	28/10/91	16:48	1600	29/10/91	8:29	1600	15.68	3.83	0.24	16.76
45	164.02	160.31	29/10/91	8:55	1600	29/10/91	16:20	1600	7.42	2.28	0.31	19.04
46	174.02	169.13	29/10/91	16:34	1600	30/10/91	2:20	25	9.77	0.83	0.09	19.87

ORNL-DWG-92-5183

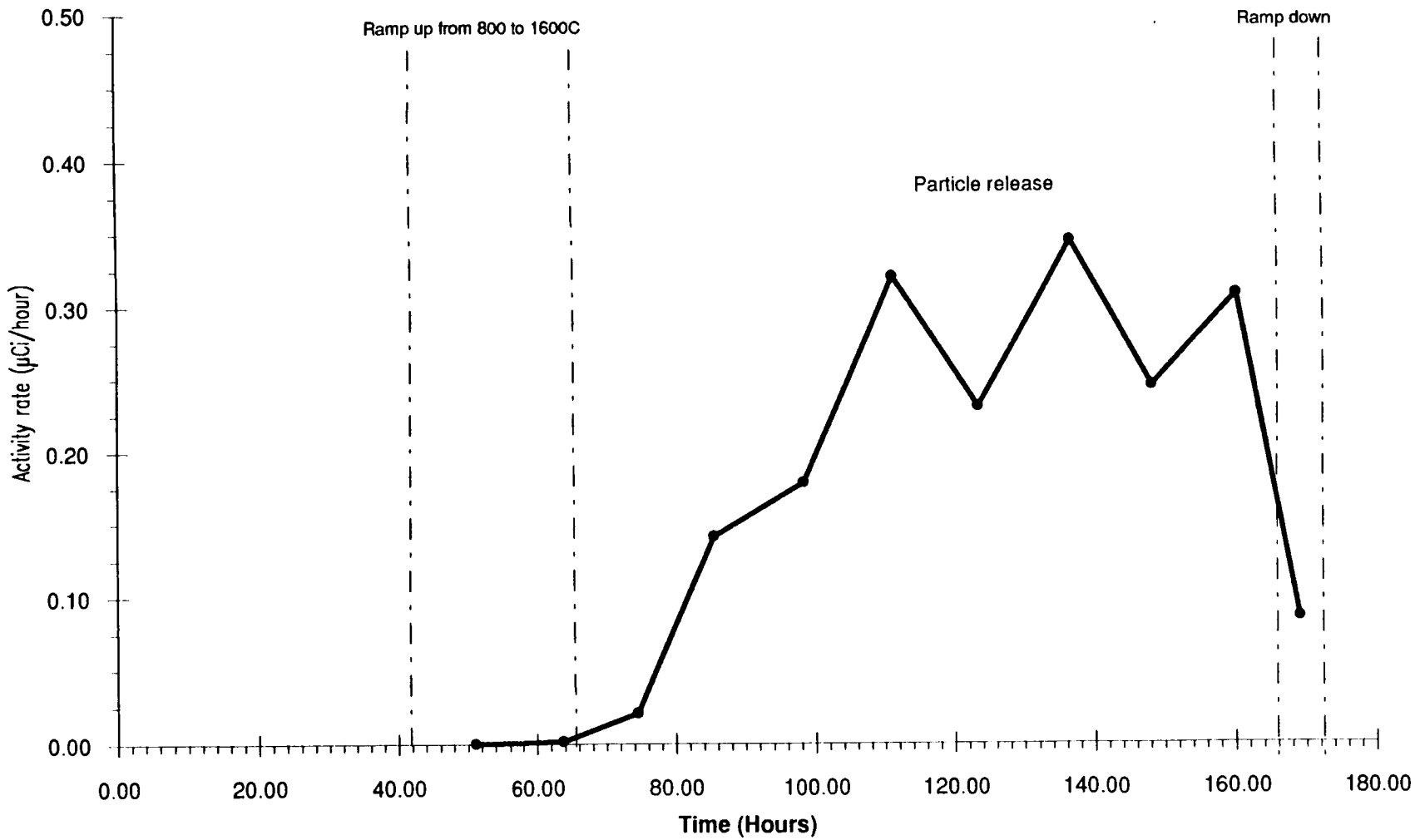

Fig. 29. Deposition cup strontium collection rate as a function of time for the 1600°C test. Corrected to 5 Feb 1986.

the fuel holder components and the fuel holder support were burned and the ash analyzed for the same radionuclides. Unfortunately, there was a factor of three disagreement between the cesium and europium values determined by this process and those measured by the gamma counting, with the leaching and burning having the lower values. It is not known whether the ^{90}Sr values of these components have acceptable error limits. Therefore, the accuracy of the computed release is low. The strontium values, in μCi and corrected to 5 Feb 1986, are:

Item	^{90}Sr	Uncertainty
Furnace components	80	100+%
Deposition cups	20	16%
Total	100	100+%
Estimated fractional loss	1.5%	100+%

The loss is based on an average particle inventory of 86 μCi (radiochemical analysis). The loss of 1.5% is similar to the cesium and europium losses.

5.4 STRONTIUM RELEASE AT 1400° C

The strontium inventory of representative deposition cups, furnace parts, and representative particles was determined in the same way as was done in the 1600° C test.

Again, five unheated and five heated particles were analyzed to obtain representative measurements. The analysis of the five unheated particles was detailed in a previous section. The analysis of five heated particles resulted in four useable inventories. Again, one particle yielded results that were orders of magnitude off and was dropped from the analysis. The average values of ^{144}Ce, ^{154}Eu, and ^{155}Eu were in good agreement with predicted inventories based on the gamma-scanning measurements, with a difference of less than 9%. As in the preheating work, poor agreement was obtained for ^{134}Cs and ^{137}Cs with an error of over 34%. The agreement between the measured ^{90}Sr and its calculated value was 5%. The average ^{90}Sr value was 94 μCi with an uncertainty of 12% (first standard deviation).

Again, the relatively large uncertainty in the ^{90}Sr inventories prevented any useful pre- and postheating comparisons.

The strontium analysis of the deposition cups for the 1400°C test was also performed by leaching. Again, the ^{134}Cs and ^{137}Cs activities were determined by radiochemical techniques and compared to the dry-counting method as a consistency check. The aggregate activity agreed within 7%.

The integrated ^{90}Sr deposition cup collection is shown in Fig. 30 and the values tabulated in Table 6. Note that, unlike the 1600°C test, the amount of ^{90}Sr collected is very small and occurs mainly in the first part of the test. The ^{90}Sr collection rate, Fig. 31, shows a collection spike during the ramp up to temperature phase of the heating program and a rapid collection decay soon afterward. As was seen in the cesium collection, this is characteristic of surface contamination.

In an effort to obtain the total ^{90}Sr release, the tantalum liner and the tantalum heat shield were leached and the furnace internal components ashed as was done for the 1600°C test. Again, there was a large disagreement between the cesium values determined by this process and those measured by the gamma counting, with the leaching and burning having the lower values. It is not known whether the ^{90}Sr values of these components have acceptable error limits. Therefore, the accuracy of the computed release is low. The strontium values, in μCi and corrected to 5 Feb 1986, are:

Item	^{90}Sr	Uncertainty
Furnace components	0.44	100+%
Deposition cups	0.01	7%
Total	0.45	100+%
Estimated fractional loss	6×10^{-3}%	100+%

The loss is based on an average particle inventory of 94 μCi. This very small loss is indicative of contamination.

5.5 COMPARISON OF 1400 AND 1600°C TEST RELEASE BEHAVIOR

The integrated cesium collection for the 1600°C test and the first half of the 1400°C test is shown in Fig. 32. In both cases the trends are similar, but the final tally is higher for the

ORNL-DWG-92-5184

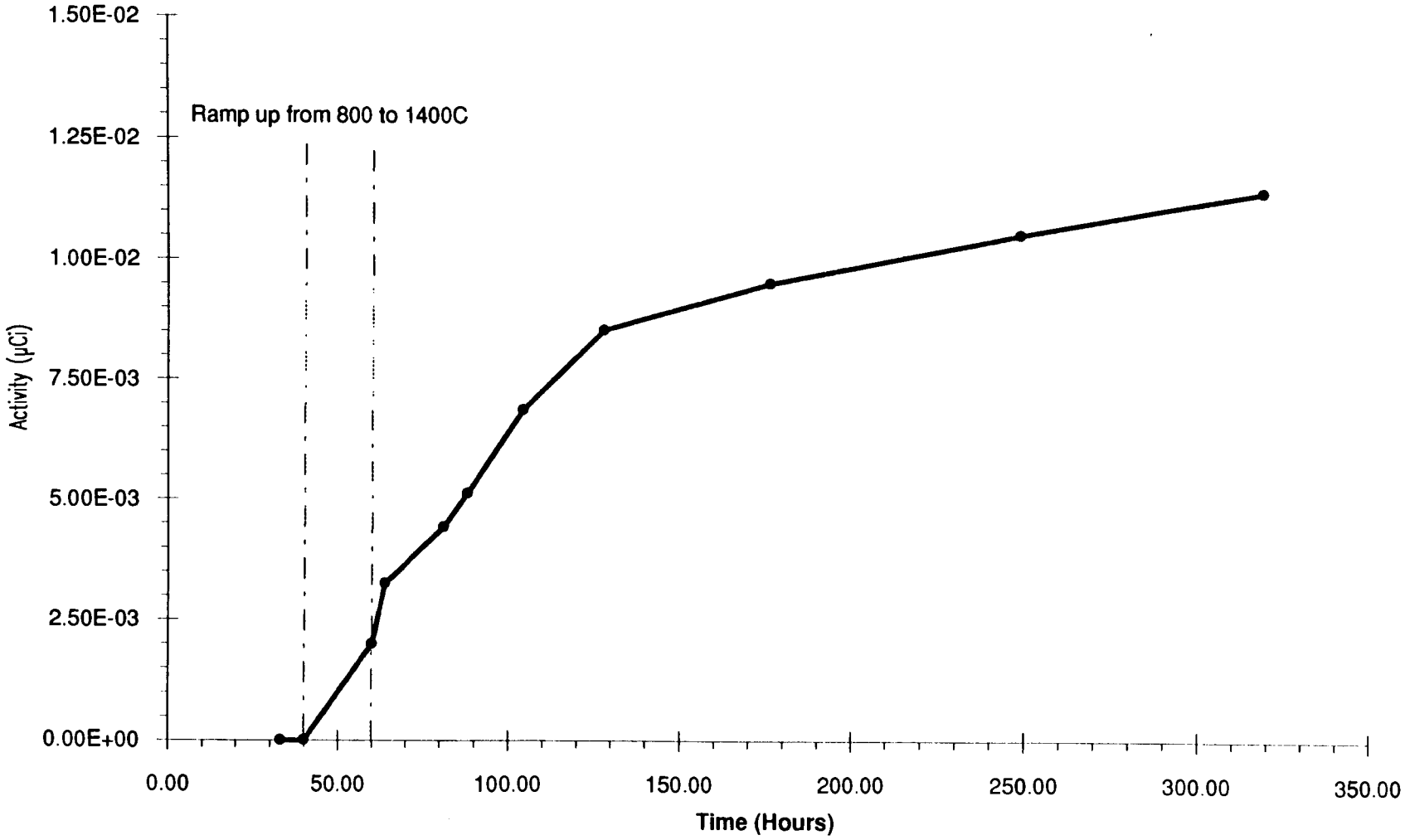

Fig. 30. Integrated deposition cup strontium collection as a function of time for the 1400°C test. Corrected to 5 Feb 1986.

Table 6. 1400°C test deposition cup strontium data. Corrected to 5 Feb 1986.

1400°C (HRB-18) Deposition Cup Results

Cup	Experimental Time (h)	Rate Time (h)	Date In	Time in	Temperature In (C)	Date Out	Time Out	Temperature Out (C)	Elapsed Time (h)	Measured Sr-90 (μCi)	Sr-90 Rate (μCi/h)	Total Sr-90 (μCi)
3	33.17	24.75	10/9/91	15:50	300	11/9/91	8:40	800	16.83	0.00E+00	0.00E+00	0.00E+00
4	40.08	36.67	11/9/91	8:45	800	11/9/91	15:35	800	6.83	0.00E+00	0.00E+00	0.00E+00
7	60.00	50.13	11/9/91	15:45	800	12/9/91	11:30	1400	19.75	1.99E-03	1.01E-04	1.99E-03
8	63.92	62.07	12/9/91	11:43	1400	12/9/91	15:25	1400	3.70	1.25E-03	3.38E-04	3.24E-03
9	81.12	72.66	12/9/91	15:42	1400	13/9/91	8:37	1400	16.92	1.17E-03	6.92E-05	4.41E-03
11	88.15	84.66	13/9/91	8:40	1400	13/9/91	15:39	1400	6.98	7.07E-04	1.01E-04	5.12E-03
13	104.55	96.46	13/9/91	15:52	1400	14/9/91	8:03	1400	16.18	1.74E-03	1.08E-04	6.86E-03
15	128.17	119.02	14/9/91	13:22	1400	15/9/91	7:40	1400	18.30	1.66E-03	9.07E-05	8.52E-03
19	176.55	168.34	16/9/91	15:38	1400	17/9/91	8:03	1400	16.42	9.82E-04	5.98E-05	9.50E-03
25	249.15	240.67	19/9/91	15:41	1400	20/9/91	8:39	1400	16.97	1.00E-03	5.89E-05	1.05E-02
31	319.33	310.51	22/9/91	13:11	1400	23/9/91	6:50	100	17.65	8.73E-04	4.95E-05	1.14E-02

ORNL-DWG-92-5185

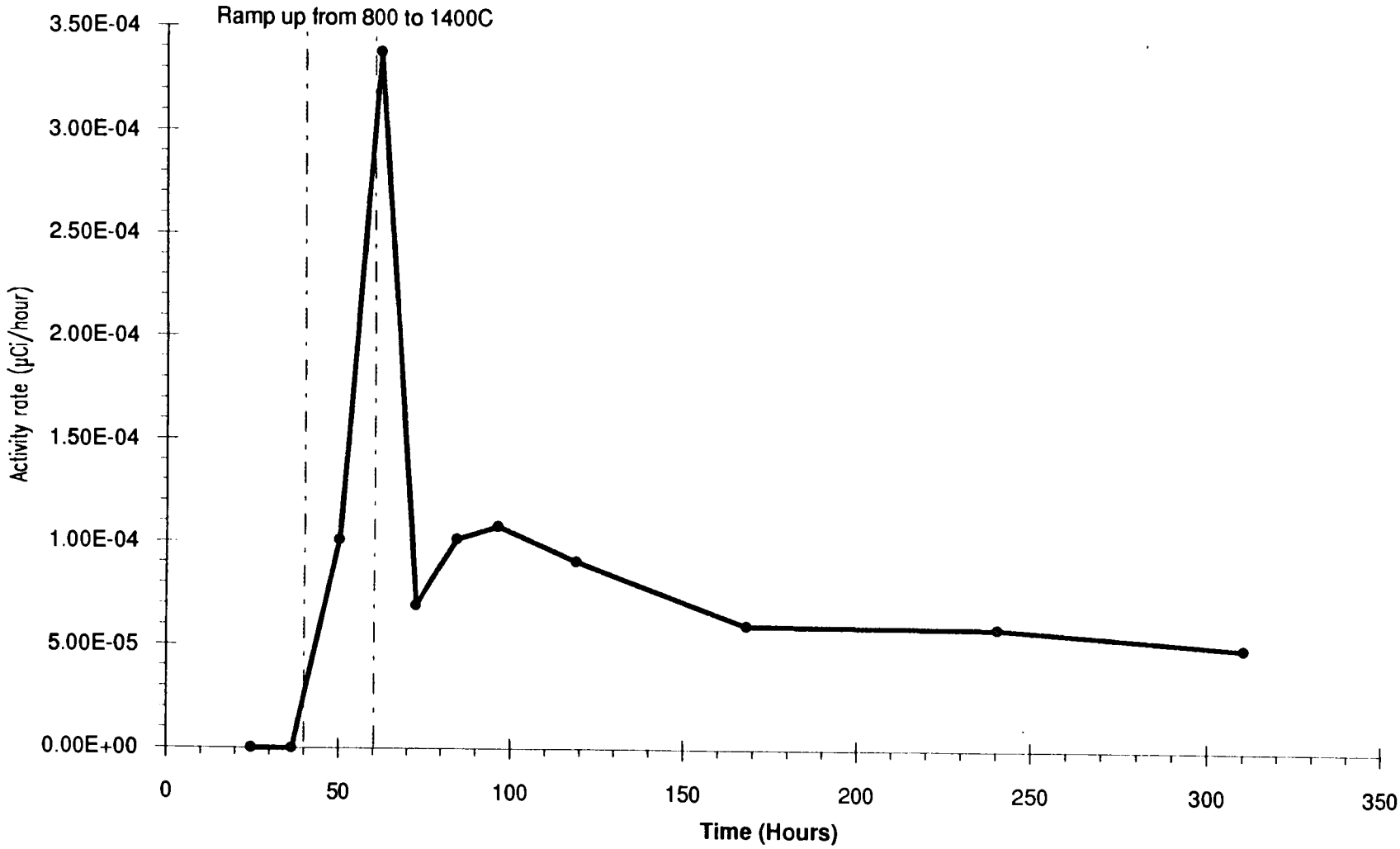

Fig. 31. Deposition cup strontium collection rate as a function of time for the 1400°C test. Corrected to 5 Feb 1986.

ORNL-DWG-92-5186

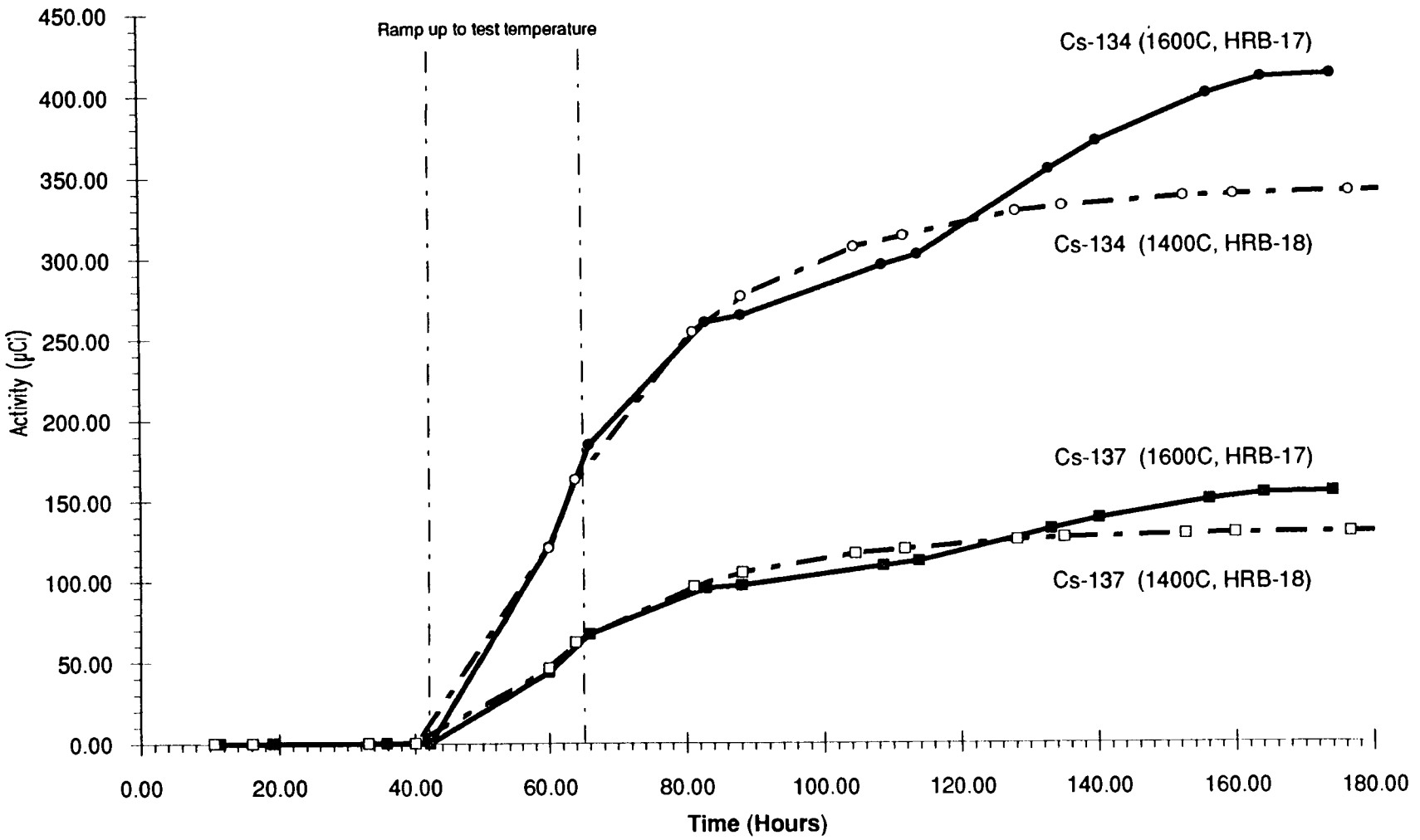

Fig. 32. Comparison between the 1600 and 1400°C integrated deposition cup cesium collection as a function of time. Corrected to 5 Feb 1986.

1600°C case because of the particle releases. The cesium collection rate for 1600 and 1400°C is compared in Fig. 33. Note that a large, initial peak in the collection rate took place during the ramp up to temperature for both tests. The time scale is approximately the same for both tests even though the final temperature was 200°C higher in the 1600°C test. The increased temperature in the 1600°C test resulted in a more rapid decay of the collection rate initial peak. This initial peak is the rapid release of the cesium surface contamination. Finally, note the second broad peak in the 1600°C (but not 1400°C) cesium release rate, indicating particle fission product release.

The strontium release in the 1400°C test is insignificant when compared with the 1600°C test. It occurs early in the test, rapidly decays, and appears to be due to a very small amount of contamination. The strontium release in the 1600°C test begins approximately 15 h after the test temperature is reached and continues throughout the experiment. The release dominates any low-level surface contamination.

In both tests, no krypton release was observed.

5.6 1600°C TEST FISSION PRODUCT MASS BALANCE

Despite the large uncertainties in the average particle loss (because of the small measurement differentials), a mass balance was estimated. This mass balance was calculated in two ways. The first method summed up the furnace component activities and the deposition cup activities and compared them with the measured particle losses. This method is the basis of this report and makes no assumptions as to the behavior of the measurement uncertainties. The second technique summed the furnace and deposition cup activities as well, but compared this sum to the particle releases normalized so that the ^{144}Ce release was zero. This approach was investigated because no ^{144}Ce was observed on the furnace parts or the deposition cups, and the particle measurements indicated a (small) nonphysical postheating ^{144}Ce gain. The cerium measurements also had reasonable counting statistics. This approach investigates the possibility that some of the measurement uncertainty may be due to a systematic error. No support for a systematic error was found.

Only ^{134}Cs, ^{137}Cs, and ^{154}Eu were considered in the mass balance calculations because they were the only detectable isotopes released in a measurable quantity; ^{155}Eu was not considered because of the poor counting statistics. Because some of the furnace parts are difficult to handle and measure, the uncertainties in the activities of these components are fairly high. A major effort to reduce these uncertainties was not considered worthwhile because of the even larger uncertainties in the average particle losses due to the measuring limits.

ORNL-DWG-92-5187

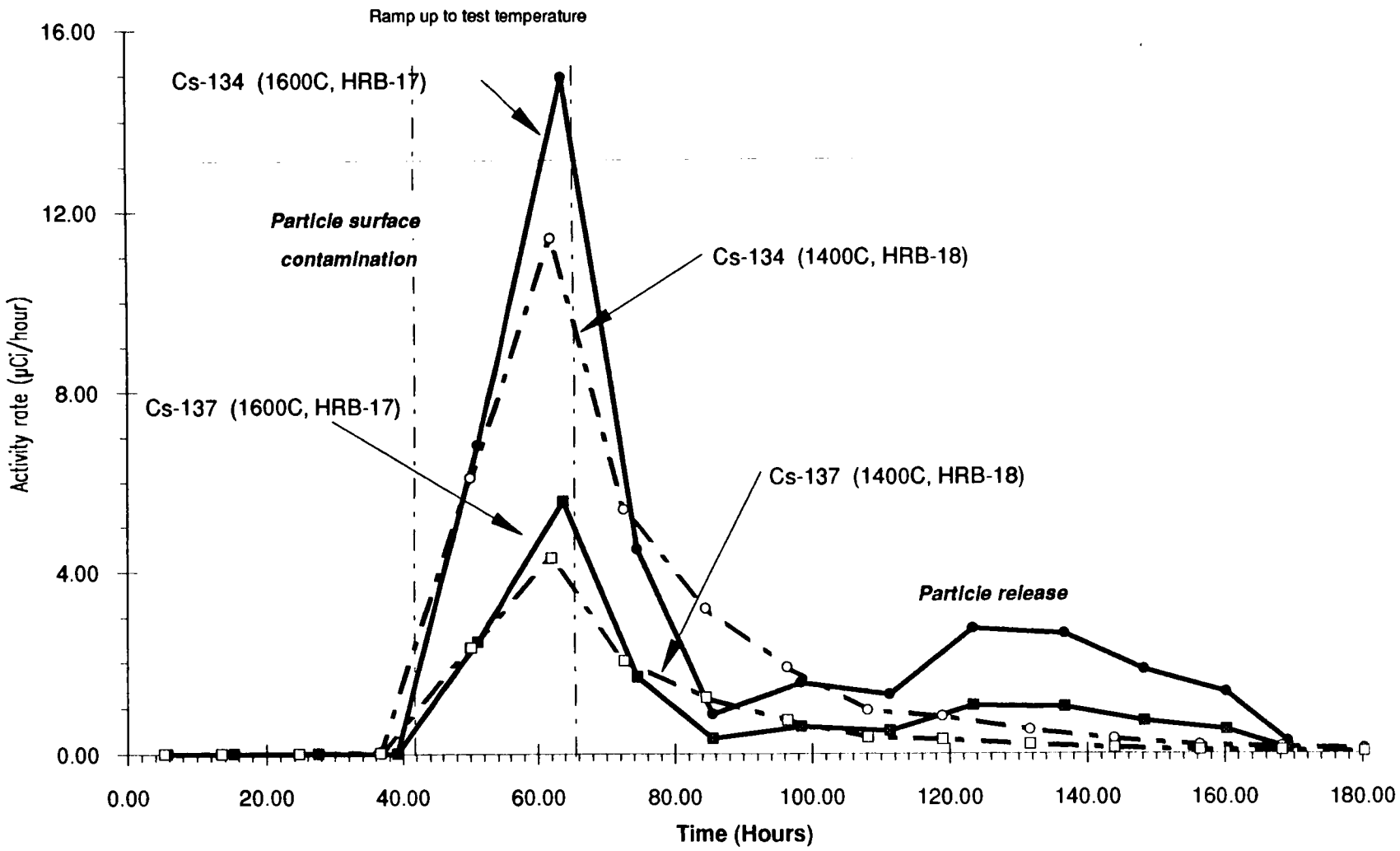

Fig. 33. Comparison between the 1400 and 1600°C deposition cup cesium collection rate as a function of time. Corrected to 5 Feb 1986.

The aggregate mass balance for the 1600°C test, measured in μCi (corrected to 5 Feb 1986), is as follows:

Item	Activity (μCi) ^{134}Cs	^{137}Cs	^{154}Eu	Uncertainty
All furnace parts	237	86	6.3	50%
Deposition cups	413	154	0	6%
Total	650	240	6.3	19%
Total loss from particles	366	195	0.0	100+%
Percent difference	-44%	-19%	-100%	

The large europium difference comes from the fact that the total-particle europium loss was buried in the uncertainty, even though individual particles were seen to have lost europium. The large overall uncertainty in the particle loss measurements is because the loss is computed as the difference between the pre- and postheating particle inventories, each of which have an uncertainty of the same order as their difference.

The cerium normalized mass balance may be computed by dividing the preheating cerium measurement by the postheating cerium measurement and using this ratio to scale the postheating cesium and europium measurements. The mass difference is computed as before.

With the particle losses normalized as above, the following mass balance, measured in μCi (corrected to 5 Feb 1986), is obtained for the 1600°C test:

Item	Activity (μCi) ^{134}Cs	^{137}Cs	^{154}Eu	Uncertainty
All furnace parts	237	86	6.3	50%
Deposition cups	413	154	0	6%
Total	650	240	6.3	19%
Total loss from particles (normalized)	721	329	5.3	100+%
Percent difference (normalized)	-11%	-37%	-16%	

The primary result of this method was the elimination of the ^{154}Eu repeatability variation. When this technique is applied to the results of the 1400° C test (see below), the results are not as favorable. This would seem to imply that the uncertainties are not due to a common systematic error.

If one compares the ratio between the ^{134}Cs and ^{137}Cs measurements in the above tables, considerable variation can be seen between the furnace and deposition cup total and the particle total. At the present time, the available particle-measuring equipment simply does not have the high level of measurement repeatability necessary to resolve these discrepancies due to very small changes in total activity. The device can, however, locate and measure individual particles that have released more than a few percent of their fission product inventory.

Overall, it appears that a detailed mass balance calculation is limited by the measurement uncertainty due to the small losses. An approximate mass balance within the large uncertainties has been obtained indicating agreement within these limits.

As a final note, the collection efficiency of the cold finger apparatus was approximately 64% for this test (cups/[cups+furnace parts]).

5.7 1400° C TEST FISSION PRODUCT MASS BALANCE

As in the 1600° C case, large uncertainties in the average particle loss limited the precision of the mass balance.

The aggregate mass balance, measured in μCi (corrected to 5 Feb 1986), is as follows:

	Activity (μCi)			
Item	^{134}Cs	^{137}Cs	^{154}Eu	Uncertainty
All furnace parts	21	8	0	50%
Deposition cups	347	132	0	6%
Total	368	140	0	6%
Total loss from particles	440	207	6.7	100+%
Percent difference	20%	48%	--	

These results are similar to those in the previous section.

Using the normalized method gives the following, measured in μCi and corrected to 5 Feb 1986:

	Activity (μCi)			
Item	^{134}Cs	^{137}Cs	^{154}Eu	Uncertainty
All furnace parts	21	8	0	50%
Deposition cups	347	132	0	6%
Total	368	140	0	6%
Total loss from particles (normalized)	550	249	5.0	100+%
Percent difference (normalized)	49%	78%	--	

In this case, the normalization technique does not seem to help, suggesting that the uncertainties are not due to a systematic error.

Again, there is considerable variation in the measured ^{134}Cs-to-^{137}Cs ratio. Since no particles were observed to have released, the collected fission products were due entirely to surface contamination. The same considerations about the mass balance being subject to the uncertainty of the measurements, as detailed above, apply. Again, an approximate mass balance within the uncertainties has been obtained.

For this test, the average cold finger collection efficiency was 94% (cups/[cups+furnace parts]). The high efficiency was probably due to the long period of time available to drive the cesium out of the furnace components.

5.8 1400/1600° C PARTICLE CONTAMINATION COMPARISON

Since both the HRB-17 (1600° C) and the HRB-18 (1400° C) particles were irradiated in similar environments, the question arises as to whether the particle contamination level can be estimated based on the results of the two heating tests. If so, the HRB-17 total release minus the four HRB-17 particle releases should equal the HRB-18 release, assuming the same level of surface contamination. This comparison can be done in two ways. The first way uses only particle release information and contains the greatest uncertainty but relies on a single instrument. The second way makes use of the deposition cups and furnace parts, as well as the releasing particles, to reduce the uncertainty.

The aggregate particle comparison using only particle gamma-scanning data, measured in μCi (corrected for decay as before), gives:

Item	Activity (μCi) ^{134}Cs	^{137}Cs	^{154}Eu	Uncertainty
HRB-17 total particle release	366	195	0.0	100
HRB-17 failed particle release	250	96	5.8	20%
Difference	116	99	(-5.8)	100+%
HRB-18 total particle release	440	206	6.7	100+%
HRB-17/18 ratio	0.26	0.48	--	100+%

As can be seen, the comparison is within a factor of four. Again, the large uncertainty due to the small average difference between the pre- and postheating measurements masks the comparison. The results do indicate, however, that the contamination levels are the same order of magnitude. Releasing particles have a smaller uncertainty than non-releasing particles because of the much larger inventory difference.

Since the aggregate particle measurements contain the greatest uncertainty, one may wish to make the contamination estimate using data with less uncertainty as was done in the previous sections. In that case, one can use the furnace parts, deposition cups, and HRB-17 releasing particles as a basis for the comparison. These data, in μCi, yield (corrected for decay as before):

Item	Activity (μCi) ^{134}Cs	^{137}Cs	^{154}Eu	Uncertainty
HRB-17 all furnace parts	237	86	6.3	50%
HRB-17 deposition cups	413	154	0	6%
HRB-17 total	650	240	6.3	19%
HRB-17 failed particle release	250	96	5.8	7%
HRB-17 difference	400	144	0.5	31%
HRB-18 all furnace parts	21	8	0	50%
HRB-18 deposition cups	347	132	0	6%
HRB-18 total	368	140	0	6%
HRB-17/18 ratio	1.09	1.03	--	34%

Using data with less uncertainty (from two sources) leads to the conclusion that the level of contamination was about the same for both sets of particles.

6.0 METALLOGRAPHY, SEM, AND RADIOGRAPHY

Because of difficulties with polishing equipment, personnel unavailability, and hot cell delays due to health and safety issues, only preliminary work on metallography was accomplished.

6.1 1600° C TEST METALLOGRAPHIC RESULTS

Preliminary metallographic results for three particles, H17D-H42, H17D-H51, and H17D-H62, indicate that fission product corrosion was not present. A cross section of particle H17D-H42, which suffered no releases, is shown in Fig. 34. While the conclusions are only preliminary, it appears that there has been no chemical attack on the SiC layer, and this layer appears to be dense and non-porous. In addition, the kernel and phase distribution appear unchanged from the unheated condition. The cracks in the coatings are believed to be a result of the polishing operation since no fission products were released.

A particle, H17D-H51, that released Eu but not Cs is shown in Fig. 35. Again, no fission product attack is evident. The SiC layer of this particle appeared to have different polishing properties relative to the particle that suffered no releases. It is not clear, at this time, whether the apparent porosity and cracks are real or artifacts of the still rather coarse polishing.

The final particle, H17D-H62, had a high cesium release and a low europium release. No fission product attack is evident; see Fig. 36. Again, the SiC layer of this particle appeared to have different polishing properties, and voids may be present, but the detail is limited by the degree of polishing. The cracks may be due to handling.

Overall, only limited information is available from the incomplete metallography, but it appears that corrosion is not a problem. The retention of ^{85}Kr and the release of the metallic fission products, along with some rough detail from the particle metallography, indicate that more examination of the SiC is necessary to explain the behavior of these particles at 1600° C.

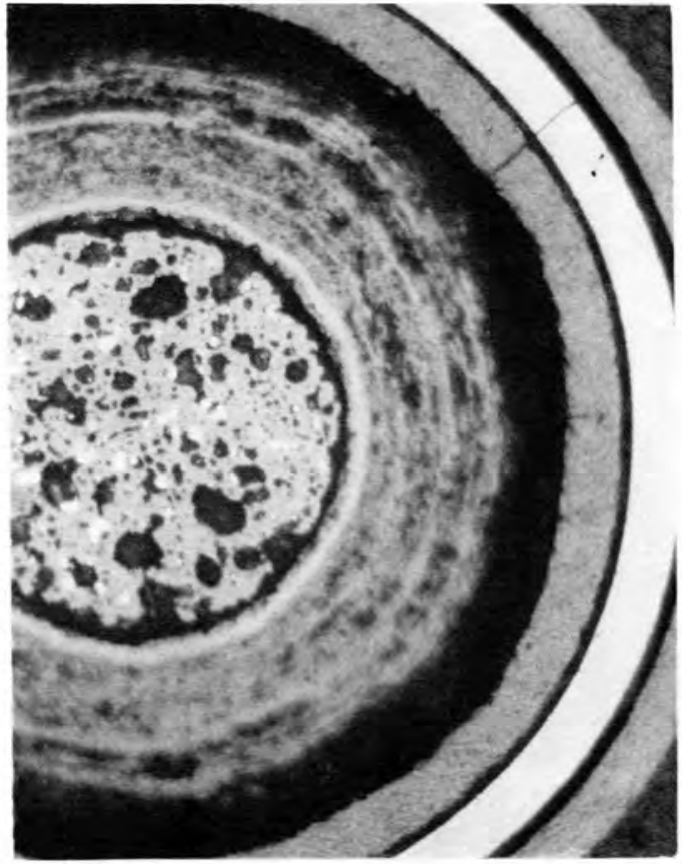

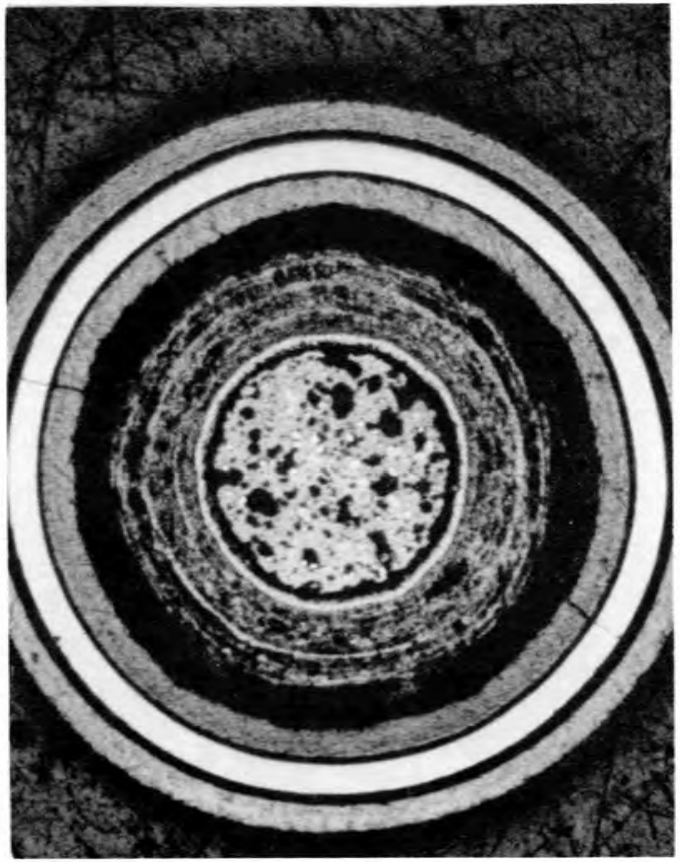

Fig. 34. Metallographic cross section of particle H17D-H42. No evidence of chemical attack. SiC appears dense and non-porous.

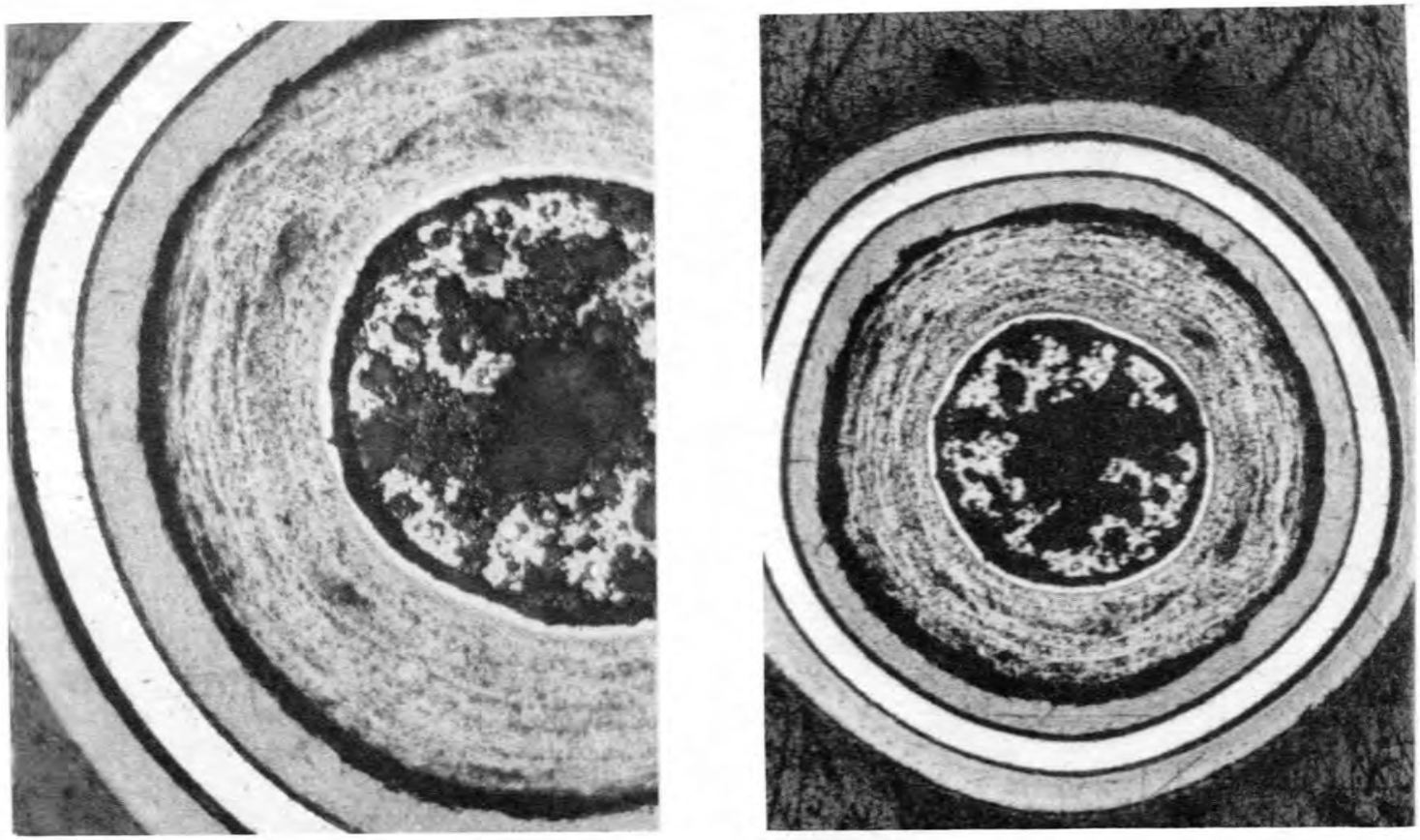

Fig. 35. Metallographic cross section of particle H17D-H51, which released europium but not cesium.

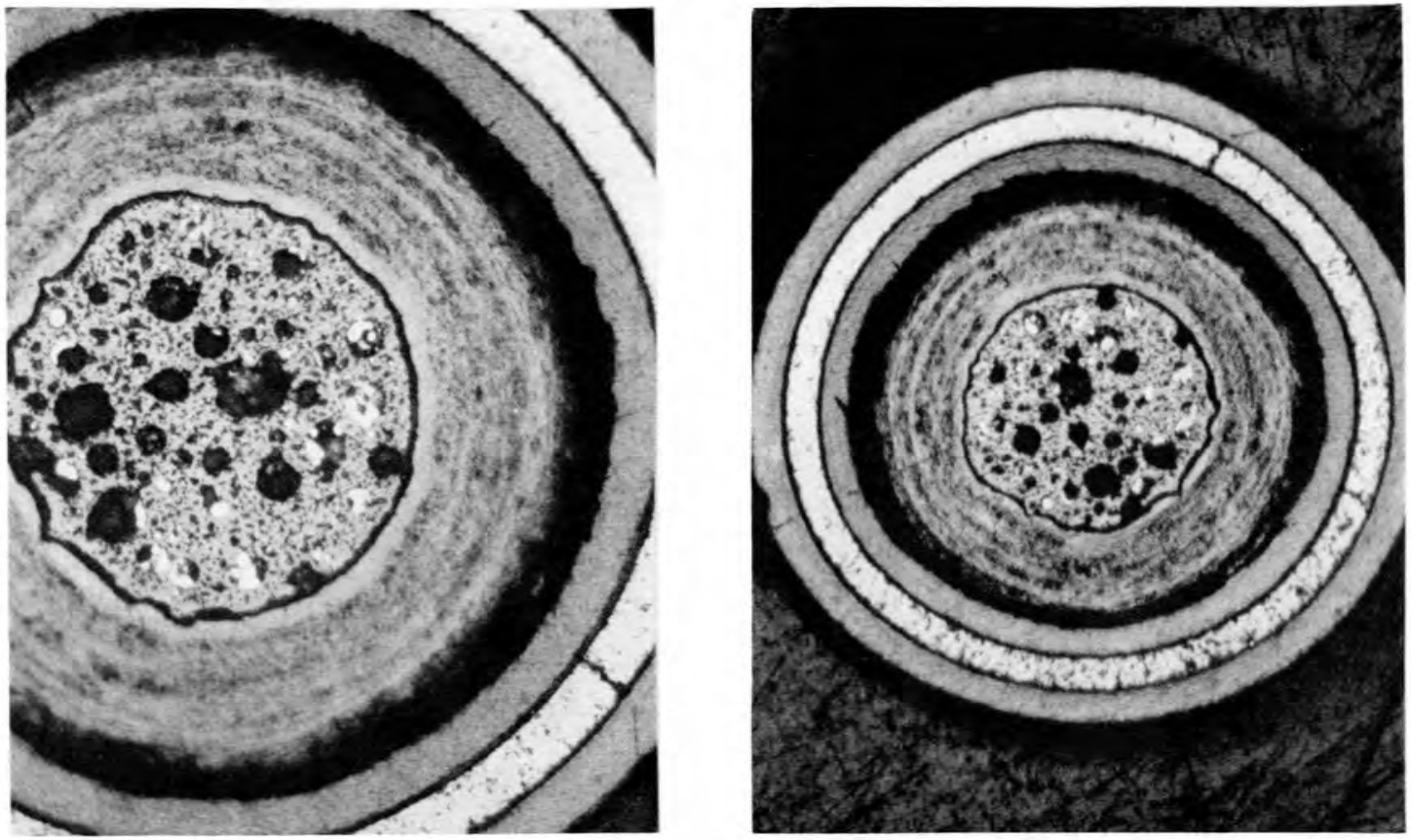

Fig. 36. Metallographic cross section of particle H17D-H62, which released cesium but little europium.

6.2 1400° C TEST METALLOGRAPHIC RESULTS

Because of the unavailability of the hot cells due to health and safety considerations, HRB-18 metallography was not performed.

6.3 SEM AND MICROPROBE ANALYSIS

Due to equipment and personnel unavailability, this work was not performed on the heated or unheated particles.

6.4 RADIOGRAPHY

Due to equipment and personnel unavailability, this work was not performed on the heated or unheated particles.

7.0 CONCLUSIONS

In general, the high-temperature furnace and its subsystems performed well. In the 1600° C test, a problem with the alignment of the deposition cup drive motor resulted in a minor cup changing delay, and a background change in the detector system resulted in a minor increase in the minimum detectable activity level. The 1400° C test suffered a premature power supply shutdown late into the heating program. Fortunately, the failure occurred near the end of the test run after the most significant data had been collected. These problems did not affect the quality of the data or compromise the usefulness of the test to the program.

The results of the 1600° C test indicate the following:

1. Three percent of the total inventory of cesium was released along with 2.1% of the europium inventory. The cesium release is believed to come from two sources. The first source is contamination that the particles received during irradiation from adjacent DTF particles and contributed 1.8%. The second source is due to large fractional inventory releases from four particles through the SiC coating, resulting in an additional 1.2%. All of the europium is believed to come from particle releases.
2. No krypton release was observed.
3. One-and-one-half percent of the strontium inventory was released. Essentially all of the collected strontium is believed to come from particle releases.

4. Preliminary metallographic results indicate that the releasing particles may have SiC coatings that differ from non-releasing particles. However, this is not conclusive.

The results of the 1400°C test indicate the following:

1. Of the total inventory of cesium, 1.8% was released. All of this activity is believed to be due to contamination.
2. No particle releases occurred during the test.
3. No krypton release was observed.
4. Trace amounts of strontium were collected; the source is believed to be surface contamination.

The results of both tests indicate that:

1. it is feasible to track particles throughout the testing program,
2. the performance of the CCCTF is as predicted, and
3. furnace contamination is contained within the internal heating zone.

Despite some problems, the overall operation of the CCCTF was good, and sound data were collected. The minor problems are being addressed, and modifications to the facility are planned.

8.0 ACKNOWLEDGMENTS

The authors thank M. R. Upton for final report preparation and K. Spence for editing.

9.0 REFERENCES

1. CEGA, *Test Specification for Post-Irradiation Heating of HRB-17/18 TRISO-Coated HEU UCO Fuel Particles*, CEGA-000337, Rev N/C.

2. *NPR MHTGR Test Plan*, NP-FFP-TP2, Martin Marietta Energy Systems, Inc., Oak Ridge Natl. Lab., February 1991.

3. R. N. Morris, C. A. Baldwin, J. L. Collins, L. C. Emerson, W. A. Gabbard, C. M. Malone, B. F. Myers, M. F. Osborne, M. L. Peters, J. C. Whitson, and J. L. Wright, *The Core Conduction Cooldown Test Facility: Current Status and Issues*, ORNL/NPR-91/7, Martin Marietta Energy Systems, Inc., Oak Ridge Natl. Lab., May 1991.

4. R. N. Morris, J. T. Collins, and J. C. Whitson, *CCCTF Shakedown Tests*, ORNL/NPR-91/25, Martin Marietta Energy Systems, Inc., Oak Ridge Natl. Lab., September 1991.

5. R. N. Morris, *Quick Look Report: HRB-18 HEU TRISO UCO Unbonded Irradiated Particle Core Conduction Cooldown Test*, ORNL/NPR-91/28, Martin Marietta Energy Systems, Inc., Oak Ridge Natl. Lab., October 1991.

6. R.N. Morris, *Quick Look Report: HRB-17 HEU TRISO UCO Unbonded Irradiated Particle Core Conduction Cooldown Test*, ORNL/NPR-91/34, martin Marietta Energy Systems, Inc., Oak Ridge Natl. Lab., December 1991.

7. J. W. Ketterer, B. F. Myers., M. J. Kania, and H. M. Henson, *Capsules HRB 17/18 PIE Report*, HTGR-86-083, G. A. Technologies, Inc., 1987.

Appendix A

Burnup Calculations
HEU UCO TRISO Particles - Capsules HRB-17/-18

Burnup calculations were made on the unbonded HEU TRISO-coated particles irradiated in Inconel-encapsulated containers in test capsules HRB-17 and HRB-18. The basis for the calculations was the fission product inventory data from the individual HEU particles obtained from gamma spectrometry. The measurements were made prior to and after long-term, high-temperature heatup tests. These data represent the most accurate information available on the fuel particles.

Previous burnup estimates for irradiation capsules HRB-17/-18 were made using neutronic calculations with the CACA-2 code coupled with empirically derived, one-group neutron flux and cross-section data set.[1] The estimates were made for the irradiated fuel compacts, containing LEU UCO and ThO_2 TRISO-coated fuel, but not for the unbonded particles in the Inconel encapsulation. The one-group, neutron flux and cross-section data base were derived with stainless steel capsule containments, but they did not include any perturbations due to the presence of the Inconel.

The individual-particle gamma spectrometry data are viewed as the most accurate data available for this current fuel. For this reason, and the lack of confidence in the available neutron flux and cross-section data, burnup was calculated from the available ^{106}Ru, ^{125}Sb, ^{137}Cs, and ^{144}Ce inventory at the end of irradiation.

Burnup, in percent fissions per initial metal atoms (FIMA) is defined as:

$$\text{Burnup (\%)} = \{\text{Total No. Fissions/Number Heavy Metal Atoms}\} \cdot 100. \qquad (1)$$

The initial quantity of uranium and its isotopic makeup are available from the pre-irradiation characterization data[2] for test capsules HRB-17/-18. It is the "Total Number of Fissions" which require a detailed analysis. The formulation for determining the number of fissions was derived from the basic rate equation for the generation of a specific fission product. For a specific fission product of N atoms, the time-dependent inventory is given by the relationship:

$$dN/dt = \text{production rate - removal rate}, \qquad (2)$$

or

$$dN/dt = \Sigma\{\phi\cdot(\sigma_i\cdot Y_i)\cdot\alpha_i\} - \lambda\cdot N - \phi\cdot\sigma_R\cdot N, \tag{2a}$$

where: ϕ = neutron flux (n/cm^2-s),

σ_i = microscopic cross section (cm^2/atom of parent),

σ_R = removal cross section (cm^2/atom of N),

Y_i = no. atoms fissile isotope i (atom of parent),

α_i = fission product yield for N (atom of N/fission), and

λ = decay constant for fission product N (s^{-1}).

For the fission products ^{106}Ru, ^{125}Sb, ^{137}Cs, and ^{144}Ce in the irradiation facilities of the High Flux Isotope Reactor (HFIR), the removal reaction rate, $\phi\cdot\sigma_R$, is much less than the removal due to radioactive decay [$\phi\cdot\sigma_R << \lambda$]. Eliminating the removal cross-section term and using an integrating factor of $e^{\lambda t}$, Eq. (2a), can be rearranged as:

$$d/dt[N\cdot e^{\lambda t}] \approx \Sigma\{\phi\cdot(\sigma_i\cdot Y_i)\cdot\alpha_i\}\cdot e^{\lambda t}. \tag{2b}$$

The production rate term, $\{\phi\cdot(\sigma_i\cdot Y_i)\cdot\alpha_i\}$, can be described as a fission-rate, $\phi\cdot(\sigma_i\cdot Y_i)$, times a yield, α_i, for each fissile isotope i. In reality, the fission rate is time dependent because the inventory of fissile isotopes changes with time. For purposes of this analysis, the production term is equated with an average fission rate, <FR>, times a weighted fission yield, α_w:

$$\Sigma\{\phi\cdot(\sigma_i\cdot Y_i)\cdot\alpha_i\} = \langle FR\rangle\cdot\alpha_w. \tag{3}$$

The average fission rate is defined as:

$$\langle FR\rangle = \text{Total No. Fissions}/t_p, \tag{4}$$

where t_p = time at power (s).

The weighted fission yield is calculated by weighing the fission yield of each fissile isotope by the fraction of fissions that result from that isotope:

$$\alpha_w = \Sigma\{(\text{Fission Fraction})_i \cdot \alpha_i\}, \tag{5}$$

where $(\text{Fission Fraction})_i$ = ratio of no. fissions due to fissile isotope Y_i to the total number of fissions

α_i = fission yield for N from fissile isotope Y_i.

The fission fraction for each fissile isotope was determined in a similar manner as were the burnups for the irradiated fuel compacts in HRB-17/-18. The only difference was that the fissile fuel material was HEU UCO rather than LEU UCO. The fission product yield data were taken from ref. 3. Table A-1 presents the fission fraction data and fission yield data for those fission products used in this analysis. The sum of the fission fractions is not quite equal to 1.0 because the fissions in the neptunium isotopes have been neglected.

Table A-1. Actinide fission fraction data and fission product yield data for HRB-17/-18 HEU UCO TRISO particle burnup calculations

	^{235}U	^{239}Pu	^{241}Pu
Fission fraction	0.9852	0.0096	0.0025
^{106}Ru	3.917×10^{-3}	4.278×10^{-2}	6.086×10^{-2}
^{125}Sb	2.999×10^{-4}	1.265×10^{-3}	4.037×10^{-4}
^{137}Cs	6.263×10^{-2}	6.692×10^{-2}	6.597×10^{-2}
^{144}Ce	5.455×10^{-2}	3.832×10^{-2}	4.145×10^{-2}

Substituting Eqs. (3) and (4), Eq. (2b) becomes, after dropping the subscripts,

$$d/dt[N \cdot e^{\lambda t}] \approx \langle FR \rangle \cdot \alpha_w \cdot e^{\lambda t}. \tag{6}$$

Now, the right side of Eq. (6) is independent of time, with the exception of the integrating term. Integrating over the time interval $t=0$ to $t=t_p$, with the initial conditions at $t=0$, $N=0$, and multiplying both sides by $e^{-\lambda t}$, the inventory of fission product N at the time the fuel was discharged from the reactor is:

$$N(t=t_p) \approx [(\langle FR \rangle \cdot \alpha_w)/\lambda] \cdot [1 - e^{-\lambda \cdot t_p}]. \quad (7)$$

After a decay time of t_d, following the radioactive decay law, the inventory of fission product N is

$$N(t_p,t_d) \approx [(\langle FR \rangle \cdot \alpha_w)/\lambda] \cdot [1 - e^{-\lambda \cdot t_p}] \cdot e^{-\lambda \cdot t_d}. \quad (8)$$

The irradiation of test capsules HRB-17/-18 occurred over a period of six fuel cycles in the HFIR. Table A-2 describes this irradiation history.

Table A-2. Irradiation history for test capsules HRB-17/-18 in HFIR[1]

		Irradiation time* (h)	
Irradiation cycle	HFIR fuel cycle	Cycle	Cumulative
1	269	422.8	422.8
2	270	503.9	926.7
3	271	508.9	1435.6
4	272	506.0	1941.6
5	273	501.2	2442.9
**	274	0.0	2442.9
6	275	511.9	2954.7

*Time at reactor full power of 100 MW(t).
**Both capsules HRB-17 and HRB-18 were out of the reactor during this cycle.

Including the downtime between fuel cycles and the irradiation time at full-reactor power, the irradiation lasted a total of 173.5 d; 123.1 d at full power, and 50.4 d at zero power. For this analysis, the reactor operation will be approximated with two time periods. The time at full power—123.1 d—is equivalent to t_p, and the downtime—50.4 d—is equivalent to t_d.

The inventory of fission products at the time of test capsule HRB-17 and HRB-18 discharge from HFIR was determined by gamma spectrometry.[4] Because of contamination present prior to the heating tests, the particle inventories measured in post-test gamma spectrometry were used in the burnup analysis. Only those particles determined not to have lost significant fission product inventories during the heatup tests were considered. The inventories for ^{106}Ru, ^{125}Sb (HRB-17 only), ^{137}Cs, and ^{144}Ce, and their respective standard deviations (s) used in this analysis, are provided in Table A-3. The individual data were obtained from Tables 1 and 2 in ref. 4. All data are corrected to the date of reactor discharge—February 5, 1986. For test capsule HRB-17, four of the 80 particles inventoried were not considered in the analysis because they were found to have lost ^{137}Cs or ^{154}Eu during the 1600°C heatup. All 80 of the particles inventoried for test capsule HRB-18 were considered.

Table A-3. Calculations for the fission rate and number of fissions for HEU UCO TRISO particles irradiated in test capsules HRB-17 and HRB-18A

Fission product	Decay constant (s^{-1})	Activity* (Bq/part.)	Std. dev. (%)	Average	
				Fiss. rate <FR>	Fissions
		Capsule HRB-17			
^{106}Ru	2.17×10^{-8}	6.85×10^{6}	11.4	8.25×10^{9}	8.77×10^{16}
^{125}Sb	8.05×10^{-9}	1.64×10^{5}	22.3	6.71×10^{9}	7.13×10^{16}
^{137}Cs	7.30×10^{-8}	3.67×10^{6}	3.33	7.61×10^{9}	8.10×10^{16}
^{144}Ce	2.82×10^{-8}	9.67×10^{7}	3.8	7.78×10^{9}	8.28×10^{16}
		Capsule HRB-18			
^{106}Ru	2.17×10^{-8}	7.07×10^{6}	10.65	8.51×10^{9}	9.05×10^{16}
^{125}Sb	8.05×10^{-9}	--	--	--	--
^{137}Cs	7.302×10^{-10}	3.65×10^{6}	3.66	7.57×10^{9}	8.05×10^{16}
^{144}Ce	2.821×10^{-8}	9.68×10^{9}	3.83	7.79×10^{9}	8.28×10^{16}

*Activity given in Bq per particle. For HRB-17, seventy-six were considered, and for HRB-18, eighty particles were considered.

Substituting for t_p and t_d and rearranging Eq. (8):

$$<FR> \approx [(N \cdot \lambda)/\alpha_w] \cdot [(1 - e^{-\lambda \cdot 123.1 \text{ days}}) \cdot e^{-\lambda \cdot 50.4 \text{ days}}]^{-1}. \quad (9)$$

The term $(N \cdot \lambda)$ is identical to the fission product activity at the time of discharge. The number of fissions is found by solving Eq. (9) for <FR> and multiplying by the time at power, t_p as described in Eq. (4). This was accomplished in a spreadsheet calculation, and the results are presented in Table A-3.

The data presented in Table A-3 for the number of fissions, derived from each fission product inventory, were then weighted according to the standard deviation of the measurement. The weighing function, ω_k, for each fission product was calculated from:

$$\omega_k = (1/s_k)^2/\Sigma(1/s_k)^2, \quad (10)$$

where s_k = standard deviation of fission product k.

The estimate for the total number of fissions for use in the burnup determination was given by:

$$\text{Total No. Fissions} \approx \omega_{(Ru106)} \cdot \text{Fissions}_{(Ru106)} + \omega_{(Sb125)} \cdot \text{Fissions}_{(Sb125)} + \omega_{(Cs137)} \cdot \text{Fissions}_{(Cs137)} + \omega_{(Ce144)} \cdot \text{Fissions}_{(Ce144)}. \quad (11)$$

The initial inventory of heavy metal atoms was estimated at 1.22×10^{17} atoms of uranium (^{235}U plus ^{238}U) from ref. 2. For test capsule HRB-17 and HRB-18, Eq. (11) was solved and, along with the initial inventory of uranium atoms, substituted into Eq. (1) to determine the burnup. The results of these burnup calculations are provided in Table A-4.

The agreement between the burnup calculations derived from independent gamma spectrometry measurements performed on individual, irradiated, HEU UCO TRISO particles from capsules HRB-17 and HRB-18 is excellent. Both capsules were irradiated under identical conditions. For HRB-17, the calculated burnup was 67.5% FIMA, and for HRB-18, it was 67.3% FIMA.

As a check of the consistency of the method used to determine burnup, the individual fission product inventories were calculated using the weighted fission product yield, α_w determined

Table A-4. Burnup determinations for HEU UCO TRISO-coated particles irradiated in test capsules HRB-17 and HRB-18

Parameter	HRB-17	HRB-18
Atoms heavy metal	1.22×10^{17}	1.22×10^{17}
Total no. fissions [Eq. (11)]	8.22×10^{6}	8.19×10^{6}
Burnup, % FIMA [Eq. (1)]	67.5	67.3

with Eq. (5) and the data of Table A-1, the total No. fissions, determined with Eq. (11) and decay constant data in Table A-3. A comparison of the calculated and measured fission product inventories is provided in Table A-5. Again, there was excellent agreement between the measured and calculated fission product inventories with the percent differences < 10% for ^{106}Ru, ^{137}Cs, and ^{144}Ce. The data for these fission products represent the most reliable post-heatup results. The ^{125}Sb data for HRB-18 exhibited excessive uncertainty and were dropped from the analysis.

Table A-5. Comparison of the fission product inventories measured (gamma spectrometry) and calculated (burnup determinations) for HEU UCO TRISO particles irradiated in test capsules HRB-17 and HRB-18

Fission product	Measured (Bq)	Calculated (Bq)	Percent diff.
	Capsule HRB-17		
^{106}Ru	6.85×10^{6}	6.40×10^{6}	6.61
^{125}Sb	1.64×10^{5}	1.88×10^{5}	-14.83
^{1137}Cs	3.67×10^{6}	3.71×10^{6}	-1.14
^{144}Ce	9.67×10^{7}	9.57×10^{7}	1.05
	Capsule HRB-18		
^{106}Ru	7.07×10^{6}	6.42×10^{6}	6.23
^{125}Sb	--	--	--
^{137}Cs	3.65×10^{6}	3.72×10^{6}	-2.01
^{144}Ce	9.68×10^{7}	9.60×10^{7}	0.84

References

1. J. W. Ketterer, B. F. Myers, M. J. Kania, and H. M. Henson, *Capsules HRB-17/-18 Final PIE Report*, DOE-HTGR-86-083, Martin Marietta Energy Systems, Inc., Oak Ridge Natl. Lab., May 1987.
2. J. W. Ketterer and K. E. Partain, *Capsules HRB-17/-18 Preirradiation Report*, GA Technologies Report 906975, August 1983.
3. B. F. Ryder and M. E. Meck, *Compilation of Fission Product Yields*, General Electric Company Report, Vallecitos Nuclear Center, NEDO-12154-2(0), Class 1, July 1977.
4. C. A. Baldwin, "Post-Heating Test Report on Unbonded HEU-UCO Particles from Capsules HRB-17 and HRB-18," unpublished data, January 1992 [ORNL Internal Correspondence, C. A. Baldwin to W. A. Gabbard, Subject: Post-Heating Test Report on Unbonded HEU UCO Particles from HRB-17 and HRB-18, January 9, 1992].

INTERNAL DISTRIBUTION

1-2. Central Research Library
3. Document Reference Section
4-5. Laboratory Records Department
6. Laboratory Records, ORNL-RC
7. ORNL NPR-RMS-DCC-RC
8. ORNL Patent Section
9-11. M&C Records Office
12-16. C. A. Baldwin
17. E. C. Beahm
18-22. J. L. Collins
23-27. T. L. Collins
28. G. L. Copeland
29. L. C. Emerson
30-34. W. A. Gabbard
35. F. J. Homan
36. H. Jones
37-41. M. J. Kania
42. J. C. Mailen
43-47. C. M. Malone
48. R. C. Martin
49-53. R. N. Morris
54. D. L. Moses
55. B. F. Myers
56. M. F. Osborne
57. N. H. Packan
58. P. L. Rittenhouse
59. P. S. Sklad
60. O. M. Stansfield
61-65. J. Travis
66-70. C. S. Webster
71. R. P. Wichner
72-76. J. C. Whitson
77-81. J. L. Wright

EXTERNAL DISTRIBUTION

82-84. CEGA, P. O. Box 85608, San Diego, CA 92138-5688

D. L. Hanson
D. W. McEachern
W. J. Scheffel

85-89. IDAHO NATIONAL ENGINEERING LABORATORY, P. O. Box 1625, Idaho Falls, ID 83415

L. J. Kay
R. K. McCardell
M. L. Russell
R. K. Southworth
E. P. Stroupe

90-91. DOE OAK RIDGE FIELD OFFICE, P. O. Box 2001, Oak Ridge, TN 37831

Office of Assistant Manager for Energy Research and Development